Investigation of the role of nucleus accumbens dopamine D1- or D2-receptor expressing neurons in cognitive, limbic, and motor functions

（側坐核
ドーパミンD1またはD2受容体発現ニューロンの認知、大脳辺縁系及び運動機能における役割の研究）

Special Integrated Science Course

Biological Science

Suthinee Attachaipanich

Osaka University, School of Science

Acknowledgements

The successful completion of my study and research project would not have been possible without the tremendous support and encouragement I have received. I am profoundly grateful for the opportunity and the time I have spent here at Osaka University. My deepest appreciation and sincere gratitude are extended to the following individuals who, in one way or another, have contributed to my professional and personal growth, enabling me to achieve the completion of this study:

First and foremost, I express my heartfelt thanks to Professor Takatoshi Hikida for his support, advice, and words of encouragement throughout my time at Osaka University. His guidance has been invaluable in shaping my research and academic development.

I am also grateful to Assistant Professor Tom Macpherson for his advice and assistance with my research project. His expertise and guidance have greatly enhanced the quality and depth of my work.

I extend my appreciation to Assistant Professor Takaaki Ozawa and Ms. Noriko Otani for their endless and dependable support. Their assistance has been crucial in ensuring the smooth progress of my study.

Furthermore, I would like to express my heartfelt gratitude to my family and friends for their love, encouragement, and unwavering support throughout my study life.

Once again, I extend my deepest gratitude to everyone mentioned above. Their support, guidance, and encouragement have played an indispensable role in my academic and personal achievements, culminating in the successful completion of this study.

Publications and Communications Arising from this Thesis

Attachaipanich S, Ozawa T, Macpherson T, Hikida T. (2023). Dual roles for nucleus accumbens core dopamine D1-expressing neurons projecting to the substantia nigra pars reticulata in limbic and motor control, *eNeuro*, 10(6):ENEURO.0082-23.2023.

Nishioka T, Attachaipanich S, Hamaguchi K, Lazarus M, de Kerchove d'Exaerde A, Macpherson T. & Hikida T. (2023). Error-related signaling in nucleus accumbens D2 receptor-expressing neurons guides inhibition-based choice behavior in mice. *Nature communications*, 14:2284(2023).

Attachaipanich S, Macpherson T, Hikida T. (2022). Nucleus accumbens core D1-MSNs microcircuits drive locomotor and reward-related behaviors (Abstract). 45th Annual Meeting of the Japan Neuroscience Society

Attachaipanich S, Macpherson T, Hikida T. (2021). The role of nucleus accumbens core D1- and D2-neurons in controlling reward and aversion (Abstract). 44th Annual Meeting of the Japan Neuroscience Society/ The 1st CJK International Meeting.

Attachaipanich S, Macpherson T, Hikida T. (2020). Optogenetic manipulation of nucleus accumbens projections to the substantia nigra pars reticulata in locomotor and reward-related behaviors (Abstract). 19th IPR Retreat

Attachaipanich S, Macpherson T, Hikida T. (2019). Optogenetic manipulation of nucleus accumbens output pathways controlling reward learning (Abstract). 18th IPR Retreat

Table of Contents

List of Abbreviations

AAV	=	Adeno-Associated Viral
Arch	=	Archaerhodopsin
A2a	=	Adenosine 2A receptor
BG	=	Basal Ganglia
cAMP	=	Cyclic Adenosine Monophosphate
CBGTC	=	Cortico-basal ganglia-thalamo-cortical
ChR	=	Channelrhodopsin
ChR1	=	Channelrhodopsin-1
ChR2	=	Channelrhodopsin-2
CPP	=	Conditioned Place Preference
DA	=	Dopamine
DLS	=	Dorsolateral Striatum
DMS	=	Dorsomedial Striatum
D1	=	Dopamine D1-receptor
D2	=	Dopamine D2-receptor
ENk	=	Enkephalin
EYFP	=	Enhanced Yellow Fluorescent Protein
FR	=	Fixed-Ratio
FSIs	=	Fast-spiking interneurons
GABA	=	GABAergic
GLUT	=	Glutamatergic
GPe	=	External segments of the Globus Pallidus
GPi	=	Internal segments of the Globus Pallidus
ITI	=	Inter-Trial Interval
LED	=	Light Emitting Diode
LH	=	Lateral Hypothalamus
LTD	=	Long-Term Depression
LTP	=	Long-Term Potentiation

lSNr	=	Lateral Substantia Nigra pars Reticulata
mPFC	=	Medial Prefrontal Cortex
mSNr	=	Medial Substantia Nigra pars Reticulata
MSNs	=	Medium Spiny Neurons
M1	=	Primary Motor Cortex
NAc	=	Nucleus Accumbens
NpHR	=	Halorhodopsin
OF	=	Optic Fiber
OFT	=	Open Field Test
PBS	=	Phosphate-Buffered Saline
PFA	=	Paraformaldehyde
PKA	=	Protein Kinase A
PV	=	Parvalbumin
RR	=	Random-Ratio
rt-pp	=	Real-time Place Preference
SNc	=	Substantia Nigra pars Compacta
SNr	=	Substantia Nigra pars Reticulata
SOM	=	Somatostatin-releasing Interneurons
SP	=	Substance P
STN	=	Subthalamic Nucleus
TH	=	Tyrosine Hydroxylase
VP	=	Ventral Pallidum
VPdl	=	Dorsolateral subregion of Ventral Pallidum
VPvm	=	Ventromedial subregion of Ventral Pallidum
VTA	=	Ventral Tegmental Area

Chapter 1

Introduction

1.1 Anatomical and Physiological Properties of the Basal Ganglia

1.1.1 The Basal Ganglia

The basal ganglia is a complex network of structures in the brain that consists of several interconnected nuclei within the cerebral hemispheres, diencephalon, and midbrain, and is comprised mainly of the striatum, globus pallidus, substantia nigra, subthalamic nucleus, ventral pallidum, and ventral tegmental area. These structures within the basal ganglia are contained within several parallel cortico-basal ganglia-thalamo-cortical (CBGTC) loop circuits that structurally and functionally distinct (Alexander & Crutcher, 1990; Haber, 2003). Although, up to six different CBGTC loops have been identified by a recent tracing study (Foster et al., 2021), these loops can be broadly categorized into three main types based upon their functional roles; motor, cognitive, and limbic CBGTC loops (Balleine et al., 2007; Haber, 2003; Macpherson & Hikida, 2019; Yin et al., 2008). These three feedback loops receive unique patterns of cortical input that enable distinct functionality. (1) The motor loop originates in the sensorimotor cortex and projects to motor-related areas of the basal ganglia and thalamus before returning to premotor areas. (2) The cognitive loop originates in the association cortex and projects to cognitive-associated areas of the basal ganglia and thalamus before returning to the prefrontal cortex. (3) The limbic loop also originates in the association cortex and projects to limbic areas of the basal ganglia and thalamus before returning to the medial prefrontal cortex (Alexander et al., 1986; DeLong & Georgopoulos, 1981; Macpherson & Hikida, 2019).

1.1.1.1 Basal Ganglia Pathways

Basal ganglia pathways begin with the input of sensory and motor information from the cerebral cortex and thalamus into the striatum, which is the main input nucleus of the basal ganglia. Then, the striatum receives excitatory input from the cortex and inhibitory inputs from the

substantia nigra pars compacta (SNc), which contains dopaminergic neurons. within the striatum, information is processed and integrated before being transmitted to basal ganglia output nuclei including the internal segment of the globus pallidus (GPi) and the substantia nigra pars reticulata (SNr). These structures serve as the main output pathways of the basal ganglia. GPi/SNr neurons send inhibitory projections to the thalamus, which serves as a relay station for motor information between the basal ganglia and motor output regions as well as sending feedback projections to the cortex to control the initiation, suppression, and execution of movements (Albin et al., 1989; DeLong, 1990).

Within the BG, information can be sent via three distinct pathways, known as the direct, indirect, and hyperdirect pathways. The direct pathway, also referred to as the "go" pathway, comprises dopamine D1 receptor-expressing striatonigral medium spiny neurons (D1-MSNs) that co-express the peptides dynorphin, and substance P (SP) (Gerfen 1990; Surmeier et al., 1996; Castro and Bruchas, 2019). These D1-MSN send GABAergic projections that inhibit the SNr/Gpi (Milardi et al., 2019; Young & Sonne, 2019), this in turn disinhibits the thalamus to which the SNr/GPi send inhibitory projections to, and facilitates voluntary movement (DeLong, 1990; Graybiel, 2000). On the other hand, the indirect pathway, also referred to as the "no-go" pathway, comprises dopamine D2 receptor-expressing striatopallidal MSNs (D2-MSNs) co-expressing adenosine 2A receptors (A2A) and enkephalin (ENk) (Gerfen 1990; Surmeier et al., 1996; Castro and Bruchas, 2019). D2-MSNs project indirectly to the SNr/GPi via a polysynaptic pathway that includes the pallidus external segment (GPe) and subthalamic nucleus (STN) (Milardi et al., 2019; Young & Sonne, 2019). This activation of this pathway results in increased inhibition of thalamus and acts to suppress unwanted or involuntary movements (DeLong, 1990; Graybiel, 2000). The hyperdirect pathway, also referred to as the "global no-go" pathway, directly connects the cortex and STN (Nambu, 2004). This pathway plays a crucial role in the rapid initiation and suppression of movements. The balance of activity within the direct and indirect pathways is regulated by the activity of the SNc, which releases dopamine into the striatum (Albin et al., 1989). Overall, the basal ganglia functions to regulate motor activity, coordinate movement, and ensure the appropriate selection and execution of actions. Dysfunction of the basal ganglia can lead to movement disorders, such as Parkinson's disease, Huntington's disease, and dystonia (Graybiel, 2000), as well as psychiatric conditions including depression and schizophrenia (Macpherson &

Hikida, 2019) A detailed anatomical model of connectivity between BG pathways is provided in Fig 1.1

Figure 1.1

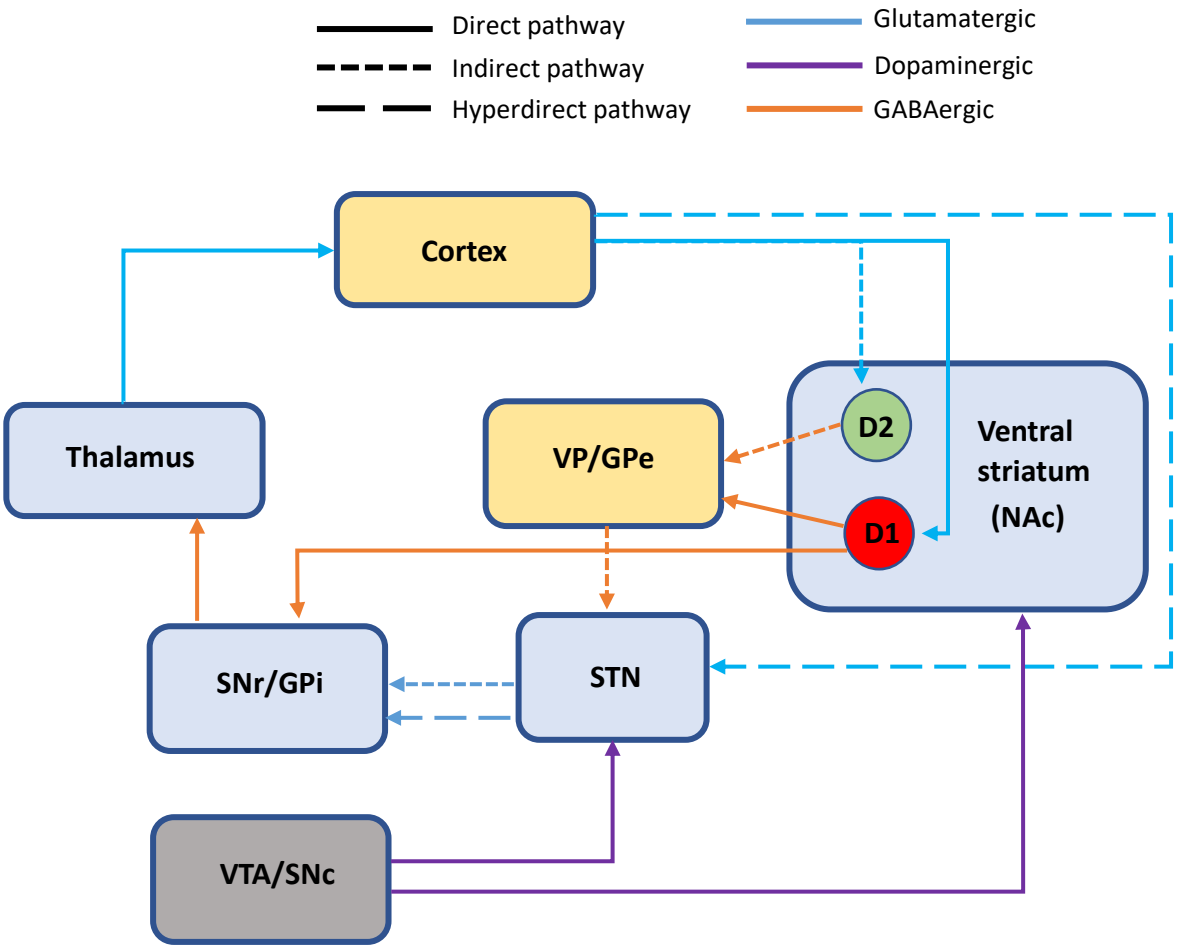

Figure 1.1 A simplified diagram of a basal ganglia circuit containing nucleus accumbens D1- and D2-MSNs. NAc, nucleus accumbens; VP, ventral pallidum; GPe, external globus pallidus; GPi, internal globus pallidus; STN, subthalamic nucleus; VTA, ventral tegmental area; SNc, substantia nigra pars compacta; SNr, substantia nigra pars reticulata.

1.2 Anatomical and Physiological Properties of the Striatum

1.2.1 The Striatum

The striatum is a crucial component of the basal ganglia that is primarily responsible for receiving and processing input from various regions of the brain related to motor control, cognition, and reward processing (Graybiel, 2000).

1.2.1.1 The Striatal Medium Spiny Neurons (MSNs)

The GABAergic inhibitory MSNs are the major output neuron type in the striatum and represent roughly 95% of all neurons (Tepper and Bolam, 2004) . These neurons are characterized by their unique morphology, electrophysiological properties, and neurotransmitter content (Surmeier et al., 2007) and can largely be divided into MSNs that express dopamine D1 receptors (D1-MSNs) and MSNs that express dopamine D2 receptors (D2-MSNs) that are present in equal proportions (Gerfen et al., 1990). D1- and D2-MSNs have distinct roles within the striatum; D1-MSNs are involved in facilitating movement initiation and reinforcement learning, while D2-MSNs are associated with inhibiting movements and aversive learning (Macpherson et al., 2014; Surmeier et al., 2007). These two neuron types are thought to be oppositely modulated by dopamine release in the striatum due to their expression of different dopamine receptors. Indeed, dopamine D1 receptors respond to phasic dopamine release to increase the activity of the neurons through Gs and Go proteins that stimulate adenylyl cyclase, elevating intracellular levels of cyclic monophosphate (cAMP), activating protein kinase A (PKA), and promoting long term potentiation (LTP) (Gerfen & Surmeier, 2011; Grace et al., 2007; Shen et al., 2008). Oppositely, dopamine D2 receptors respond to tonic dopamine to reduce the activity of the neurons through Gi and Go proteins that inhibit adenyl cyclase, decreasing intracellular levels of cAMP and PKA, and promoting long-term depression (LTD) (Gerfen & Surmeier, 2011; Kreitzer & Malenka, 2007; Shen et al., 2008).

1.2.1.2 The Striatal Interneurons

Interneurons comprise approximately 5% of all striatal neurons and can be anatomically and histochemical separated into GABAergic and cholinergic interneurons (Tepper & Bolam, 2004). GABAergic interneurons can further be subdivided into various types, including

parvalbumin (PV)-expressing fast-spiking interneurons (FSIs) and somatostatin-releasing interneurons (SOM) (Castro & Bruchas, 2019). These PV and SOM interneurons have distinct functional roles, with PV interneurons contributing to a feedforward inhibition network (Swadlow, 2003), whereas SOM interneurons control to feedback inhibition (Isaacson & Scanziani, 2011). These populations help to prevent excessive recurrent excitation (Scudder et al., 2018). SOM interneurons are also known to play a role in regulating DA release in the striatum, and have been reported to modulate DA-dependent turning behavior (Ikeda et al., 2012). Cholinergic interneurons are the main endogenous source of acetylcholine in the striatum (Castro & Bruchas, 2019; Lee et al., 2016) and play a modulatory or faciliatory role rather than a directive role on behavior by regulating DA release in the striatum (Chuhma et al., 2014; Yorgason et al., 2017).

1.2.1.3 The Striatal Structure

The striatum has segregated output projections between distinct sections of the striatum: the dorsal and ventral striatum. The dorsal striatum is composed of the caudate nucleus and the putamen which have distinct anatomical connections and are involved in motor control and cognitive processing, while the ventral striatum is composed of the nucleus accumbens (NAc) and the olfactory tubercle and is involved in reinforcement learning and motivational control of instrumental performance (Haber, 2016; Macpherson & Hikida, 2019; Yin et al., 2008).

Within the dorsal striatum, D1- and D2-MSNs differ in their projection targets. As mentioned above, in the dorsal striatum, D1-MSNs project directly to the SNr/GPi in a “direct” monosynaptic pathway, while D2-MSNs project to the GPe in an “indirect" pathway (Milardi et al., 2019; Young & Sonne, 2019). However, within the nucleus accumbens (NAc) of the ventral striatum, recent studies indicate that the coding of D1- and D2-MSNs to direct and indirect pathways, respectfully is not valid (Kupchik et al., 2015; Young & Sonne, 2019). Indeed, while D2-MSNs project exclusively to the ventral pallidum (VP), D1-MSNs project to both the SNr/VTA and VP, meaning that they could possibly contribute to both direct and indirect pathways (Kupchik et al., 2015).

1.2.1.4 The Nucleus accumbens (NAc)

The NAc is a key structure located in the basal forebrain and it is considered a part of the ventral striatum. The NAc plays a crucial role in reward, motivation, and reinforcement processes within the brain (Wise, 2004). The NAc is further divided into two primary subregions: the core and shell subregions which have distinct anatomical connections and functional roles (Groenewegen et al., 1999; Voorn et al., 2004). From the NAc core, D1-MSNs project primarily to the VP and SNr, while D2-MSNs project to the VP (Kupchik et al., 2015). Whereas, from the NAc shell, D1-MSNs project largely to the VP, VTA, and lateral hypothalamus (LH), while D2-MSNs project primarily to the VP, with minor innervation of the VTA and LH (Gibson et al., 2018; O'Connor et al., 2015). These differences in projection targets are thought to enable different functionality between these two NAc regions (discussed further below) (Ambroggi et al., 2011). Additionally, the retrograde tracing studies have demonstrated differing innervation patterns between the NAc core and shell, with the NAc core primarily receiving input from cortical and allocortical structures (Li et al., 2018; Scofield et al., 2016) that are involved in reward processing and goal-directed behavior (Scofield et al., 2016), while the NAc shell receives inputs from the lateral hypothalamus that involved in reward learning and motivation (Castro & Bruchas, 2019).

Previous studies have revealed that the NAc core is primarily involved in the processing of reward-related information that plays a role in evaluating rewards, initiating motivated behaviors, and facilitating reinforcement learning (Klawonn & Malenka, 2018; Sicre et al., 2020). The NAc core is also a critical structure for refining action selection that facilitates goal-direct behavior by inducing approach behavior toward motivationally associated stimuli (Floresco, 2015) such as food outcomes (Ambroggi et al., 2011; Floresco, 2015; Nicola, 2010). The NAc core is also known to be involved in the rewarding and reinforcing the effects of addictive substances, mediating the attribution of incentive salience to drug stimuli and controlling motivation to seek and consume drug rewards (Crespo et al., 2008; Macpherson & Hikida, 2019; Yee et al., 2011). In contrast, the shell is more closely associated with the affective and emotional aspects of natural rewards the integration of reward-related information with affective valence, and motivated behavior. The NAc shell also plays a role in refining action selection that facilitates goal-direct behavior by suppressing non-rewarded actions (Floresco, 2015). For drug rewards, the NAc shell also plays crucial role in addiction-related processes, and is known to be involved in the processing of drug-

related cues (Lobo et al., 2010), the attribution of incentive salience to drug stimuli, and the regulation of drug-seeking and drug-taking behavior (Schlosburg et al., 2013; Whitfield et al., 2015). Thus, while NAc core and shell regions show some differences in their functional roles, they both contribute to the reward, motivation, and emotional regulation in the brain

1.2.1.5. Nucleus accumbens D1- and D2-MSN roles

Canonically, NAc D1- and D2-MSNs have been reported to have different and sometimes opposing functional roles. Indeed, studies over the last decade have reported activation of D1-MSNs to be associated with reward (Hikida et al., 2010, 2013; Kravitz et al., 2012; Lobo et al., 2010), while activation of D2-MSNs to be associated with aversion (Hikida et al., 2010, 2013; Kravitz et al., 2012; Lobo et al., 2010). Interestingly, recent evidence has revealed that both NAc D1- and D2-MSNs may be able to control reward or aversion. While brief stimulation of either cell type was found to promote positive reinforcement in a real-time place preference task, prolonged stimulation promoted aversion in the same task (Soares-Cunha et al., 2020). Similarly, activation of either NAc D1- or D2-MSNs has been reported to promote instrumental self-stimulation behavior in an operant chamber test. (Cole et al., 2018). NAc D2-MSNs are also known to play an important role in controlling motivation; however, it has been unclear how these neurons mediate both aversion and motivation. A recent finding suggests that the activation of D2-MSNs projecting to the VP during reward-paired cues can increase motivation to seek the reward, wheras activation of the same neurons during the delivery of rewarding outcomes results in aversion (Soares-Cunha et al., 2022).

1.2.2 The Ventral Pallidum (VP)

The VP is a structure within the basal ganglia pathway that receives a major GABAergic input from both NAc D1-MSNs and D2-MSNs (Kupchik et al., 2015). The VP is a critical brain structure in the neural circuitry underlying reward-related behaviors (Creed et al., 2016; Smith et al., 2009), and motivation (Robinson et al., 2014). Histologically the VP has been suggested to act as a site for the ‘limbic-motor’ interface due to its closely connect with motor output regions (Mogenson et al., 1980). Indeed, Swerdlow & Koob, (1987) evidence revealed that the NAc-VP circuit links the mesoaccumbal dopamine system to motor circuitry. Within the VP, primarily

GABAergic (GABA) and glutamatergic (GLUT) neurons were found. It was observed that stimulation of VP GABA neurons can drive positive reinforcement by inhibiting VTA GABA neurons. Conversely, activation of VP GLUT neurons leads to the inhibition of reward effects through the lateral habenular (Faget et al., 2018; Tooley et al., 2018) These studies highlight the specific role of VP cell types and their projections in behavioral reinforcement. Interestingly, recent evidence has revealed that the VP is involved in processing both rewarding and aversive stimuli.

This region can be classified into ventromedial (VPvm) and dorsolateral (Vpdl) subregions which receive a projection from the NAc shell and core, respectively (Root et al., 2015). These two subregions have distinct functional roles. It is assumed that VPdl neurons have a similar function to NAc core neurons in biasing the direction of subsequent behavior towards approaching a reward (Floresco, 2015). In contrast, the VPvm has a similar function to NAc shell neurons in biasing behavior towards persisting with the current task (Floresco, 2015), and is also thought to be involved in reward prediction (Root et al., 2015).

1.2.3 The Substantia Nigra pars Reticulata (SNr)

The SNr is the major output nuclei of the basal ganglia. The SNr receives inputs from various structures within the basal ganglia, including NAc, GPe, and STN. These inputs converge onto the GABAergic neurons in the SNr, allowing it to integrate and process information from different components of the BG circuitry (Gerfen et al., 1990). The SNr sends inhibitory projections to several key targets, including the thalamus, super colliculus, and brainstem structures that are involved in motor control (Alexander et al., 1986; McHaffie et al., 2005). As such, the SNr is known to play an important role in motor control via its GABAergic afferent projection to the motor thalamic nuclei (Antal et al., 2014; Lai et al., 2021) and the sensory-motor system (Gerashchenko et al., 2006; Lai et al., 2021; Liu et al., 2020).

The SNr can be divided into two distinct subregions, the lateral (lSNr) and medial (mSNr), which receive innervation from the dorsal and ventral striatum, respectively (Aoki et al., 2019). These two subregions are known to play different functional roles in the modulation of sleep and motor activity. It has been reported that GABAergic neurons in mSNr regulate sleep, whereas PV neurons in the lSNr control motor activity (Liu et al., 2020). However, other studies have suggested

that the lSNr, rather than the mSNr, is responsible for sleep control (Gerashchenko et al., 2006; Lai et al., 2021).

A detailed anatomical model of connectivity between NAc-VP and -SNr structure involved in this study is provided in Fig 1.2

Figure 1.2

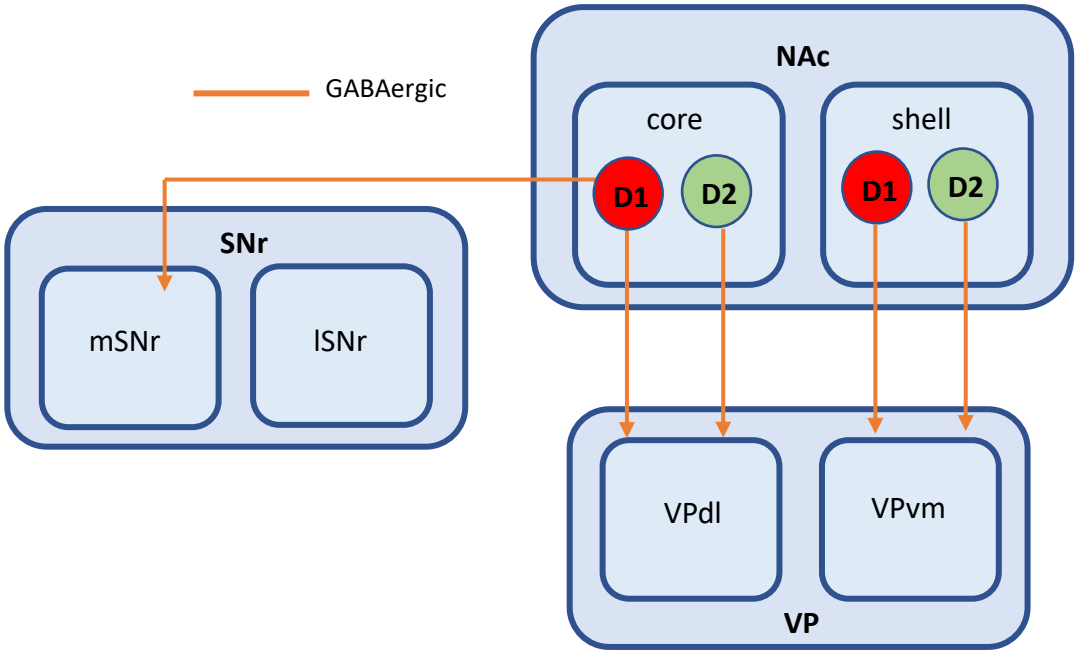

Figure 1.2 A simplified diagram of the subregion-specific NAc output pathways. NAc, nucleus accumbens; core, NAc core; shell, NAc shell; VP, ventral pallidum; VPdl, dorsolateral ventral pallidum; VPvm, ventromedial ventral pallidum; SNr, substantia nigra pars reticulata; lSNr, lateral substantia nigra pars reticulata; mSNr, medial substantia nigra pars reticulata

1.3 Optogenetics

Optogenetic technology is a combination of optics, genetics, and bioengineering to either activate or silence cellular activity through genetically encoded proteins (opsins) (Boyden et al., 2005; Deisseroth et al., 2006; Yizhar et al., 2011). This technique has emerged as a powerful method for controlling cellular activity that can precisely and non-invasively manipulate specific brain circuits and specific cell types (Tye & Deisseroth, 2012) with high-temporal resolution (Boyden et al., 2005). Optogenetics uses genetically encoded proteins called opsins to control the activity of target cells. Opsins can be categorized into two major classes: excitatory opsins and inhibitory opsins.

Excitatory opsins, also known as Channelrhodopsins (ChR), are capable of generating electrical signals in response to light. When activated by light, excitatory opsins allow the influx of positive ions, typically sodium or calcium, into the cell. This influx of ions depolarizes the cell membrane and triggers an action potential, leading to activation of the neuron and subsequent transmission of signals in neural circuits. ChR2 is a non-selective cation channel that is permeable to positively charged ions. ChRs can be divided into channelrhodopsin-1 (ChR1) and channelrhodopsin-2 (ChR2). In general, ChR2 is widely used to activate neural circuits and is maximally excited by blue light at 450-490 nm (Nagel et al., 2003; Rein & Deussing, 2012) and can provide millisecond-timescale temporal resolution (Boyden et al., 2005).

Inhibitory opsin refers to a class of light-sensitive proteins that can inhibit or suppress the activity of neurons when exposed to light. These opsins can be divided into two categories: light-driven inward chloride pumps or light-driven outward proton pumps. Following exposure to light, chloride pumps like halorhodopsin (NpHR) actively pump Cl- ions into the cell, whereas proton pumps like achaerhodopsin (Arch/ArchT), pump protons (H+) out of the cell, causing cell hyperpolarization. NpHR is maximally excited at wavelengths of approximately 589 nm, while Arch and ArchT are maximally excited at wavelengths of approximately 566 nm (Chow et al., 2010; Han et al., 2011).

In vivo, viral gene transfer by adeno-associated viral (AAV) vectors has effectively been used in rodents to deliver optogenetic constructs into genetically defined cell populations. Using Cre-dependent AAV vectors alongside transgenic mice expressing Cre in specific cell types, robust

expression can be achieved in these specific cell types (Atasoy et al., 2008). Then, laser light is delivered directly to the specific brain region for stimulation via an optic fiber which is chronically implanted in the target area (Pama et al., 2013). This allows us to investigate the effects of either silencing or increasing the activity of specific neural cells on behavior and brain function.

The use of optogenetics has various advantages when compared with classic electrical or multicomponent manipulation approaches. Using genetic targeting, optogenetic manipulation of diverse brain tissues can be performed in a cell-type-specific manner. Indeed, optogenetics has been used to precisely identify neural circuits implicated in various brain functions and diseases, including anxiety disorders, addiction, depression, and schizophrenia (Tye & Deisseroth, 2012).On the other hand, electrical manipulation acts on all neural cells in the area it is used, and therefore makes it different to separate the roles of various cell types within brain circuits (Rein & Deussing, 2012).

1.4 Aims and structure of thesis

While much is known about the functional roles of the NAc and its constituent cell types, much more is still unknown. With the creation of new bioengineering technologies including cell-type specific targeting of virus delivery and optogenetics, we are now able to precisely explore the role of specific neural circuits. In this thesis, my aim is to further elucidate the functional roles of NAc D1- and D2-MSNs in cognitive, limbic, and motor control. As such my thesis is divided into two projects, the first (Chapter 2) that describes research into the role of NAc D1- and D2-MSNs in decision-making, and the second (Chapter 3) that describes research into elucidating the roles of NAc D1-MSNs in circuits projecting to either the VP or the SNr in reinforcement and motor control.

1.4.1 Chapter 2

The aim of this research project was to explore the precise role of the NAc in decision-making. Previous studies have indicated that the NAc is a critical structure for goal-directed decision-making (Balleine, 2019; Floresco, 2015; Macpherson et al., 2021; Mannella et al., 2013), however, the roles that NAc D1- and D2-MSNs play in decision-making has been unclear. Here, a novel cue-guided cognitive-behavioral task was used to test mice's ability to make correct decisions based upon previous experience of failure (i.e. the ability to learn from its mistakes). Given that NAc D1-MSNs have been implicated in reward learning, while D2-MSNs have been implicated in aversion learning and behavioral flexibility (Hikida et al., 2010, 2013; Kravitz et al., 2012; Macpherson and Hikida, 2018; Macpherson et al., 2022; Yawata et al., 2012), it is hypothesized that D1-MSNs may be important for learning based on successful decisions (learning based on reward), while D2-MSNs may be useful for learning based on decision errors (learning based on failure).

1.4.2 Chapter 3

While NAc D1-MSNs are known to be involved reinforcement and motor control (Salgado & Kaplitt, 2015), the specific roles that D1-MSNs contained in pathways projecting to either the

VP or SNr play in these functions is still unknown. Here, cell type-specific optogenetics was used to investigate the effect of activation or inhibition of D1-MSNs projecting to the VP or SNr on reward-related behaviors as well as motor control. Given that the VP has been implicated in reward and addiction-related behaviors sensitization (Stefanik et al., 2013; Creed et al., 2016; Pardo-Garcia et al., 2019), while the SNr is known to contribute to motor control, it was hypothesized that D1-MSN projections to the VP might influence reward-related behavior and D1-MSNs projecting to the SNr might influence locomotion.

Chapter 2

Choice-based inhibition behavior is influenced by error-related signaling in nucleus accumbens D2-receptor expressing neurons

2.1 Introduction

Choice behavior can be influenced not only by strategies focused on achieving desirable outcomes, but also by strategies aimed at avoiding undesirable outcomes. In situations where the appropriate response to achieve desired outcomes is unclear or ambiguous, previous experiences of failure can serve as a guide to inhibit inappropriate responses. The importance of negative outcomes in influencing behavioral inhibition has been recognized, from Thorndike's (1927) law of effect to more contemporary concepts like loss aversion in behavioral economics (Kahneman & Tversky, 1979; Kubanek et al., 2015; Rasmussen & Newland, 2008). However, the neural mechanisms underlying the utilization of inhibition-based strategies for decision-making are still not fully understood, as existing studies have predominantly focused on investigating behaviors leading directly to rewarding outcomes (Horner et al., 2013; Iino et al., 2020; Xiong et al., 2015).

Within a signaling loop involving the limbic cortico-basal ganglia-thalamo-cortical circuitry, the nucleus accumbens (NAc), particularly the NAc core subregion, is believed to play a crucial role in decision-making (Balleine, 2019; Floresco, 2015; Macpherson et al., 2021; Mannella et al., 2013). It achieves this by connecting information about outcome values with information relevant to goal selection. The principal neuronal population in the NAc, known as medium spiny neurons (MSN), can be roughly divided into two equal subpopulations: dopamine D1 receptor-expressing MSNs (D1-MSNs), which predominantly send their projections to the ventral pallidum (VP) and substantia nigra pars reticulata (SNr), while dopamine D2 receptor-expressing MSNs (D2-MSNs) primarily project to the VP (Kupchik et al., 2015; Lu et al., 1997). While previous studies have demonstrated the involvement of NAc D1-MSNs in reward-related learning and D2-MSNs in aversion-related learning and behavioral flexibility, their specific role in inhibiting behavioral responses is less clear (Hikida et al., 2010; Soares-Cunha et al., 2016; Yawata et al., 2012).

To examine and quantify the capacity for inhibition-based decision-making, a visual discrimination-based cue-guided inhibition learning (VD-Inhibit) task was designed for mice. In

this task, mice were needed to suppress a touch response when presented with a visual cue related to the absence of a reward. Alternatively, they had to respond to a random cue that was no previous association with any outcome to obtain a liquid reward. Time-specific optogenetic suppression of NAc D1-MSNs and D2-MSNs during the specific time windows of the task was used to determine whether inactivating these two subpopulations would impair the utilization of inhibition-based behavioral strategies.

2.2 Material and Methods

2.2.1 Animals

Experiments were conducted using male D1-Cre (FK150Gsat) and A2a-Cre (2MDkde) transgenic mice, aged 8-12 weeks old, on a C57BL/6 background, as well as their wildtype counterparts. Mice were housed in groups of 2-3 and kept on a 12-h light/dark cycle, with lights on at 8:00 a.m. The temperature was maintained at 24 ± 2 ºC, and the humidity was kept at 50 ± 5%. Behavioral experiments were performed during the light period. Throughout the study, mice had access to water and standard lab chow *ad libitum*, except during touchscreen operant chamber experiments when they were food restricted to maintain their motivation to instrumentally respond. All animal experiments conformed to the guidelines of the National Institutes of Health experimental procedures and were approved by the ethical committee of the Institute for Protein Research at Osaka University.

A2a-Cre mice were used to target D2-MSNs because A2a receptors are selectively expressed on D2-MSNs within the striatum, while D2 receptors are expressed on other cell types including cholinergic interneurons (Alcantara et al., 2003; Svenningsson et al., 1997).

2.2.2 Stereotaxic Virus Injection and optical Cannula Implantation

After administering anesthesia (using an i.p. injection of 90 mg/kg Ketamine and 20 mg/kg Xylazine), mice were placed in a stereotaxic apparatus. A midline incision was made on the scalp, followed by creating a craniotomy using a dental drill. The injections were performed bilaterally into the NAc core of D1-Cre and A2a-Cre mice, targeting specific coordinates (Bregma coordinates: anterior/posterior, +1.2 mm; medial/lateral, ± 1.25 mm; dorsal/ventral, -3.50 mm). Adeno-associated virus (AAV) expressing archaerhodopsin (ArchT) under a FLEX cre-switch promotor (AAV5-CAG-FLEX-ArchT3.0-tdTomato; Addgene ID: 28305) was injected at concentrations of 1.3 x 10^{13} virus molecules/ml. As a control, an optically-inactive virus (AAV5-EF1a-DIO-EYFP; Addgene ID: 27056) was injected at the same concentration. The injections were carried out using graduated pipettes with a tip diameter of 10-15 μm, and the injection rate was 100 nl/min, with each site receiving 400 nl of the virus. To allow for optogenetic experiments,

chronically implantable optic fibers (200-µm core 0.37 N.A., Thorlabs, Newton, NJ, USA) were bilaterally implant above the same region as the virus injection (Bregma coordinates: anterior/posterior, +1.2 mm; medial/lateral, ± 1.30 mm; dorsal/ventral, -3.20 mm). Additionally, three skull screws were implanted 1 mm into the skull surrounding the optic fibers, and the whole skull was secured using dental cement.

In this chapter, D1- and A2a-expressing ArchT or EYFP mice, the continuous LED stimulation at 550 nm light, 1-3 mW LED was used.

2.2.3 Behavioral Experiments

2.2.3.1 Apparatus

The training and testing sessions were conducted within a Bussey-Saksida touchscreen chamber (Lafayette Instruments, IN, USA). In front of the touchscreen, a black plastic mask with two windows (70 × 75 mm 2 spaced, 5 mm apart, 16 mm above the floor) was positioned. To control the operant system and collect data, ABET II and Whisker Server software (Lafayette Instruments, IN, USA) were utilized. Additionally, laser delivery within the chamber was controlled using Radiant v2 software (Plexon Inc, TX, USA).

2.2.3.2 Pretraining.

Mice were subjected to food restricted, limiting their intake to 85-90% of their free-feeding weight before the experiment. Prior to the main experiment, a pretraining phase was carried out with slight modifications to a previously described method (Horner et al., 2013). In the initial Habituation sessions, mice were familiarized with the chamber over three consecutive daily sessions lasting, each lasting 40 minutes. During these sessions, a small amount of diluted condensed milk (7 µl, Morinaga Milk, Tokyo, Japan) was dispensed into the reward magazine every 10 seconds. Moving on to the subsequent Must initiate session, one out of 51 random visual stimuli was presented in one of the two windows. After displaying the stimulus for 30 seconds, a milk reward (20 µl) was delivered along with a tone (3 kHz), and the inside of the magazine was illuminated. Once the mice collected the reward, the magazine light turned off, and the next trial

began with a 20-second intertrial interval (ITI) (60 trials completed in 60 minutes). In the next Must touch session, stimuli were randomly presented in one of the two windows, and the mice were had to touch the stimulus to receive a reward (60 trials completed in 60 minutes). The final phase of the pretraining, punish incorrect sessions, involved a punishment for incorrect responses. If the mice touched an empty window, they were subjected to a 5-second time-out period where the house light was illuminated. Mice had to achieve a criterion of >75% correct trials within 35 minutes for two consecutive days to proceed to the basic training phase.

Typically, mice took approximately one day to complete the "Must initiate" session, another day for the "Must touch" session, and approximately 2-4 days to complete the "Punish incorrect" session. These completion times align with previous studies that used a similar pretraining protocol.

2.2.3.3 Basic training.

The mice underwent testing sessions 5-6 days per week, with each session consisting of 60 trials or lasting up to 60 minutes. To initiate each trial, the mice nose-poked in the reward magazine. Visual cues were displayed until the mice responded by touching one of the two windows. In the VD-Attend task, the touchscreen showed two visual cues: a marble and a random image. The random image was selected in a pseudorandom menner from a pool of 51 images. When the mouse correctly responded to the visual cue (marble), a milk reward (7 µl) was delivered along with a tone (3 kHz), and the magazine was illuminated. After the mouse collected the reward, the magazine light turned off, and the next trial began after a 20-second intertrial interval (ITI). However, in the case of an incorrect response to the visual cue (random image), mice experienced a 5-second time-out punishment with the house light turned on. In the VD-inhibit task, the touchscreen presented two visual cues: a flag and a random image. If the mouse correctly responded to the visual cue (random image), it received a milk reward (7 µl) was delivered along with a tone (3 kHz), and the magazine was illuminated. On the other hand, if the mouse responded to the incorrect visual cue (flag), it received a 5-second time-out punishment with the house light turned on. A response to a random image was considered a correct response, while a response to the "Flag" visual cue was considered as an incorrect response. Once the mice achieved a criterion

of over 80% accuracy for two consecutive days, they proceeded to undergo cable habituation for either optogenetic or miniature microscope imaging experiments.

In the optogenetic suppression experiments, once the mice showed stable performance with an accuracy of over 80% for two consecutive days while the fiber optic cables were attached, they proceeded to undergo optogenetic stimulation test sessions. During these session, continuous LED stimulation at 1-3 mW, utilizing a 550 nm LED attached to a rotary joint (Plexon, TX, USA) was applied at different periods of the test session: during the inter-trial interval (ITI) (-5 to 0 seconds from trial onset), Cue presentation (from trial initiation to the response), or Outcome period (0-5 seconds after a response). Each type of stimulation (ITI, Cue, or Outcome) was performed in different sessions on consecutive days, using a pseudo-randomized order based on a Latin-square design. Additionally, LED stimulation was applied to only in 50% of the trials, in a pseudo-randomized manner, ensuring that there no more than three consecutive trials of the same type (LED on/off) occurred. Both VD-Inhibit and VD-Attend tasks were conducted on the same mice, with VD-Inhibit always conducted before VD-Attend.

In all behavioral experiments, we monitored several parameters including the percentage of correct responses (calculated as the number of correct trials divided by the sum of correct and incorrect trials, expressed as a percentage). Additionally, we recorded the latencies for correct responses, incorrect responses, and reward collection.

2.2.4 Histological analysis

Following the completion of behavioral experiments, mice were anesthetized with 90 mg/kg Ketamine and 20 mg/kg Xylazine and then transcardially perfused. First, they were perfused with 0.1 M phosphate-buffered saline (PBS) for 2 minutes, followed by 4% paraformaldehyde (PFA) dissolved in 0.1 M Na_2HPO_4/NaH_2PO_4 buffer (PH 7.5) in PBS for 5 minutes at a flow rate 10 ml/min. The brains were subsequently removed and postfixed for 2 days in 4% PFA. Then the brains were placed in sucrose solutions with concentrations of 7.5%, 15%, and 30% in PBS, and kept at 4°C until the brain tissue sank to the bottom at each stage. The brains were fully frozen by embedded them in Optimal Cutting Temperature (O.C.T.) compound, which provides support during cryostat sectioning. Next, the brain tissue attached to a circular cryostat block was sectioned into slices that were 40-μm-thick, with the cryostat set at -17 to -20°C. The Coronal brain slices

(40 μm) were stored in PBS solution at 4°C. For immunohistochemical staining, each brain section was treated with a blocking solution (5% Bovine serum albumin in PBS) for 1 h at room temperature, followed by three times PBS washes. After rinsing in PBS, the slices were incubated overnight at 4°C with the anti-red fluorescent protein rabbit IgG primary antibody (1:1000; ABCAM, Cambridge, UK) in 1x PBS with 0.3% Triton-X (Nacalai Tesque Inc, Kyoto, Japan) (PBST). Subsequently, all brain sections were washed three times for 10 min in PBS and stained with Alexa Fluor 568 goat anti-rabbit IgG secondary antibody (1:500; Thermo Fisher Scientific, MA, USA) in 1x PBST for 1 hour at room temperature. Following three times 10-minutes washes in 1x PBS, the sections were mounted using Fluoroshield mounting medium containing DAPI (Abcam, Cambridge, UK) and then observed using a KEYENCE BZ-X800E All-in-one Fluorescence Microscope (Keyence, Osaka, Japan).

2.2.5 Statistical Analysis

Experimental data were represented as the mean ± SEM using Prism v8.0 software (GraphPad Software Inc, CA, USA). Behavioral performances were analyzed through two-way repeated measures ANOVAs with factors such as virus (ArchT, EYFP) and laser stimulation (OFF vs ON), or history (After Correct, After Error) and laser stimulation (OFF vs ON). *Post hoc* Sidak's multiple comparisons tests were conducted in cases where significant main effects or interactions were observed in the ANOVA ($p < 0.05$). The Geisser-Greenhouse correction was applied when non-normal distribution was observed. ± SEM, *$p<0.05$ was considered to be significant.

2.3 **Results**

2.3.1 Inhibition-based decision-making is impaired by optogenetic inhibition of NAc D2-MSNs during the outcome phase of error trials

To test whether inactivation of D1- and D2-MSNs impairs the utilization of inhibition-based behavioral strategies, I performed optogenetic inhibition of D1-Cre and A2a-Cre transgenic mice that had been microinjected with a Cre-dependent archaerhodopsin (ArchT) (AAV5-CAG-FLEX-ArchT3.0-tdTomato) or EYFP control virus (AAV5-Ef1a-DIO-EYFP), then bilaterally implanted optic fibers directly above the NAc core (Fig1,2; D1-Cre ArchT, n=9 , D1-Cre EYFP, n=8 , A2a-Cre ArchT, n=10 , A2a-Cre EYFP, n=9). A new task, known as the inhibition-based visual discrimination task (VD-Inhibit), was developed by modifying a touchscreen-based visual discrimination task to evaluate the mice's ability for inhibition-based choice behavior. In this task, mice used visual cues to determine which of the two touchscreen response windows should be inhibited in order to receive a liquid reward by responding at the alternate window.

At the start of each trial, a visual cue appeared in both response windows (Fig. 3). After trial initiation, a visual cue was presented in each of the two response windows. One visual cue (correct cue) was randomly changed with each trial, offering 51 possible images, and resulted in the delivery of a liquid reward (7 µl condensed milk at the reward magazine) when the mouse responded by touching the correct cue. On the other hand, the other visual cue (incorrect cue) remained the same throughout all trials and resulted in no reward, followed by a 5-second time-out, when the mouse responded by touching the incorrect cue. Importantly, the randomization of the correct cue prevented the mice from forming an association between the cue and the outcome. Therefore, the mice had to rely on the cue-outcome association related to the incorrect cue to guide their behavior effectively. This required them to inhibit the known visual cue and respond by touching the unknown visual cue to receive the reward.

After the mice achieved the required performance levels on the VD-Inhibit task (≥80% correct on two consecutive days or ≥75% correct on three consecutive days), laser stimulation was conducted to suppress NAc activity during three distinct time periods of the task (ITI period; the last 5 seconds of the ITI, Cue period; from the trial initiation to the response, Outcome period; 5 seconds after the response). These stimulations were conducted in separate sessions on consecutive

days, following a pseudo-randomized order (Fig 4). In each test session, LED stimulation was applied in a pseudo-random order, ensuring that no more than three consecutive trials of the same trial time occured, and was used in 50% of the trials. Additionally, as previous studies have suggested that NAc D2-MSNs play a crucial role in behavior modification following reward omission, I investigated whether suppression of activity affected performance in trials immediately following correct or error responses (Nonomura et al., 2018; Tai et al., 2012; Tsutsui-Kimura et al., 2017; Yawata et al., 2012). The results indicated that optogenetic inhibition of D1-MSNs during outcome period did not affect performance on the VD-Inhibit task (Fig 5C). However, optogenetic inhibition of D1-MSNs during ITI period impaired performance on trials after the incorrect response (Fig 5A: significant laser x history interaction: $F_{(1,14)} = 5.725$, $p<0.05$), while inhibition during the Cue period improved performance on the trial after the incorrect response (Fig 5B: significant laser x history interaction: $F_{(1,12)} = 29.45$, $p<0.001$). On the contrary, performance on the VD-Inhibit task was unaffected by optogenetic inhibition of D2-MSNs during ITI and Cue periods (Fig 5G,H), but optogenetic inhibition of D2-MSNs during the Outcome period reduced performance on trials immediately after a response error in the VD-Inhibit task (Fig 5I: significant main effect of virus: $F_{(1,18)} = 15.84$, $p<0.001$). Mice expressing EYFP in D1-MSNs (Fig 5D-F) or D2-MSNs (Fig 5J-L) showed no behavioral changes as a result of LED stimulation. In addition, indicators of motivation such as response latencies (Fig 6) and the number of rewards gained (Fig 7) did not change in response to LED stimulation throughout any of the time windows (ITI, Cue, Outcome). These findings demonstrate that suppression of NAc D2-MSNs is able to impair inhibition-based decision-making by blocking error-signaling during the outcome period of error trials.

2.3.2 Stimulation of following in response errors of D2-MSNs does not affect performance for attendance-based choice behavior

To investigate whether the observed post-error outcome-selective contribution of D2-MSNs in the VD-Inhibit task is specific to tasks guided by response inhibition or occurs in a task-independent manner, I performed the same optogenetic protocol during the performance of an attendance-based decision-making (VD-Attend) task. This task is a more classical reward learning paradigm where a consistent visual cue indicated the rewarded response window that should be

attended to, while a randomly-assigned visual cue indicated an unrewarded response window (Fig 8). Similar to the previous experiment, these tests were conducted on animals that had already reached the performance criterion, achieving at least 80% accuracy on two consecutive days or at least 75% accuracy on three consecutive days. The results revealed that optogenetic inactivation of NAc D1- or D2-MSNs during the ITI, Cue, or Outcome periods did not affect performance in trials immediately following either correct or error trials (Fig 9). These findings suggest that the stimulation of NAc D2-MSNs after the Outcome period of response errors plays a role in choice behavior in a context-dependent manner and is not necessary for effective performance of attendance-based choice behavior.

Figure 1.

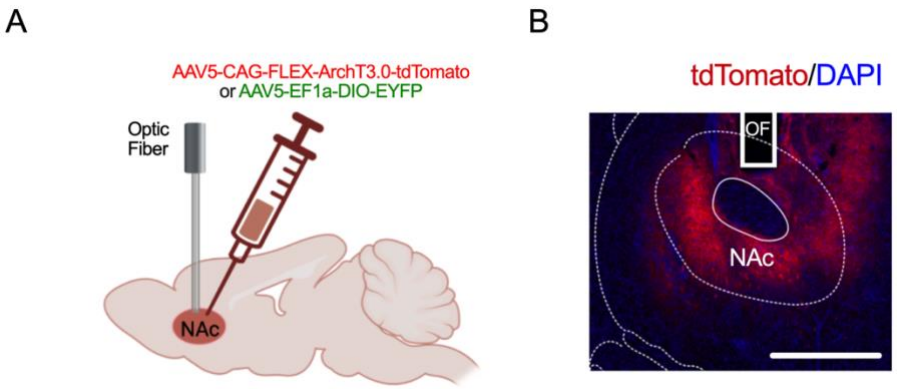

Fig 1. Histology of virus expression and fiber implantations site. (A) The diagram illustrates the locations of viral infusion and optic fiber implantation in the NAc of D1-Cre and A2a-Cre mice. (B) Representative coronal brain section showing the expression of ArchT tagged with tdTomato fluorescent protein along with optic fibers (OF) in the NAc; tdTomato is shown in red, and DAPI in blue, with a scale bar of 500 μm.

Figure 2.

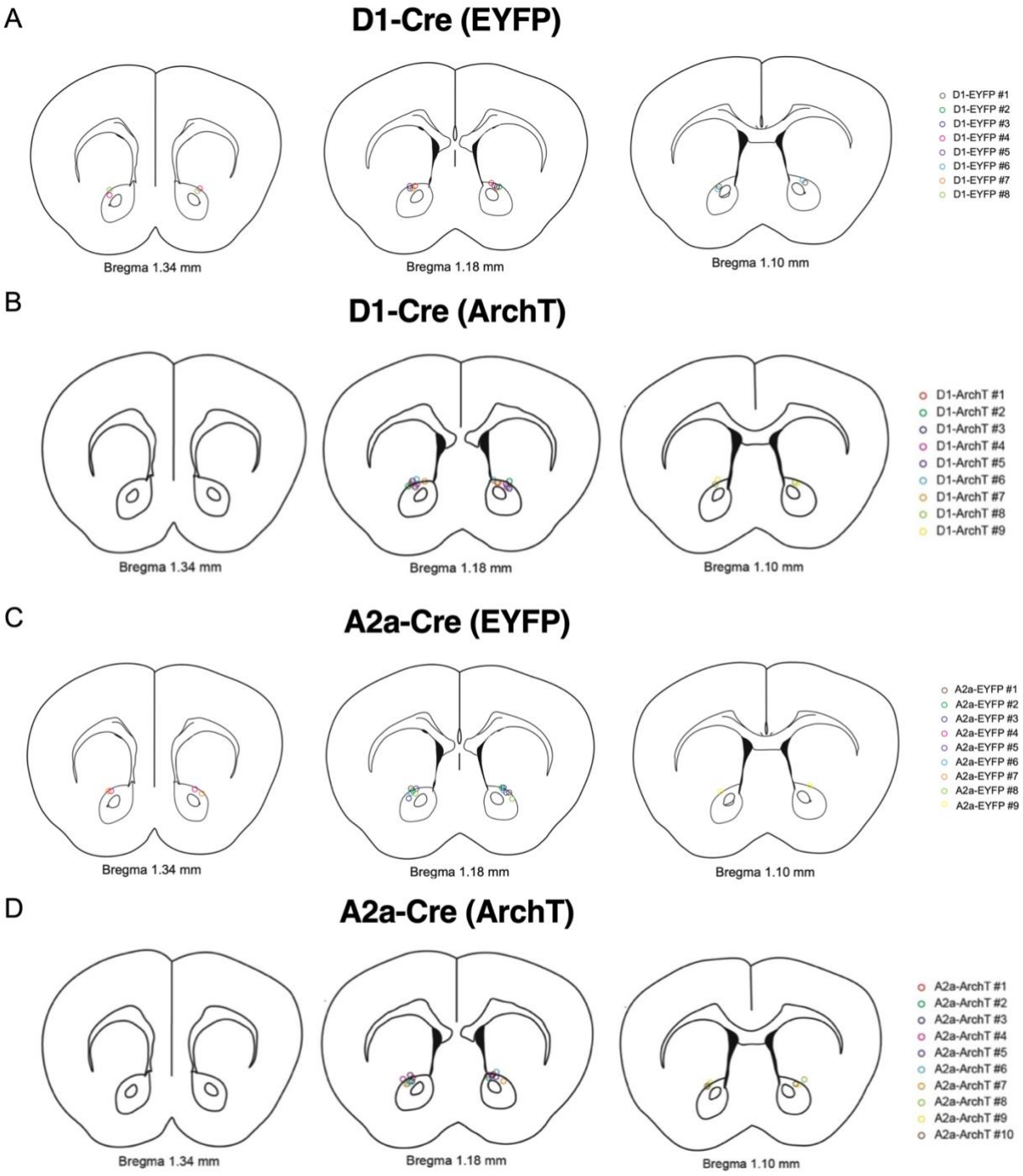

Fig 2. Optic fiber placements (A-B) Representative coronal brain sections of optic fiber placements in the NAc at three different anterior-posterior coordinates from the Bregma at +1.34 mm, +1.18 mm, and +1.10 mm of D1-Cre mice expressing (A) EYFP (n=8) and (B) ArchT (n=9).

(C-D) Representative coronal brain sections of optic fiber placements in the NAc at three different anterior-posterior coordinates from the Bregma at +1.34 mm, +1.18 mm, and +1.10 mm of A2a-Cre mice expressing (C) EYFP (n=9) and (D) ArchT (n=10).

Figure 3.

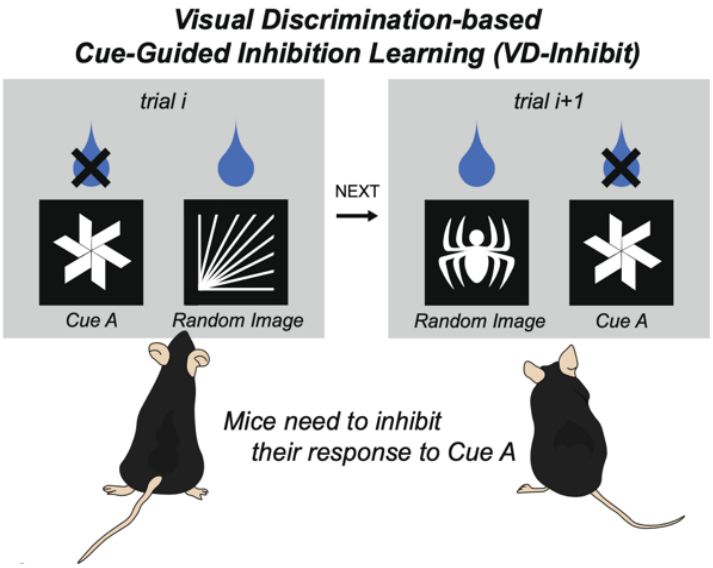

Figure 3. The experiment design of the visual discrimination-based cue-guided inhibition learning (VD-Inhibit) task consisted of two different visual cues presented on either the left or right touch panel. Cue A (Flag) served as a consistent image throughout all sessions and was associated with punishment following a response to this cue. A random image was selected from 51 possible images and associated with milk reward delivery following a response to this cue.

Figure 4.

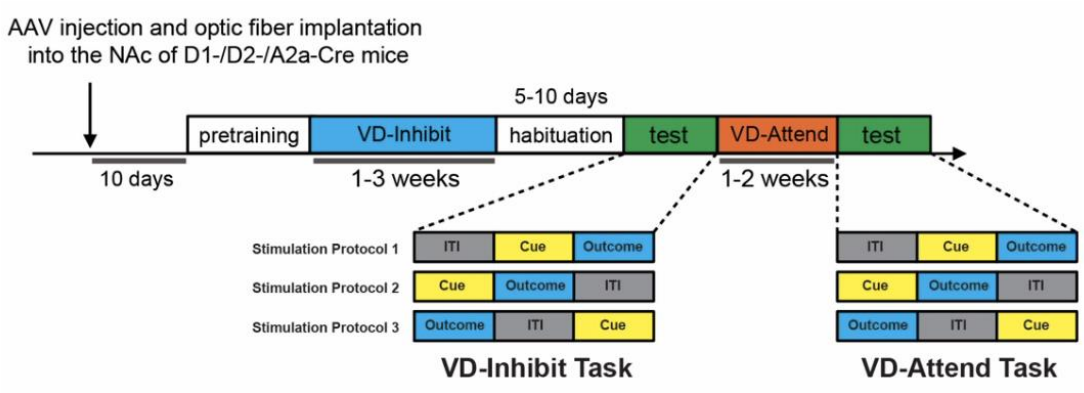

Figure 4. Experimental timeline. VD-Inhibit and VD-attend are two different tasks, as mentioned in the method section. During the test session (highlighted in green), the stimulation protocols were pseudo-randomized based on the Latin-square design. Visual discrimination-based cue-guided inhibition learning; VD-Inhibit, Visual discrimination-based cue-guided attendance learning; VD-Attend; Inter-trial interval; ITI.

Figure 5.

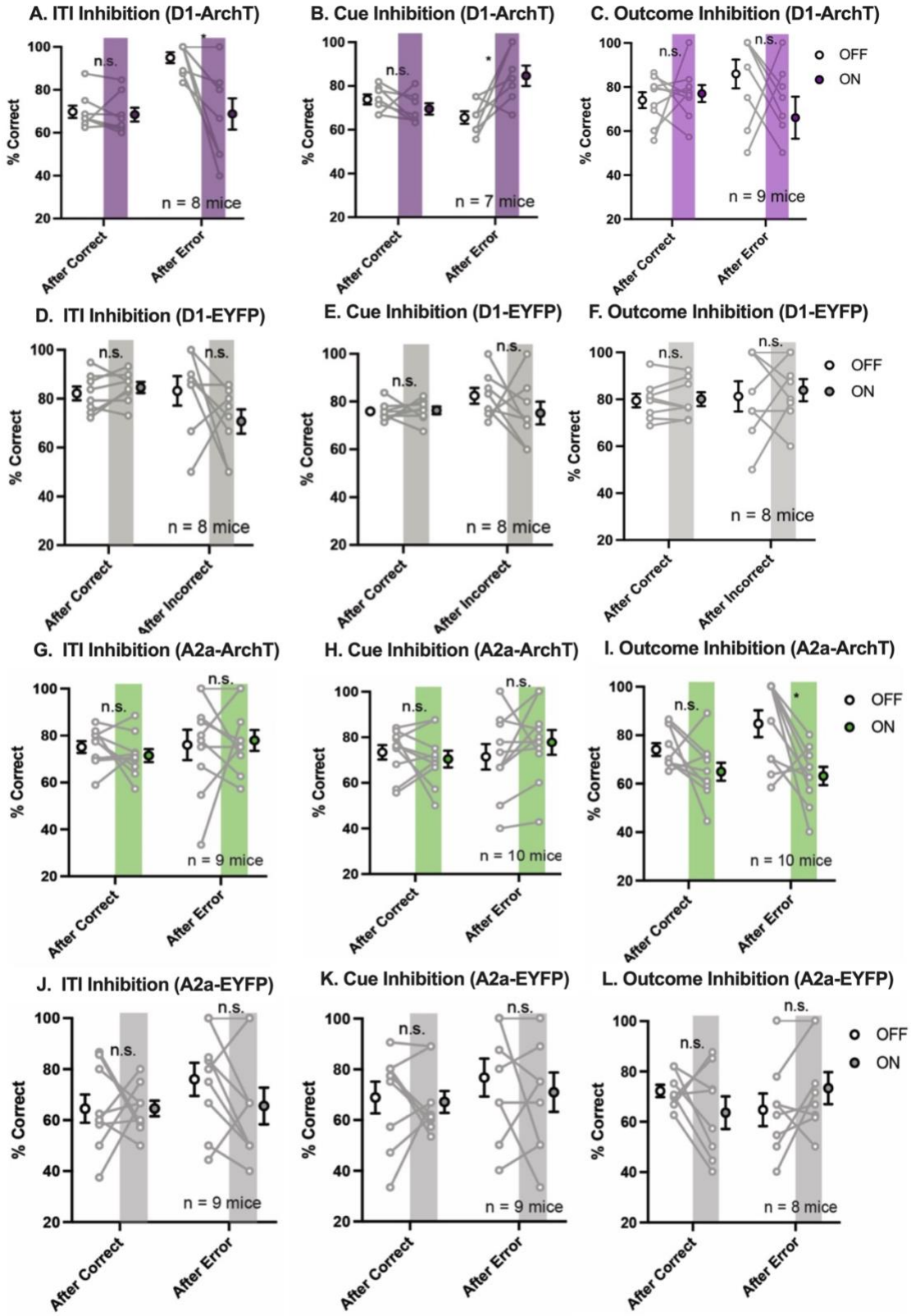
A. ITI Inhibition (D1-ArchT)
B. Cue Inhibition (D1-ArchT)
C. Outcome Inhibition (D1-ArchT)
D. ITI Inhibition (D1-EYFP)
E. Cue Inhibition (D1-EYFP)
F. Outcome Inhibition (D1-EYFP)
G. ITI Inhibition (A2a-ArchT)
H. Cue Inhibition (A2a-ArchT)
I. Outcome Inhibition (A2a-ArchT)
J. ITI Inhibition (A2a-EYFP)
K. Cue Inhibition (A2a-EYFP)
L. Outcome Inhibition (A2a-EYFP)
% Correct
n.s.
*
OFF
ON
n = 8 mice
n = 7 mice
n = 9 mice
n = 10 mice
After Correct
After Error
After Incorrect

Fig 5. Activation of D2-MSNs after response errors is necessary for inhibition-based decision-making. All results were collected from the percentage of corrections in the trials following a correct choice and trials following respond an incorrect choice during laser ON and OFF. The shaded areas represent the optogenetic suppressing results during inter-trial interval (ITI), cue or outcome period. (A-C) Optogenetic suppression of NAc D1-MSNs (D1-ArchT) during the ITI (A) (Two-way RM-ANOVA; After Correct, p =0.8655; After Error, *p = 0.0195), Cue (B) (Two-way RM-ANOVA; After Correct, p =0.4624; After Error, *p = 0.0487), and Outcome (C) periods of correct or error trials. (D-F) Laser delivery during ITI (D), Cue, (E), and Outcome (F) periods in control mice expressing EYFP in D1-MSNs (D1-EYFP). (G-I) Optogenetic suppression of NAc D2-MSNs (A2a-ArchT) during the ITI (G), Cue (H), and Outcome (I) periods of correct or error trials (Two-way RM-ANOVA; After Correct, p =0.2765; After Error, *p = 0.0257). (J-L) Laser delivery during ITI (J), Cue, (K), and Outcome (L) periods in control mice expressing EYFP in D2-MSNs (A2a-EYFP). Data represent the mean ± SEM, *post hoc* Sidak comparisons were performed with *p<0.05 indicating statistical significance.

Figure 6.

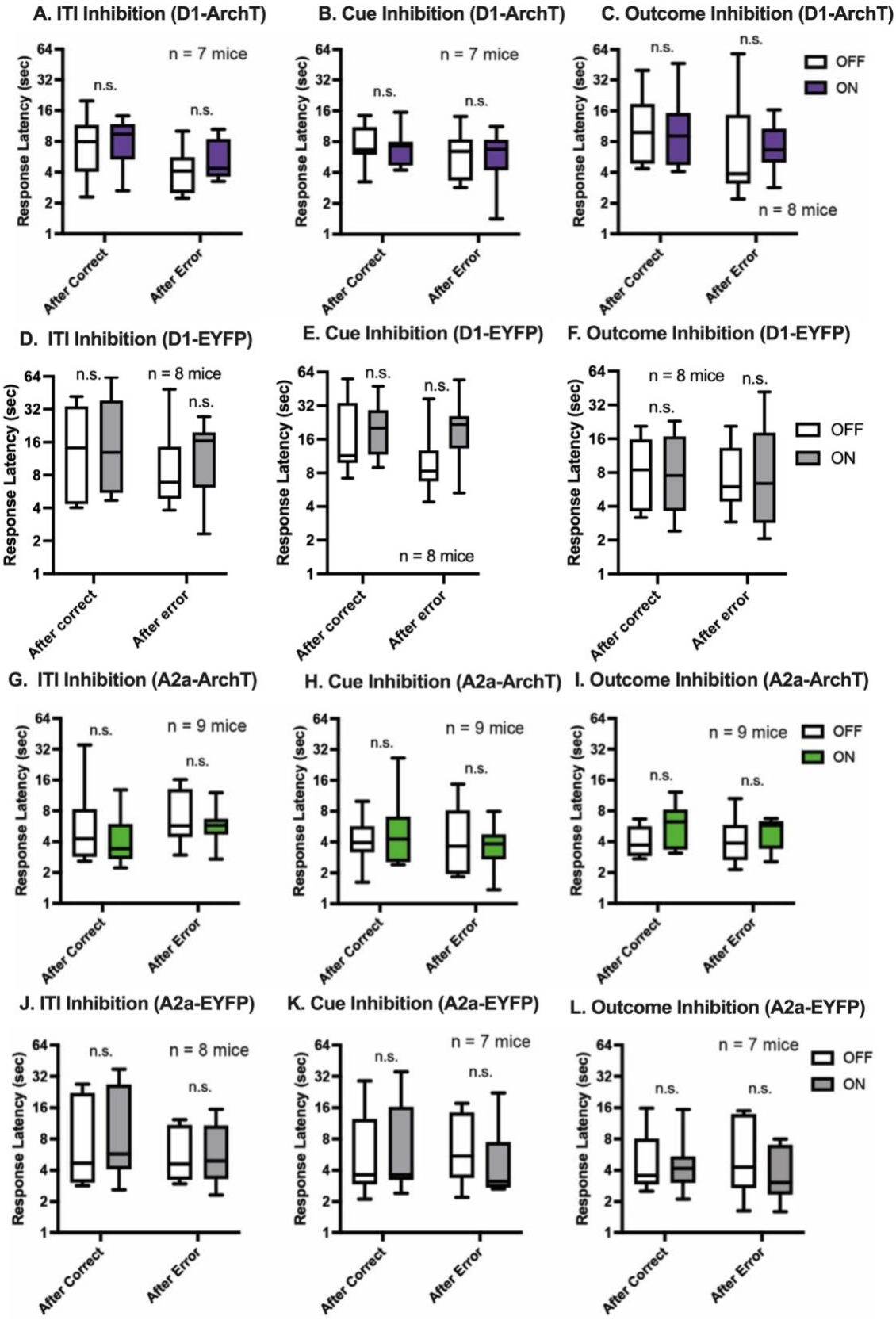
A. ITI Inhibition (D1-ArchT)
B. Cue Inhibition (D1-ArchT)
C. Outcome Inhibition (D1-ArchT)
D. ITI Inhibition (D1-EYFP)
E. Cue Inhibition (D1-EYFP)
F. Outcome Inhibition (D1-EYFP)
G. ITI Inhibition (A2a-ArchT)
H. Cue Inhibition (A2a-ArchT)
I. Outcome Inhibition (A2a-ArchT)
J. ITI Inhibition (A2a-EYFP)
K. Cue Inhibition (A2a-EYFP)
L. Outcome Inhibition (A2a-EYFP)
Response Latency (sec)
64
32
16
8
4
2
1
n.s.
n = 7 mice
n = 8 mice
n = 9 mice
OFF
ON
After Correct
After Error
After correct
After error

Fig 6. The response latencies were unaffected by optogenetic suppression of D1- and D2-MSNs. All results were collected from the latencies for correct and incorrect response (in second) in the trials following a correct choice and trials following respond an incorrect choice during laser ON and OFF (A-C) Optogenetic inhibition of NAc D1-MSNs (D1-ArchT) during the ITI (A), Cue (B), or Outcome (C) did not affect the response latency. (D-F) Laser delivery during ITI (D), Cue, (E), and Outcome (F) periods in control mice expressing EYFP in D1-MSNs (D1-EYFP). (G-I) Optogenetic inhibition of NAc D2-MSNs (A2a-ArchT) during the ITI (G), Cue (H), or Outcome (I) did not affect the response latency. (J-L) Laser delivery during ITI (J), Cue, (K), and Outcome (L) periods in control mice expressing EYFP did not affect the response latency.

Figure 7.

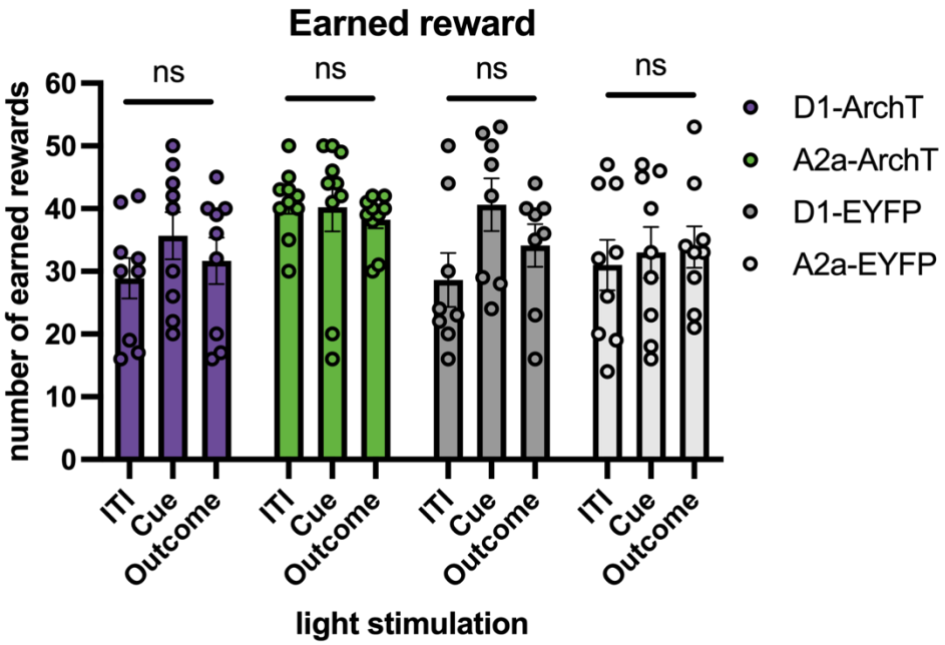

Fig 7. Optogenetic inactivation of D1- and D2-MSNs did not affect the number of earned rewards. All results were collected form the total number of reward collection during optogenetic suppression during ITI, cue, or outcome period of D1- and A2a-Cre mice expressing ArchT or EYFP.

Figure 8.

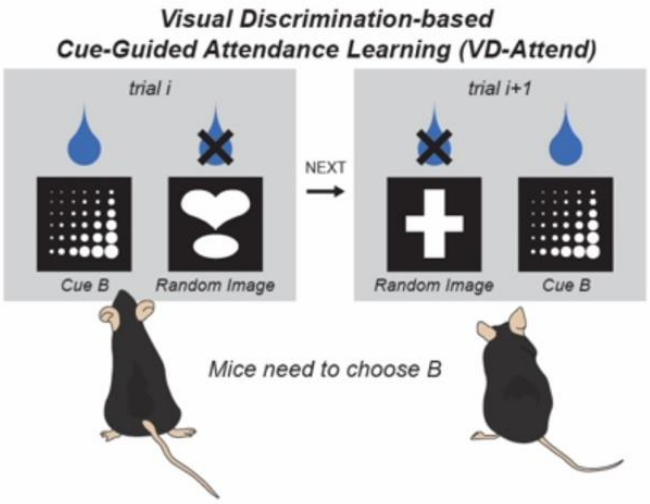

Figure 8. The experiment design of visual discrimination-based cue-guided attendance learning (VD-Attend) task consisted of two different visual cues presented on either the left or right touch panel. Cue B (Marble) served as a consistent image throughout all sessions and was associated with milk reward delivery following a response to this cue. A random image was selected from 51 possible images and associated with punishment following a response to this cue.

Figure 9.

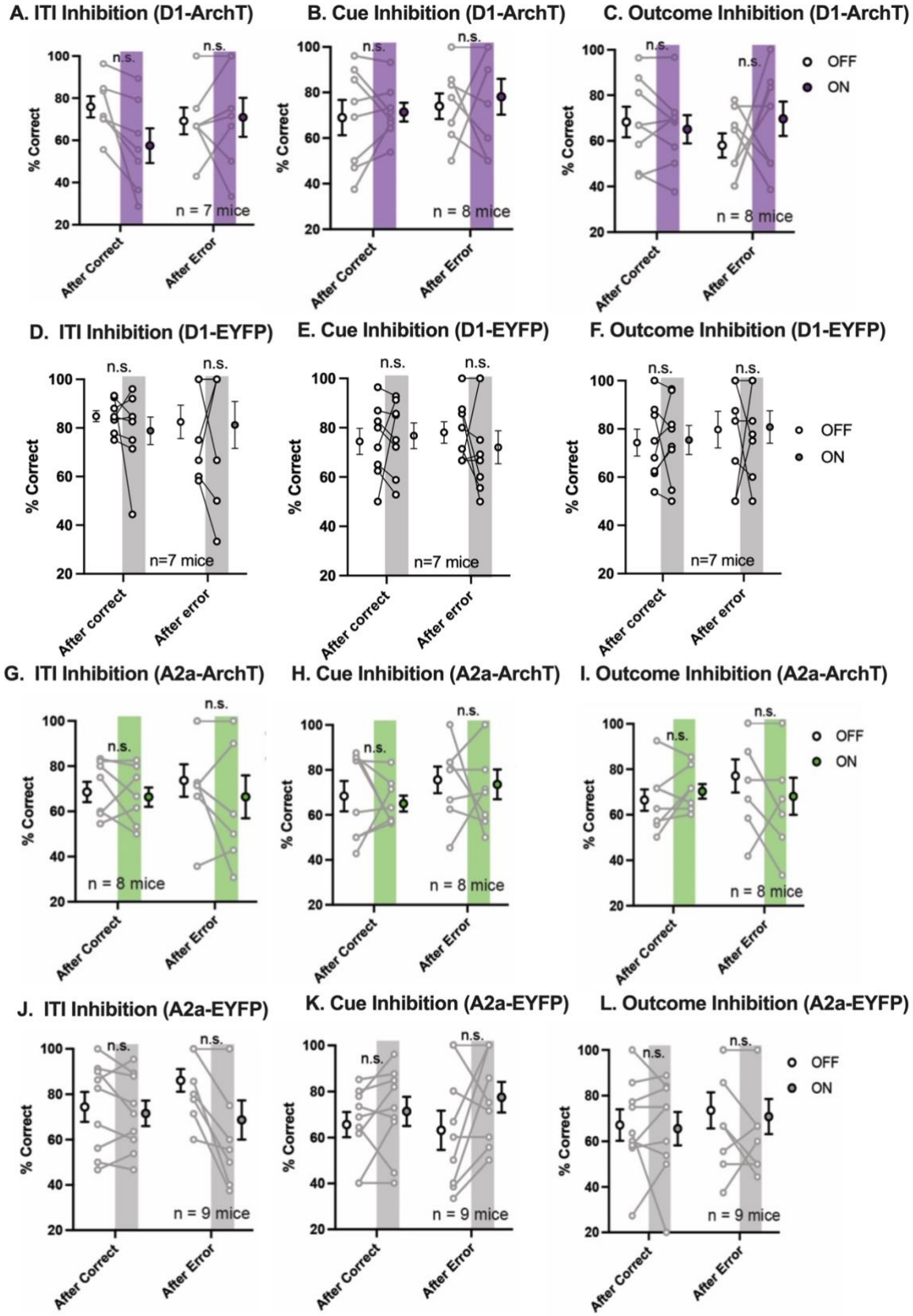
A. ITI Inhibition (D1-ArchT)
B. Cue Inhibition (D1-ArchT)
C. Outcome Inhibition (D1-ArchT)
D. ITI Inhibition (D1-EYFP)
E. Cue Inhibition (D1-EYFP)
F. Outcome Inhibition (D1-EYFP)
G. ITI Inhibition (A2a-ArchT)
H. Cue Inhibition (A2a-ArchT)
I. Outcome Inhibition (A2a-ArchT)
J. ITI Inhibition (A2a-EYFP)
K. Cue Inhibition (A2a-EYFP)
L. Outcome Inhibition (A2a-EYFP)
% Correct
n.s.
OFF
ON
n = 7 mice
n = 8 mice
n = 9 mice
n=7 mice
After Correct
After Error
After correct
After error

Fig 9. Attendance-based decision-making is not affected by NAc D1- or D2-MSN inhibition during ITI, Cue, or Outcome periods. All results were collected from the percentage of corrections in the trials following a correct choice and trials following respond an incorrect choice during laser ON and OFF. The shaded areas represent the optogenetic suppressing results during inter-trial interval (ITI), cue or outcome period. (A-C) Optogenetic suppression of NAc D1-MSNs (D1-ArchT) during the ITI (A), Cue (B), or Outcome (C) periods of correct and error trials. (D-F) Laser delivery during ITI (D), Cue, (E), and Outcome (F) periods in control mice expressing EYFP in D1-MSNs (D1-EYFP). (G-I) Optogenetic suppression of NAc D2-MSNs (A2a-ArchT) during the ITI (G), Cue (H), or Outcome (I) periods of correct and error trials. (J-L) Laser delivery during ITI (J), Cue, (K), and Outcome (L) periods in control mice expressing EYFP.

2.4 Discussion

The NAc is a crucial component of the basal ganglia and is believed to contribute to the assessment of rewards and the control of motivation by integrating glutamatergic inputs from the cerebral cortex and dopaminergic inputs from the ventral tegmental area (Gallo et al., 2018; Iino et al., 2020; Ikemoto & Panksepp, 1999; Mannella et al., 2013; Reynolds & Berridge, 2002). While the significance of the NAc has been discussed in various models of behavioral control (Balleine, 2019; Floresco, 2015; Mannella et al., 2013; Nicola, 2007; Schultz et al., 1997), its precise role, particularly the involvement of specific cell types, in choice behavior has remained unclear. In this study, a novel visual discrimination task in mice was created to examine the neural mechanisms underlying cue-guided inhibition-based decision-making. Importantly, optogenetic inhibition of NAc core D2-MSNs during the outcome period of trials in which a response error was made was sufficient to inhibit decision-making ability in the subsequent trial. The findings suggested that error-related activity in a subset of NAc D2-MSNs guides future choice behavior by steering mice away from environmental cues associated with incorrect choices.

The importance of NAc core activity during the outcome period in our study suggests that D2-MSNs may play a primary role in monitoring and updating choice behavior rather than directly selecting actions. Interestingly, previous research indicates that optogenetic stimulation of the dorsomedial striatum (DMS) during cue presentation influences action selection (Tai et al., 2012), supporting models proposing the DMS as an "actor" and the NAc as a "critic" in the process of action selection and evaluation, respectively (Bornstein & Daw, 2011; Penner & Mizumori, 2012). The NAc is a component of limbic processing loop that converges with associative/cognitive and motor processing loops associated with the DMS and DLS (dorsolateral striatum), respectively (Aoki et al., 2019; Foster et al., 2021). This circuitry allows for the integration of action value information from the limbic loop with current goal information from the associative/cognitive loop, enabling dynamic control over choice behavior, as supported by computational models (Mannella et al., 2013, 2016).

Interestingly, in this study, using optogenetic to suppress NAc D1-MSN activity during the ITI period resulted in decreased performance in the VD-Inhibit task. Conversely, Optogenetic suppression of NAc D2-MSN activity during the ITI period did not affect performance, indicating that D1- and D2-MSNs of the NAc contribute to performance of the task during different time

windows. Additionally, optogenetic suppression of D1- and D2-MSNs during ITI and outcome periods, respectively, led to reduced performance in trials following errors, suggesting that both D1- and D2-MSNs play a role in updating action value. Previous studies have highlighted the importance of D1-MSNs in associative learning and approach behavior towards conditioned stimuli (Macpherson & Hikida, 2018). Therefore, it is plausible that the optogenetic inhibition of D1-MSNs may have improved performance in trials after response errors by inhibiting approaches to visual cues related to response errors.

These behavioral findings of this study are also partially supported by recent single cell resolution in-vivo imaging data that showed that, in general, large populations of NAc core D1-MSNs were activated by the delivery of a reward during the outcome period of correct trials, while large populations of NAc core D2-MSNs were activated by reward omission during the outcome period of error trials in the VD-Inhibit task (Nishioka et al., 2023). Interestingly, while these results suggest that D1-MSNs may play an important role in signaling correct decisions, optogenetic silencing of D1-MSNs in the current study had no effect on performance of the VD-Inhibit or VD-Attend tasks. One potential explanation is that the optogenetic suppression of NAc D1-MSNs as a whole population led to a cancellation of the functional effects of these opposing populations, thereby neutralizing their impact on task performance. Another hypothesis is that alterations in the activity of NAc D1-MSNs during the task, especially in the Outcome period, could be associated with signaling of salient events rather than signaling outcome value, which when silenced does not adversely affect task performance. Previous research has indeed highlighted the significant role of the NAc core in signaling salience (Kutlu et al., 2021).

Impairments in response control have been linked to risk-taking behaviors observed in drug addiction and attention-deficit/hyperactivity disorder (Constantinople et al., 2019; Frank et al., 2004; Robbins et al., 2012; Strickland et al., 2016). A previous study demonstrated that activating D2-MSNs in the NAc reduced risky choices in rats with a propensity for risk-taking, indicating the importance of D2-MSN activity in inhibiting such behavior (Zalocusky et al., 2016). The findings of the current study largely support and expand upon these observations, revealing that NAc D2-MSN activity not only inhibits risky choices but also actions associated with negative outcomes. Moreover, the aforementioned previous study showed a decrease in the probability of making risky choices on subsequent trials following a failure to obtain a reward and the reduction of risky behavior through optogenetic activation of NAc D2-MSNs, which aligns well with the

results of the current study. Previous studies have also demonstrated that repetitive cocaine treatment leads to decrease in the frequency of miniature excitatory postsynaptic currents in D2-MSNs (Kim et al., 2011). This research aligns with theoretical model proposing that enhanced excitability of D2-MSNs promotes the strategy of inhibiting unfavorable options, whereas decreased excitability impairs the ability to inhibit such options (Frank, 2006; Frank et al., 2004; Nakanishi et al., 2014). These bidirectional effects on the strategy provide additional support for the hypothesis in the current study that activation of D2-MSNs plays a crucial role in inhibiting unfavorable options.

In conclusion, the current study's findings highlight the crucial role of NAc core D2-MSNs activation using cues to facilitate the inhibition of undesirable responses. These data suggest that controlling the neural activity of D2-MSNs in the NAc core through D2-receptor-selective drugs could potentially offer benefits for the treatment of disorders related to impaired ability for inhibitory control, such as drug addiction (Strickland et al., 2016) and attention-deficit/hyperactivity disorder (Frank et al., 2004; Robbins et al., 2012).

Chapter 3

Dual roles for nucleus accumbens core dopamine D1-expressing neurons projecting to the substantia nigra pars reticulata in limbic and motor control

3.1 Introduction

In addition to their well characterized roles in limbic control (Hikida et al., 2010; Lobo et al., 2010; Macpherson et al., 2014; Macpherson & Hikida, 2018), NAc D1- and D2-MSNs might also play a role in regulating locomotor activity. Administering D1 and D2 receptor agonists directly into the NAc has been reported to increase locomotion in rats, whereas intra-NAc infusion of D1 and D2 antagonists reduced their locomotor activity (Dreher & Jackson, 1989; Plaznik et al., 1989). Supporting these earlier findings, a more recent study using chemogenetic techniques demonstrated that stimulating NAc D1-MSNs increased wheel running and locomotor activity in an open field arena, while activating NAc D2-MSNs led to a decrease in these effect (Zhu et al., 2016). These results suggest that both NAc D1-MSNs and D2-MSNs may play a role in controlling both limbic and locomotor processing.

D1-MSNs in the NAc core are known to send equal projections to both the ventral pallidum (VP) ($NAc^{D1\text{-}MSN}$-VP) and the substantia nigra pars reticulata (SNr) ($NAc^{D1\text{-}MSN}$-SNr), whereas D2-MSNs primarily project their connections to the VP (Heimer et al., 1991; Kupchik et al., 2015; Kupchik and Kalivas, 2017; Matsui and Alvarez, 2018; Pardo-Garcia et al., 2019; Robertson and Jian, 1995). Previous studies have reported the $NAc^{D1\text{-}MSN}$-VP pathway to play an important role in motivation and reward-related behaviors, including as cue-induced reinstatement of cocaine (Stefanik et al., 2013; Pardo-Garcia et al., 2019),cocaine-context-associated memory formation (Wang et al., 2014), and cocaine-induced locomotor sensitization (Creed et al., 2016). However, contrastingly, a recent report indicated that optogenetic stimulation of the $NAc^{D1\text{-}MSN}$-VP pathway induces aversion in mice (Liu et al., 2022). Thus, the role of this pathway in limbic control is still unclear and further functional characterization is required. The $NAc^{D1\text{-}MSN}$-VP pathway is also suggested to be involved in locomotor control (Root et al., 2015). Indeed, it has been reported that intra-VP infusion of substance P, a neuropeptide released from D1-MSNs projecting to the VP,

increases locomotor activity (Napier et al., 1995). Similarly, intra-VP infusion of a muscimol, a GABA receptor agonist, is able to block increased locomotion induced by intra-NAc infusion of dopamine and NMDA agonists (Churchill et al., 1998; Patel & Slater, 1988; Wallace & Uretsky, 1991). However, the functional effect of direction optogenetic manipulation of the $NAc^{D1\text{-}MSN}$-VP pathway has yet to be tested.

In contrast to the $NAc^{D1\text{-}MSN}$-VP pathway, these is currently limited knowledge regarding the functional role of the $NAc^{D1\text{-}MSN}$-SNr pathway. Classically, it has been suggested that the NAc D1-MSN projections to the SNr form an integral part of a limbic information processing basal ganglia loop circuit (Alexander et al., 1986; Foster et al., 2021; Haber, 2003; Macpherson et al., 2021; Parent & Hazrati, 1995). According to this theory, activation of the $NAc^{D1\text{-}MSN}$–SNr pathway is hypothesized be responsible for driving reinforcement. However, this proposed function has not been empirically tested as of yet (Balleine, 2019; Macpherson et al., 2021; Peak et al., 2019). Interestingly, recent study has suggested that the $NAc^{D1\text{-}MSN}$–SNr pathway might have an impact on motor behavior as well. Indeed, optogenetic stimulation of axon terminals in the SNr from NAc D1-MSNs has been shown to increase activity not only in the mPFC, but also in the primary motor cortex (M1) (Aoki et al., 2019). Although this study highlights the potential influence of the $NAc^{D1\text{-}MSN}$–SNr pathway on motor areas such as the M1, it has not yet been definitively established whether stimulation of this pathway results in changes in motor behavior.

In this study, I used optogenetic activation of the axon terminals of NAc core D1-MSNs in the VP or SNr to investigate the contribution of $NAc^{D1\text{-}MSN}$-VP and $NAc^{D1\text{-}MSN}$-SNr pathways to limbic and motor functions. To access the limbic functions, mice performed reward-related learning tasks including real-time place preference and self-stimulation tests. Next, to investigate motor functions, these pathways were stimulated either bilaterally or unilaterally while mice were placed an open field arena and tracked using locomotor activity tracking software.

3.2 Material and Methods

3.2.1 Animals

Experiments utilized male D1-Cre (FK150Gsat) transgenic mice aged between 8 and 12 weeks old and on a C57BL/6 background, as well as their wild-type counterparts. The animals were housed in groups of 2-3 and were maintained on a 12-h light/dark cycle (lights on at 8:00 a.m.), with the temperature regulated at 24 ± 2 ºC and humidity maintained at 50 ± 5%. Behavioral experiments were performed during the light period. Mice had unrestricted access to water and standard lab chow *ad libitum*, except during touchscreen operant chamber experiments, which they were food-restricted to ensure their motivation to respond instrumentally. All animal experiments were conducted in accordance with the National Institutes of Health experimental procedures and were approved by the ethical committee of the Institute for Protein Research at Osaka University. The same mice were used for all experiments.

3.2.2 Stereotaxic Virus Injection and optical cannula Implantation

After administrating anesthesia (90 mg/kg Ketamine and 20 mg/kg Xylazine, i.p. injection), mice were positioned in the stereotaxic apparatus. A midline incision was made on the scalp, and a craniotomy was performed using a dental drill. The injections were then carried out using graduated pipettes with a tip diameter of 10-15 μm.

Bilateral injections were administered to the mice in the NAc core (Bregma coordinates: anterior/posterior, +1.2 mm; medial/lateral, ± 1.35 mm; dorsal/ventral, -3.75 mm, 250 nl/site at a rate of 100 nl/min) using an adeno-associated virus (AAV) virus expressing channelrhodopsin-2 (ChR2) under a FLEX Cre-switch promotor (AAV2-EF1-FLEX-hChR2(H134R)-EYFP; Addgene ID: 20298), or an optically-inactive control virus (AAV5-EF1a-DIO-EYFP; Addgene ID: 27056). The concentrations for the ChR2 virus and the control virus were 4.4 x 10^{12} virus molecules/ml and 1.3 x 10^{13} virus molecules/ml, respectively. Following infusion, the needle was left at the injection site for 10 minutes to allow for diffusion of the virus, and then it was slowly withdrawn. Optic fibers (200-μm core 0.22 N.A., Thorlabs, Newton, NJ, USA) were bilaterally implanted into either the VP (Bregma coordinates: anterior/posterior, -0.11 mm; medial/lateral, ± 1.40 mm;

dorsal/ventral, -4.25 mm) or medial SNr (Bregma coordinates: anterior/posterior, -3.3 mm; medial/lateral, ±1.0 mm; dorsal/ventral, -4.4 mm) using ceramic zirconia ferrules. Finally, three skull screws were inserted 1 mm into the skull area surrounding the optic fibers, and the entire skull was firmly secured with dental cement. For robust viral expression, the viral infusions occurred at least 3-4 weeks before conducting the behavioral experiments.

In total; 9 D1-Cre $NAc^{D1\text{-}MSN}$-VP ChR2, 9 D1-Cre $NAc^{D1\text{-}MSN}$-VP EYFP, 10 D1-Cre $NAc^{D1\text{-}MSN}$-SNr ChR2, and 9 D1-Cre $NAc^{D1\text{-}MSN}$-SNr EYFP mice were used. The same mice were used for all behavioral experiments.

Laser stimulation at a frequency of 20 Hz using a 473 nm wavelength was delivered by DPSS (diode-pumped solid-state) lasers (Shanghai Laser & Optics Century Co., Ltd.), with the laser intensity at the fiber tip controlled by a microcontroller (Arduino) set at 8-10 mW.

3.2.3 Real-time place preference (rt-pp) test

The rt-pp experiment was conducted in a white rectangular box, which was divided lengthways into two equal-sized rectangular chambers (W:15cm x L:20cm x H:25cm). Each chamber had distinct contextual cues; one chamber featured green triangles on the walls, while the other chamber had blue dots on the walls.

The rt-pp task consisted of two stages: (1) a pre-conditioning test (pre-test) and (2) test sessions (laser test). In the pre-test, mice were given 15 minutes to freely explore the entire apparatus, and the time spent in each chamber was measured to evaluate any bias towards either side using automated video tracking software (EthoVision XT 16, Noldus). Next, the laser-test sessions were conducted with an unbiased experimental design across 3 consecutive days for 20 min each day. During these sessions, whenever an animal entered one chamber, the laser stimulation was delivered for the duration that the animal stayed in the chamber. Conversely, when the animal entered the other chamber, no stimulation was delivered. The chamber (either with triangle or dot walls) paired with laser stimulation was randomized between the animals. The duration of time spent in the chamber paired with laser was measured across the three test sessions to assess the mouse’s preference.

3.2.4 Operant chamber test of reinforcement

Operant tasks were conducted in trapezoidal Bussey–Saksida touchscreen operant chambers (Lafayette Instrument) situated within a sound- and light-attenuating cubicle. Each chamber was equipped with a front touchscreen divided into two touch response panels (70 × 75 mm^2 spaced, 5 mm apart, 16 mm above the floor), along with a liquid delivery magazine at the back end of the chamber. The self-stimulation tests were managed using ABET II and Whisker Server software (Lafayette Instrument), while laser delivery within the chambers was controlled by Radiant version 2 software (Plexon).

3.2.5 Two-choice optogenetic self-stimulation task

Initially, mice underwent food restriction until they reached 85-90% of their free-feeding weight, which took approximately 7 days, to enhance their motivation for producing instrumental behavioral responses. Subsequently, they underwent four consecutive daily training sessions under a fixed-ratio 1 (FR1: 1 response produces the outcome) schedule to instrumentally respond at a touch panel paired with the delivery of laser stimulation (S+: 30 sec laser delivery), while another touch panel no outcome (S-). The spatial location (left/right) of the S+ response panel was counterbalanced across mice. The outcome of each trial was followed by a 10-sec intertrial interval (ITI). This task was conducted for four consecutive days, with a duration of 60 minutes or up to 60 trials. Throughout all trials, the number of touch responses for both the S+ and S- panels, as well as the response latencies, were recorded to evaluate the potential reinforcing effect of laser stimulation.

3.2.6 Two-choice task with optogenetic stimulation paired with a liquid reinforcer

The mice underwent training to respond at two specific response panels in order to receive a sucrose liquid reward (7μl of 10% sucrose diluted in water). One of the panels (previously associated with laser delivery) was additionally paired with the delivery of the the liquid reward (S+), while the other panel (previously associated with no outcome) delivered only the liquid reward alone (S-). Each outcome was followed by a 10-second ITI. The position of the S+ panel

was counterbalanced across the previous S+ and S- panels used in the earlier self-stimulation task. However, no significant main effect or interaction of the previous panel location was observed, leading to the grouping together of the data.

Animals underwent training on consecutive days using a previously described reinforcement schedule with slight modifications (Robinson et al., 2014; Soares-Cunha et al., 2022). The training schedule comprised the following stages: a fixed-ratio 1 (FR1) schedule for 5 days, a FR4 schedule (4 response produces the outcome) for 1 day, a random ratio 4 (RR4) schedule (a random number of responses between 1-4 produces the outcome) for 4 days, and finally a RR6 schedule (a random number of responses between 1-6 produces the outcome) for 4 days each (lasting 60 minutes or up to 60 trials). Throughout all trials, data were recorded for each session, including the number of touch responses for both the S+ (sucrose & laser) and the S- (sucrose), as well as the response latencies and time taken to collect the liquid rewards.

During this test, one D1-Cre $NAc^{D1\text{-}MSN}$-VP EYFP mouse was excluded from the study due to low responses at both touch panels.

3.2.7 Open field tests (OFT) of motor activity

For bilateral stimulation tests, mice were placed in a grey cylindrical open field apparatus with dimensions of 42 cm in diameter and 42 cm in height. Bilateral fiber optic cannulae were attached to patch cords and suspended above the animal, allowing them to move freely throughout the apparatus. The animals were given three minutes to freely explore the entire arena and become habituated to the before the start of testing. The test consisted of a 12-min session, divided into four alternating 3-minute trials. During these trials, bilateral laser stimulation was applied in an alternating manner, switching between OFF or ON states (OFF-ON-OFF-ON), according to a previously described method (Tye et al., 2013). During the laser ON trials, photostimulation was applied following the protocol described in the “Stereotaxic virus injection and optical cannula implantation” subsection. The video tracking software (EthoVision XT 16, Noldus) automatically recorded the total distance moved, velocity, and speed of animals during these trials.

Unilateral stimulation was conducted following the previous mentioned, but with the exception that only one patch cable was conected to either the contralateral or ipsilateral fiber optic cannulae. The contralateral and ipsilateral tests were conducted on consecutive days, and the order

of these tests was randomized across mice. The test session consisted of 18 minutes and was divided into four alternating 3-minute trials: OFF-ON-OFF-ON-OFF-ON. During these trials, video tracking software (EthoVision XT 16, Noldus) automatically recorded body rotations (>180° turn).

3.2.8 Retrograde Tracing of NAc Core D1-MSNs

To investigate the monosynaptic inputs of D1-VP and -SNr projection, I injected two different retrograde viruses, pAAV$_{retro}$-hSyn-DIO-EYFP and pAAV$_{retro}$-hSyn-DIO- mCherry, into the SNr and VP of D1-Cre mice, respectively. After four weeks, the animals were transcardially perfused, and their brains were fixed and coronally sectioned at a thickness of 40 μm. I quantified the individual mCherry, EYFP, and the overlap of both mCherry and EYFP co-labeled cells in the NAc core, using three mice per group. Immunofluorescence was used to visualize both the mCherry and EYFP labeled neurons, ensuring verification of the retrograde transport injection site in the NAc core. The labeled neurons in each mouse brain were manually marked using the ImageJ program.

3.2.9 Histological analysis

Once behavioral experiments were completed, the mice were anesthetized using 90 mg/kg Ketamine and 20 mg/kg Xylazine. Subsequently, they were transcardially perfused with 0.1 M phosphate-buffered saline (PBS) for 2 minutes, followed by 4% paraformaldehyde (PFA; dissolved in 0.1 M Na_2HPO_4/NaH_2PO_4 buffer, pH 7.5) in PBS for 5 minutes, at a flow rate of 10 ml/min. The brains were removed and postfixed in 4% PFA overnight, then placed in 7.5%, 15%, and 30% sucrose in PBS solution at 4°C until the brains sank to the bottom at each stage. Once the brains were then completely frozen, they were embedded in Optimal Cutting Temperature (O.C.T.) compound, providing support for tissue specimens during cryostat sectioning. Next, the brain tissue was affixed to a circular cryostat block and sliced into 40-μm-thick sections at temperatures ranging from -17 to -20°C. These coronal brain slices (40 μm) were then stored in a PBS solution at 4°C. For the immunohistochemical staining process, each brain section was treated with a blocking solution (5% Bovine serum albumin in PBS) for 1 hour at room temperature, followed

by three times washes in PBS. After the PBS rinsing, the brain slices were incubated at 4°C overnight in a solution containing anti-green fluorescent protein rabbit IgG primary antibody (diluted 1:1000; Molecular Probes, OR, USA) and anti-Tyrosine Hydroxylase (TH) antibody (diluted 1:500; EMD Millipore, USA) in 1x PBS with 0.3% Triton-X (Nacalai Tesque Inc, Kyoto, Japan) (PBST). All brain sections were washed three times for 10 minutes in PBS, then stained with either Alexa Fluor 488 or 555 goat anti-rabbit IgG secondary antibody (diluted 1:500; Thermo Fisher Scientific, MA, USA) in 1x PBST for 1 hour at room temperature. Following three times 10-minutes washes in 1x PBS, the sections were mounted using Fluoroshield mounting medium containing DAPI (Abcam, Cambridge, UK) and then observed using a KEYENCE BZ-X800E All-in-one Fluorescence Microscope (Keyence, Osaka, Japan).

3.2.10 Statistical Analysis

The experimental data were presented as the mean ± SEM and plotted using Prism v8.0 software (GraphPad Software Inc, CA, USA). The rt-pp and OFT (bilateral stimulation) data underwent analysis using two-way repeated measures ANOVAs. The factors considered in the analysis were the virus type (ChR2 vs EYFP) as a between-subjects factor and laser state (OFF vs ON) as a within-subjects factor. The dependent variable for rt-PP was the time spent in the laser-paired chamber minus time spent in the non-laser paired chamber, while for OFT, the dependent variable was velocity or distance traveled. The data from the two-choice optogenetic stimulation and OFT (unilateral stimulation) were analyzed using three-way repeated measures ANOVAs. The between-subjects factor was the virus (ChR2 vs EYFP), and within-subjects factors were the panel (S+ vs S-) and session (day of training) for two-choice optogenetic stimulation. For OFT, the within-subjects factors were Laser (ON vs OFF) and turn direction (contralateral vs ipsilateral rotation), with the dependent variables being responses or turns. *Post hoc* Bonferroni's multiple comparisons tests were performed when ANOVA main effects or interactions were significant ($p < 0.05$). Mauchly's sphericity test was used to assess the assumption of sphericity, and the Greenhouse-Geisser correction was applied where necessary (Mauchly's test $p < 0.05$). The results are presented as mean ± SEM, and statistical significance is denoted as follows: *p<0.05, **p<0.01, ***p<0.001, ****p<0.0001.

3.3 Results

3.3.1 Optogenetic stimulation of $NAc^{D1\text{-}MSN}$-VP and $NAc^{D1\text{-}MSN}$-SNr pathway drives reinforcement

Given the established role of NAc D1-MSNs in reinforcement (Cole et al., 2018; Hikida et al., 2010; Lobo et al., 2010), my initial investigation focused on determining whether optogenetic activation of either the $NAc^{D1\text{-}MSN}$–VP or $NAc^{D1\text{-}MSN}$–SNr pathways, utilizing the excitatory ChR2, could effectively control reinforcement. To achieve pathway-specific control of axon terminal activity, optic fibers were bilaterally implanted into the VP or SNr region of D1-Cre mice that had been microinjected with either a Cre-dependent ChR2 (AAV2-Ef1a-FLEX-hChR2(H134R)-EYFP) or an EYFP control virus (AAV5-Ef1a-DIO-EYFP) (Fig 1A-B,2). Furthermore, I further confirmed that expression of the virus at SNr terminal sites did not overlap with the presence of dopaminergic neurons in the substantia nigra pars compacta (SNc) and the ventral tegmental area (VTA), as this overlap could potentially influence the behavior response (Fig 1C).

In an rt-PP task, mice were allowed to freely explore a two-chamber apparatus with distinct contextual stimuli in each chamber (circles vs triangles) during a 15-minute learning session (Fig 3A; Pretest). Subsequently, for the following three consecutive days, mice were placed back in the apparatus for a 20-minute session, during which laser stimulation was applied through optic fibers whenever mice entered one of the two chambers (circles vs triangles, randomized between mice; Fig 3A, Laser test).

Mice expressing ChR2 in the D1-Cre $NAc^{D1\text{-}MSN}$-VP and $NAc^{D1\text{-}MSN}$-SNr, but not in mice expressing EYFP, exhibited a significant increase in the time spent in the laser-paired chamber during the laser test sessions compared to the pretest session ($NAc^{D1\text{-}MSN}$-VP: Fig 3B, significant virus x session interaction: $F_{(3,48)} = 16.87$, $p<0.0001$; $NAc^{D1\text{-}MSN}$-SNr: Fig 3C, significant virus × session interaction: $F_{(3,51)} = 17.28$, $p<0.0001$). These findings strongly indicate that activation of the $NAc^{D1\text{-}MSN}$-VP and $NAc^{D1\text{-}MSN}$–SNr pathways had a reinforcing effect on the mice.

3.3.2 Optogenetic activationn of VP and SNr-projecting NAc D1-MSNs is sufficient to facilitate instrumental self-stimulation and enhances instrumental responses for a liquid reinforcer

To further confirm their functional role in the reinforcing properties, I next performed optogenetic stimulation of $NAc^{D1\text{-}MSNs}$-VP and $NAc^{D1\text{-}MSNs}$-SNr pathways in a two-choice schedule of operant self-stimulation. In four consecutive daily 60-minute sessions, mice were trained to nose-poke for intracranial optical self-stimulation using a fixed-ratio 1 (FR1) schedule of reinforcement. This involved making a touch response at one of two response panels. One of two touchscreens is randomly assigned for a 30-second delivery of laser stimulation through optic fibers (S+), while the other touchscreen is assigned without optical stimulation (S-) (Fig 4A). Throughout the four test sessions, a significant increase in responding at the S+ panel was observed compared to the S- panel in D1-Cre mice expressing ChR2 in $NAc^{D1\text{-}MSNs}$-VP (Fig 4B, significant virus x panel x session interaction: $F_{(3,48)} = 25.99$, $p<0.0001$) or $NAc^{D1\text{-}MSNs}$-SNr (Fig 4C, significant virus x panel x session interaction: $F_{(3,51)} = 3.193$, $p<0.05$) pathways, but not in mice expressing EYFP (Fig 4B,C). These results suggest that the activation of both $NAc^{D1\text{-}MSNs}$-VP and $NAc^{D1\text{-}MSNs}$-SNr pathways provides sufficiently reinforcement to sustain instrumental responding. There were no significant differences in the response latencies at either response panels between ChR2- and EYFP-expressing mice during the training sessions (Fig 4D,E).

Next, to investigate the possibility that activation of these pathways might not only directly reinforce behavior but also influence the attractiveness of a liquid reward. To explore this, I paired laser delivery to a response that earned a sucrose reward in a two-choice schedule of reinforcement (Fig 5A). As previously, mice were given the option to respond at one of two response panels. However, in this modified setup, a touch response at one randomly assigned panel resulted in both a sucrose reward and a 30-second laser delivery (S+), while a response at the other panel provided the sucrose reward by itself (S–). Mice underwent training following a previously described schedule of reinforcement with minor adjustments (Robinson et al., 2014; Soares-Cunha et al., 2022), which progressed from a FR1 to a RR6 (an average of six responses were needed to produce the outcome) over consecutive days. Similarly to the previous self-stimulation task, D1-Cre mice expressing ChR2 in $NAc^{D1\text{-}MSNs}$-VP or $NAc^{D1\text{-}MSNs}$-SNr pathways exhibited a significantly increase in responses at the S+ panel compared to the S– panel, and this effect gradually became stronger as the reinforcement schedules progressed ($NAc^{D1\text{-}MSNs}$-VP: Fig 5B, significant virus × panel × session interaction: $F_{(13,195)} = 4.168$, $p<0.0001$; $NAc^{D1\text{-}MSNs}$-SNr: Fig 5C, significant virus × panel × session interaction: $F_{(13,195)} = 3.365$, $p<0.0001$). In contrast, EYFP-expressing animals

did not show any significant difference in the number of responses for the S+ and S- across the four days (Fig 5B,C).

Analysis of response latencies revealed that ChR2-expressing mice in both $NAc^{D1\text{-}MSNs}$-VP and $NAc^{D1\text{-}MSNs}$-SNr pathways exhibited quicker response times at both S+ and S– panels throughout all sessions compared to EYFP-expressing mice ($NAc^{D1\text{-}MSNs}$-VP: Fig 5D, significant main effect of virus: $F_{(1,15)} = 19.75$, $p<0.001$; $NAc^{D1\text{-}MSNs}$-SNr: Fig 5E, significant main effect of virus: $F_{(1,17)} = 17.65$, $p<0.001$). It is possible that the substantial reward (liquid reinforcer and laser) obtained from responding at the S+ panel might have resulted in quicker response times, which also generalized to influence S– responses. Interestingly, mice expressing ChR2 in $NAc^{D1\text{-}MSNs}$-VP or $NAc^{D1\text{-}MSNs}$-SNr exhibited a significantly increased latency to collect the reward when responding at the S+ panel compared to the S- panel, while there was no such effect in mice expressing EYFP ($NAc^{D1\text{-}MSNs}$-VP: Fig 5F, significant virus × panel interaction: $F_{(1,15)} = 33.29$, $p<0.0001$; $NAc^{D1\text{-}MSNs}$-SNr: Fig 5G, significant virus × panel interaction: $F_{(1,17)} = 15.25$, $p<0.01$). I propose that receipt of the rewarding laser stimulation might lead to reduced motivation in mice to obtain the liquid reinforcer, as they are already receiving a rewarding outcome.

Altogether, the results from the rt-PP, two-choice self-stimulation, and laser paired with liquid reinforcer two-choice task demonstrate that the activation of the $NAc^{D1\text{-}MSN}$–VP or $NAc^{D1\text{-}MSN}$–SNr pathways is reinforcing and capable of sustaining and enhancing instrumental responding for the laser itself and a liquid reinforcer, respectively.

3.3.3 Stimulation of VP and SNr-projecting NAc D1-MSNs increases motor activity

Next, as NAc core D1-MSN activation has been related to enhanced motor behavior (Dreher & Jackson, 1989; Plaznik et al., 1989; Zhu et al., 2016), I investigated the effect of optogenetic activation or inhibition of the $NAc^{D1\text{-}MSN}$–VP or $NAc^{D1\text{-}MSN}$–SNr pathways on motor activity in an open field arena (Fig 6A). Initially, mice were habituated to the arena for 3 minutes, followed by four alternating 3-minute periods of laser OFF and laser ON epochs, in total 12 minutes (Fig 6A). The assessment of motor activity during the laser ON versus the laser OFF epochs showed that optogenetic stimulation of NAc core D1-MSNs projecting to the VP and SNr resulted in a significant enhancement of velocity ($NAc^{D1\text{-}MSN}$–VP: Fig 6B, significant virus × time period interaction: $F_{(11,176)} = 2.683$, $p<0.01$ (Left); Fig 6B, significant virus × laser interaction: $F_{(1,16)} =$

12.21, $p<0.01$ (Right); $NAc^{D1\text{-}MSN}$–SNr: Fig 6C, significant virus x time period interaction: $F_{(11,187)} = 3.243$, $p<0.001$ (Left); Fig 6C, significant virus x laser interaction: $F_{(1,17)} = 16.86$, $p<0.001$ (Right) and distance moved ($NAc^{D1\text{-}MSN}$–VP: Fig 7A, significant virus × time period interaction: $F_{(11,176)} = 2.093$, $p<0.05$ (Left); Fig 7A, significant virus × laser interaction: $F_{(1,16)} = 7.481$, $p<0.05$ (Right); $NAc^{D1\text{-}MSN}$–SNr: Fig 7B, significant virus x time period interaction: $F_{(11,187)} = 3.360$, $p<0.001$ (Left); Fig 7B, significant virus x laser interaction: $F_{(1,17)} = 14.07$, $p<0.01$ (Right)) in ChR2-expressing mice, but no change in EYFP-expressing mice.

Next, I examined whether unilateral stimulation of VP or SNr-expressing D1-MSNs could influence motor behavior, biasing it towards the same side as the stimulation (ipsilateral direction) or the opposite side (contralateral direction) in an open field arena. Mice were habituated to the circular chamber for 3 minutes and then underwent 6 alternating 3-minute period with laser off and laser on across 18-minute sessions. Mice underwent two sessions on consecutive days in which they received stimulation to either the right or left hemisphere (Fig 8A). As unilateral stimulation of motor-related circuitry typically induces turning behavioral rather than forward motion (Guillaumin et al., 2021), total number of rotations to the ipsilateral and contralateral directions were counted during the laser on and off epochs, using automated tracking software. An increase in rotations was observed during laser stimulation of mice expressing ChR2 in $NAc^{D1\text{-}MSNs}$-VP (Fig 8B: significant virus x laser by turn direction interaction: $F_{(1,16)} = 10.55$, $p<0.01$; Fig 8C: significant virus x laser by turn direction interaction: $F_{(1,16)} = 11$, $p<0.01$) or $NAc^{D1\text{-}MSNs}$-SNr (Fig 8D: significant virus x laser by turn direction interaction: $F_{(1,17)} = 6.118$, $p<0.05$; Fig 8E significant virus x laser by turn direction interaction: $F_{(1,17)} = 14.31$, $p<0.01$), but not those expressing EYFP.

Altogether, these data indicate that activity in $NAc^{D1\text{-}MSNs}$-VP and $NAc^{D1\text{-}MSNs}$-SNr is able to increase motor activity, indicating that these projection pathways may play a significant role in motor regulation.

3.3.4 Retrograde tracing of VP and SNr-projecting NAc D1-MSNs

Finally, while it was demonstrated that $NAc^{D1\text{-}MSNs}$-VP and $NAc^{D1\text{-}MSNs}$-SNr pathways play similar functional roles in limbic and motor control, it was still unclear whether these pathways are completely separated or whether the same NAc core D1-MSNs send collateral projections to both the VP and SNr. Thus, in order to elucidate the anatomical characteristics of these pathways,

fluorescent retrograde tracing was performed using retrogradely-travelling AAV-retro-hSyn-DIO-EYFP and AAV-retro-hSyn-DIO- mCherry injected into the SNr and VP, respectively, of D1-Cre mice (Fig 9A). Following adequate viral expression, brains were sliced and the amount of individual mCherry, EYFP expressing cells, and co-labeled mCherry and EYFP expressing cells in the NAc core were quantified (Fig 9B-C,10). It was found that approximately 73.6% of fluorescence-expressing cells were co-labeled with both EYFP and mCherry, indicating dual projection of NAc core D1-MSNs to both the VP and SNr. 6.2% of neurons were found to express only EYFP (projecting exclusively to the VP), while 20.2% of neurons expressed only mCherry (projecting exclusively to the SNr) (Fig 11). These results suggest that a majority of NAc core D1-MSNs project to both the VP and SNr, potentially explaining why these two pathways appear to share the same functional roles.

Figure 1.

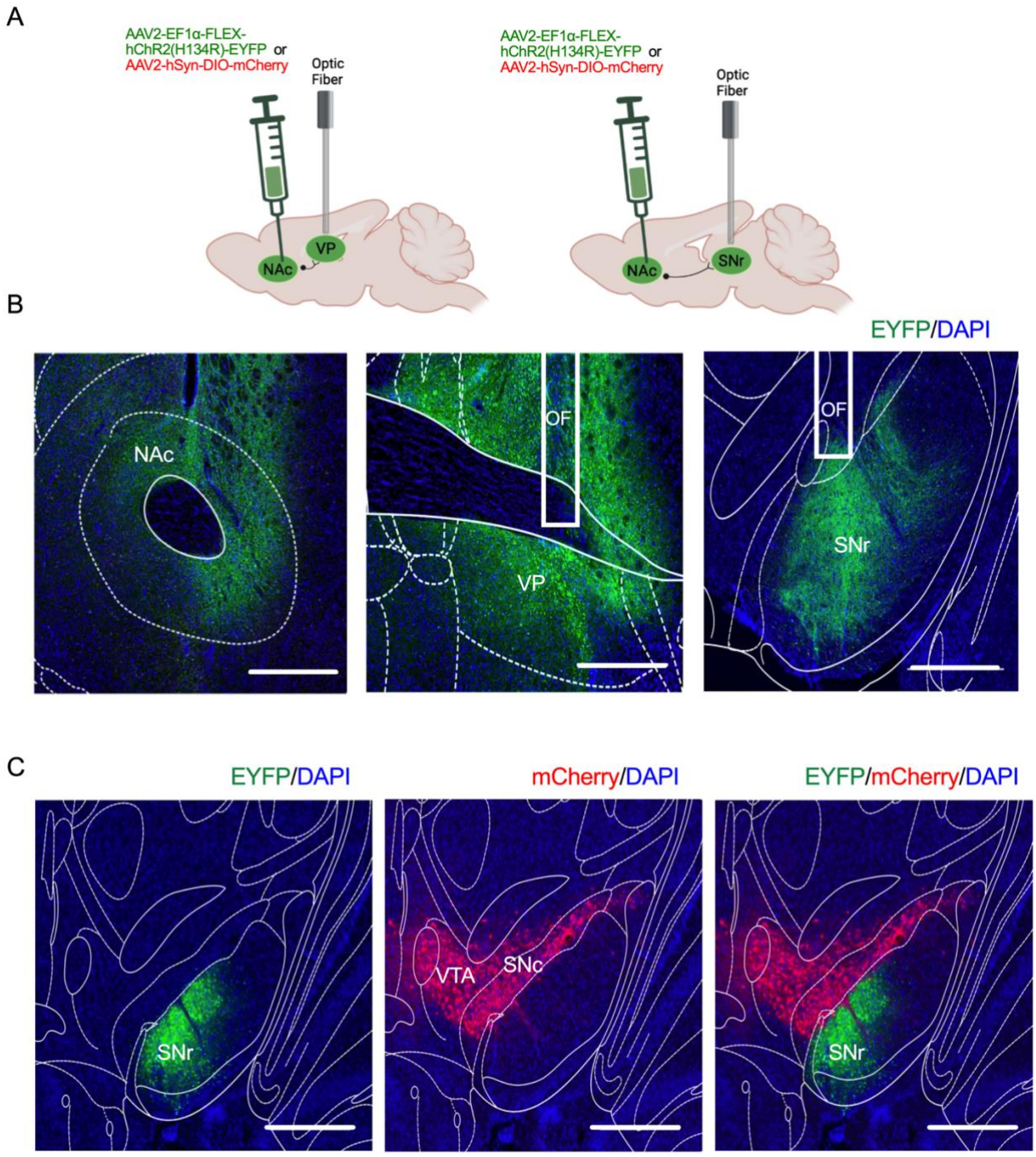

Fig 1. Histology of virus expression and fiber implantations site. (A) The diagram illustrates the location of viral infusion in the nucleus accumbens (NAc) and optic fiber implantation in the terminal target area, including ventral pallidum (VP) and substantia nigra pars reticulata (SNr), in D1-Cre transgenic mice. (B) Representative coronal sections show the expression of ChR2 tagged

with EYFP fluorescent protein in the NAc core (Left), VP (Middle) and SNr (Right) of D1-Cre mice; Optic fiber (OF); nuclear marker DAPI is shown in blue, and EYFP in green, with a scale bar of 500 μm. (C) The representative image demonstrates the expression of EYFP in the SNr (Left), the expression of TH-positive dopaminergic neurons tagged with mCherry fluorescent protein in the substantia nigra pars compacta (SNc) and ventral tegmental area (VTA) (Middle), and a merged expression of both EYFP and mCherry (Right); mCherry is shown in red, EYFP in green, and DAPI in blue, with a scale bar of 500 μm.

Figure 2.

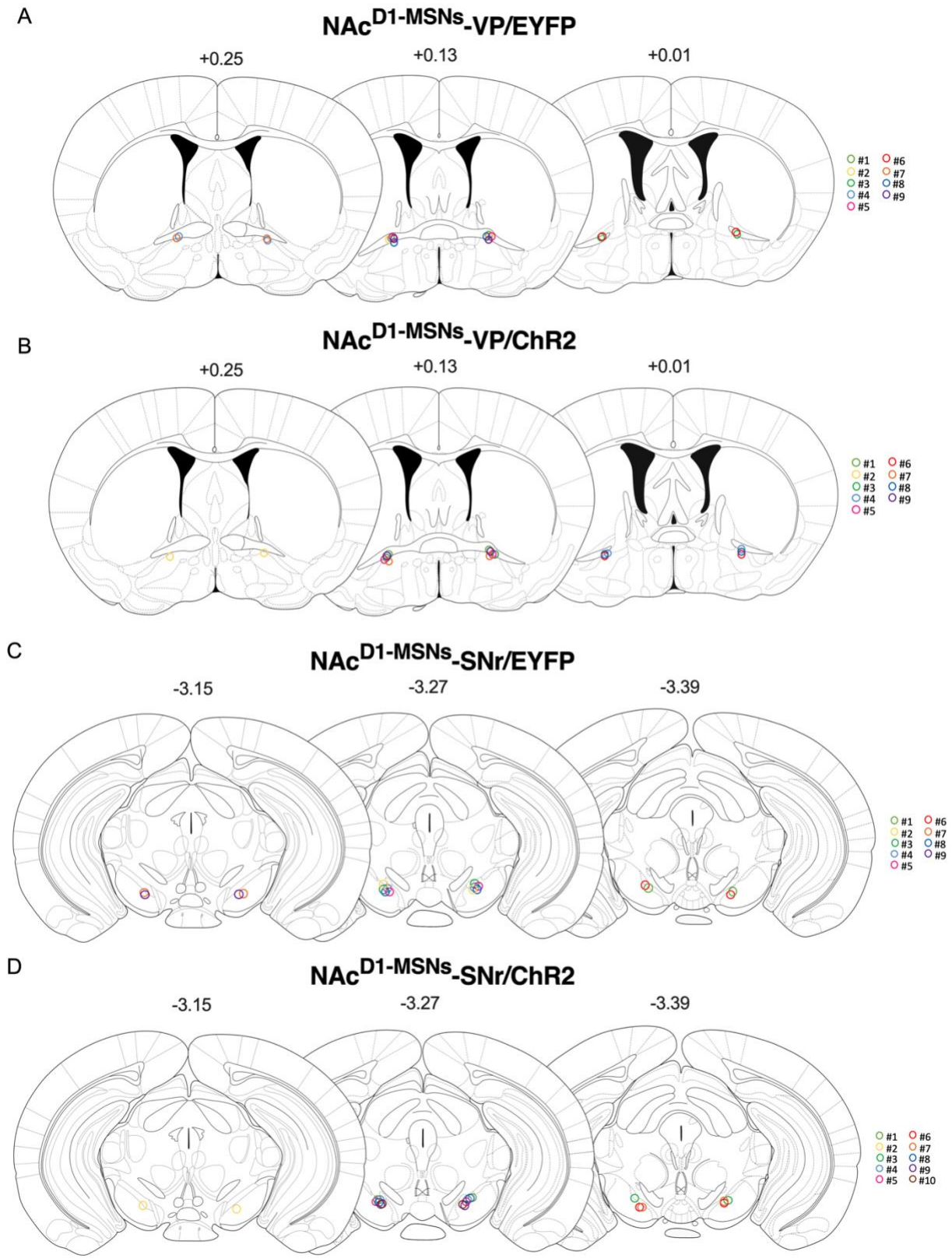
A
NAc D1-MSNs-VP/EYFP
+0.25
+0.13
+0.01
#1 #2 #3 #4 #5 #6 #7 #8 #9
B
NAc D1-MSNs-VP/ChR2
+0.25
+0.13
+0.01
#1 #2 #3 #4 #5 #6 #7 #8 #9
C
NAc D1-MSNs-SNr/EYFP
-3.15
-3.27
-3.39
#1 #2 #3 #4 #5 #6 #7 #8 #9
D
NAc D1-MSNs-SNr/ChR2
-3.15
-3.27
-3.39
#1 #2 #3 #4 #5 #6 #7 #8 #9 #10

Fig 2. Optic fiber placements (A) Representative coronal sections of optic fiber placements in the VP at three different anterior-posterior coordinates from the Bregma at +0.25 mm, +0.13 mm, and +0.01 mm for two different groups of mice: EYFP-expressing mice (n=9), and (B) ChR2-expressing mice (n=9). (C) Representative coronal sections of optic fiber placements in the SNr at three different anterior-posterior coordinates from the Bregma at -3.15 mm, -3.27 mm, and -3.39 mm for two different groups of mice: EYFP-expressing mice (n=9), and (D) ChR2-expressing mice (n=10).

Figure 3.

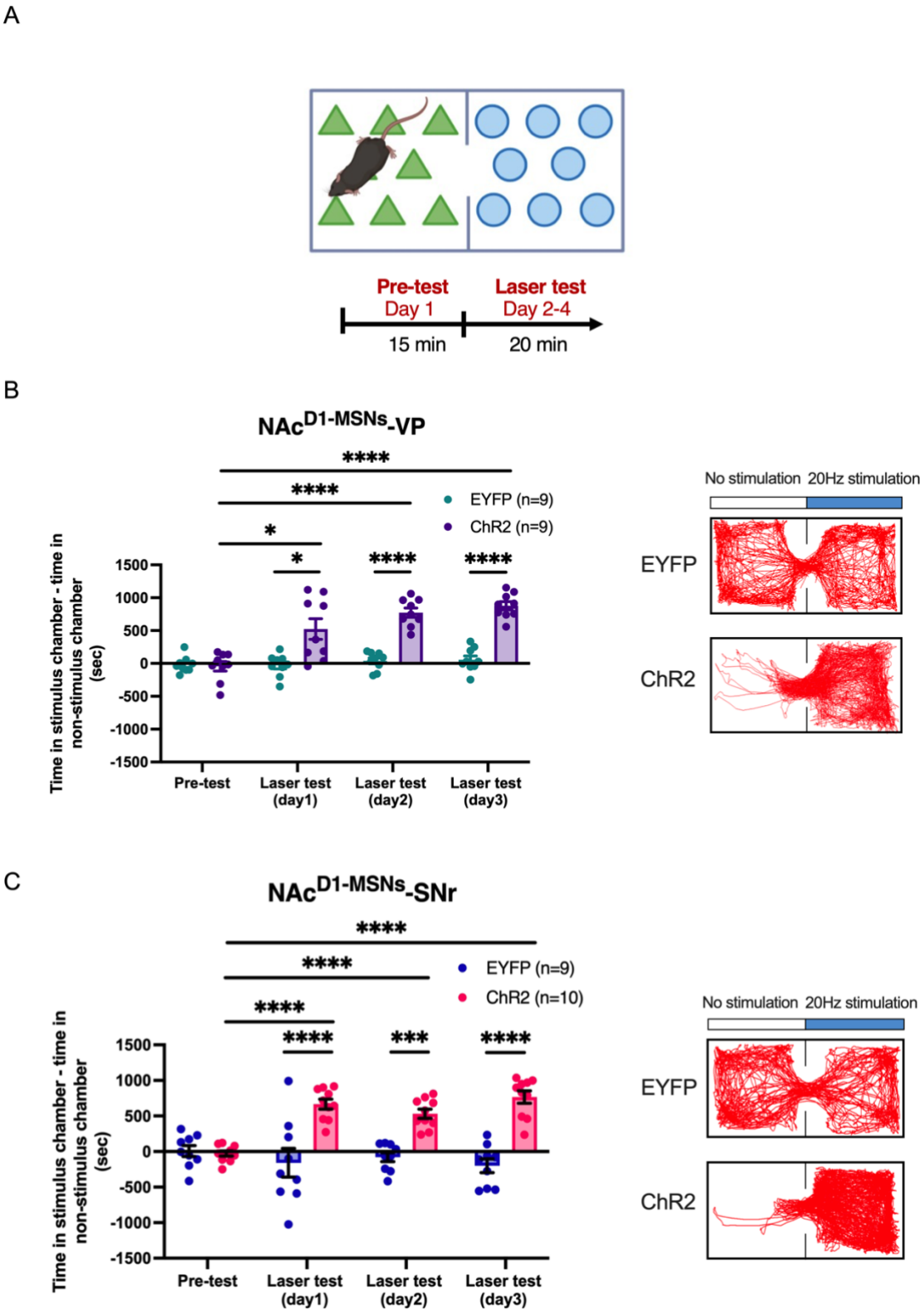
A
Pre-test
Day 1
15 min
Laser test
Day 2-4
20 min
B
NAcD1-MSNs-VP
EYFP (n=9)
ChR2 (n=9)
Time in stimulus chamber - time in non-stimulus chamber (sec)
Pre-test
Laser test (day1)
Laser test (day2)
Laser test (day3)
No stimulation
20Hz stimulation
EYFP
ChR2
C
NAcD1-MSNs-SNr
EYFP (n=9)
ChR2 (n=10)
Time in stimulus chamber - time in non-stimulus chamber (sec)
Pre-test
Laser test (day1)
Laser test (day2)
Laser test (day3)
No stimulation
20Hz stimulation
EYFP
ChR2

Fig 3. Optogenetic stimulation of the $NAc^{D1\text{-}MSN}$-VP and -SNr pathways is reinforcing (A) The diagram illustrates the apparatus used for the real-time place preference (rt-pp) assay and its experimental timeline. (B) The different in time spent between the laser-paired compartment and the non-laser-paired chamber in mice expressing EYFP (n=9) or ChR2 (n=9) in the $NAc^{D1\text{-}MSNs}$-VP pathway during pre-test and laser test across 3 sessions (Left) (Two-way RM-ANOVA; EYFP vs ChR2; Laser test (day1), *p=0.0316; Laser test (day2), ****p<0.0001; Laser test (day3), ****p<0.0001), along with representative movement traces of the time spent in each compartment during the last session of the laser-test for two example mice expressing EYFP and ChR2, respectively (Right). (C) The different in time spent between laser-paired compartment and the non-laser-paired chamber in mice expressing EYFP (n=9) or ChR2 (n=10) in the $NAc^{D1\text{-}MSNs}$-SNr pathway during pre-test and laser test across 3 sessions (Left) (Two-way RM-ANOVA; EYFP vs ChR2; Laser test (day1), ****p<0.0001; Laser test (day2), ***p=0.0001; Laser test (day3), ****p<0.0001), along with representative movement traces of the time spent in each compartment during the last session of the laser-test for two examples mice expressing EYFP and ChR2, respectively (Right). Data represent the mean ± SEM, *post hoc* Bonferroni comparisons were performed with *p<0.05, ***p<0.001, ****p<0.0001 indicating statistical significance.

Figure 4.

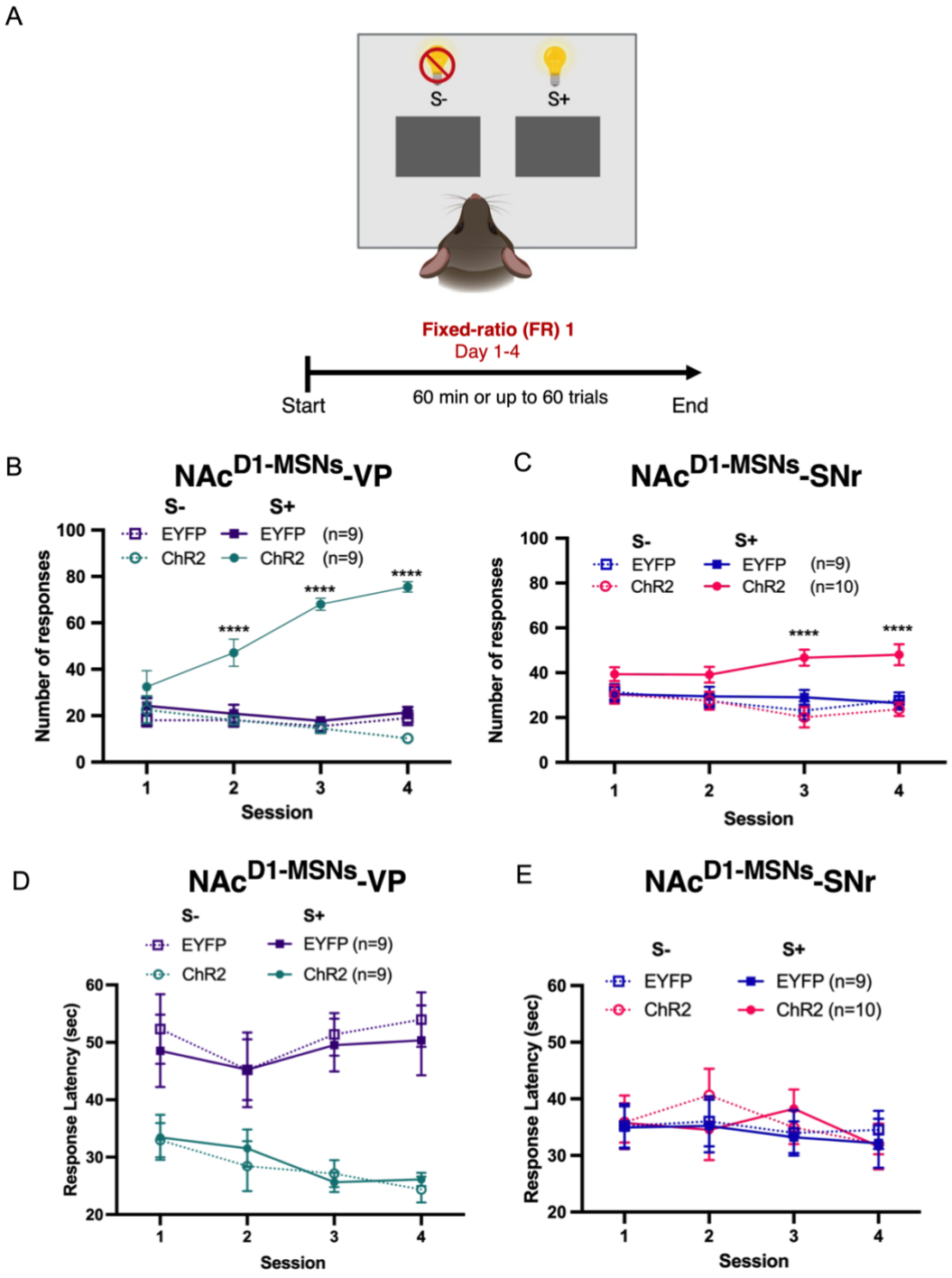

Fig 4. Optogenetic stimulation of SNr and VP-projecting NAc D1-MSNs promotes instrumental self-stimulation. (A) Diagram representation and experimental timeline of the two-choice task in which mice performed instrumental responses at two response panels following a FR1 schedule (1 response produces the outcome), allowing them to choose between self-stimulation by the laser

(S+) or receiving no outcome (S-). (B) The total number of touches at the S- and S+ panels in mice expressing EYFP (n=9) or ChR2 (n=9) in the $NAc^{D1\text{-}MSNs}$-VP pathway and (C) mice expressing EYFP (n=9) or ChR2 (n=9) in the $NAc^{D1\text{-}MSNs}$-SNr pathway. (D) The response latency at the S+ and S- panel during the two-choice optogenetic self-stimulation task in mice expressing either EYFP (n=9) or ChR2 (n=9) in the $NAc^{D1\text{-}MSNs}$-VP pathway and (E) mice expressing EYFP (n=9) or ChR2 (n=10) in the $NAc^{D1\text{-}MSNs}$-SNr pathway. Data represent the mean ± SEM, *post hoc* Bonferroni comparisons were performed with ****$p<0.0001$ indicating statistical significance.

Figure 5.

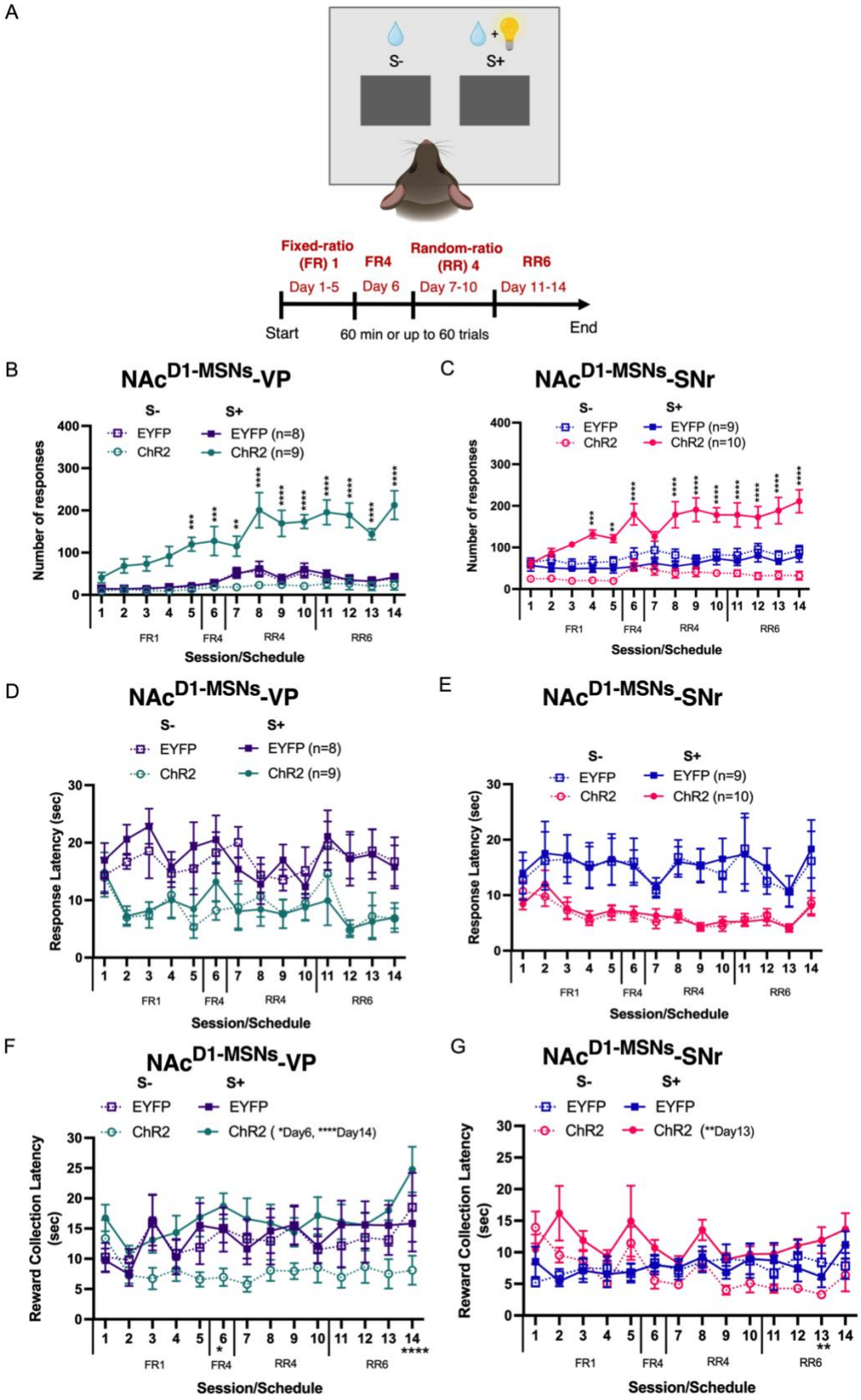
A
S-
S+
Fixed-ratio (FR) 1
FR4
Random-ratio (RR) 4
RR6
Day 1-5
Day 6
Day 7-10
Day 11-14
Start
60 min or up to 60 trials
End
B
NAcD1-MSNs-VP
C
NAcD1-MSNs-SNr
EYFP
ChR2
EYFP (n=8)
ChR2 (n=9)
EYFP (n=9)
ChR2 (n=10)
Number of responses
Session/Schedule
D
NAcD1-MSNs-VP
E
NAcD1-MSNs-SNr
Response Latency (sec)
F
NAcD1-MSNs-VP
ChR2 (*Day6, ****Day14)
G
NAcD1-MSNs-SNr
ChR2 (**Day13)
Reward Collection Latency (sec)
FR1
FR4
RR4
RR6

Fig 5. Optogenetic stimulation of SNr and VP-projecting NAc D1-MSNs enhances instrumental responding for a liquid reinforcer. (A) Diagram representation and experimental timeline of the two-choice task in which mice performed instrumental responses at two response panels under consecutive FR1-RR6 schedules, choosing between a liquid reinforcer paired with laser delivery (S+) or the liquid reinforcer alone (S-). A fixed-ratio 1 (FR1) schedule for 5 days, a FR4 schedule (4 response produces the outcome) for 1 day, a random-ratio 4 (RR4) schedule (a random number of responses between 1-4 produces the outcome) for 4 days, and finally a RR6 schedule (a random number of responses between 1-6 produces the outcome). (B) The total number of touches at the S- and S+ panels during FR1, FR4, RR4, and RR6 sessions in mice receiving optogenetic activation of the $NAc^{D1\text{-}MSNs}$-VP pathway (ChR2; n=9) and control mice (EYFP; n=8) (Three-way RM-ANOVA; ChR2 (S+ vs S-); day5, ***p=0.0005; day6, ***p=0.0002; day7, **p=0.0048; day8-14, ****p<0.0001), and (C) mice receiving optogenetic activation of the NAc $NAc^{D1\text{-}MSNs}$-SNr pathway (ChR2; n=10) and control mice (EYFP; n=9) (Three-way RM-ANOVA; ChR2 (S+ vs S-); day4, ***p=0.0004; day5, **p=0.0030; day6, and day8-14 ****p<0.0001. (D) The response latency at the S+ and S- panel during the two-choice laser and liquid reinforcer task in mice expressing EYFP or ChR2 in the $NAc^{D1\text{-}MSNs}$-VP and (E) $NAc^{D1\text{-}MSNs}$-SNr pathway. (F) The latency to collect the liquid reward at food magazine in the two-choice laser and liquid reinforcer task in mice expressing EYFP or ChR2 in the $NAc^{D1\text{-}MSNs}$-VP and (G) $NAc^{D1\text{-}MSNs}$-SNr pathway. Mice expressing ChR2 exhibited increased latency to collect the liquid reward at food magazine following an S+ response. Data represent the mean ± SEM, *post hoc* Bonferroni comparisons were performed with **p<0.01, ***p<0.001, ****p<0.0001 indicating statistical significance.

Figure 6.

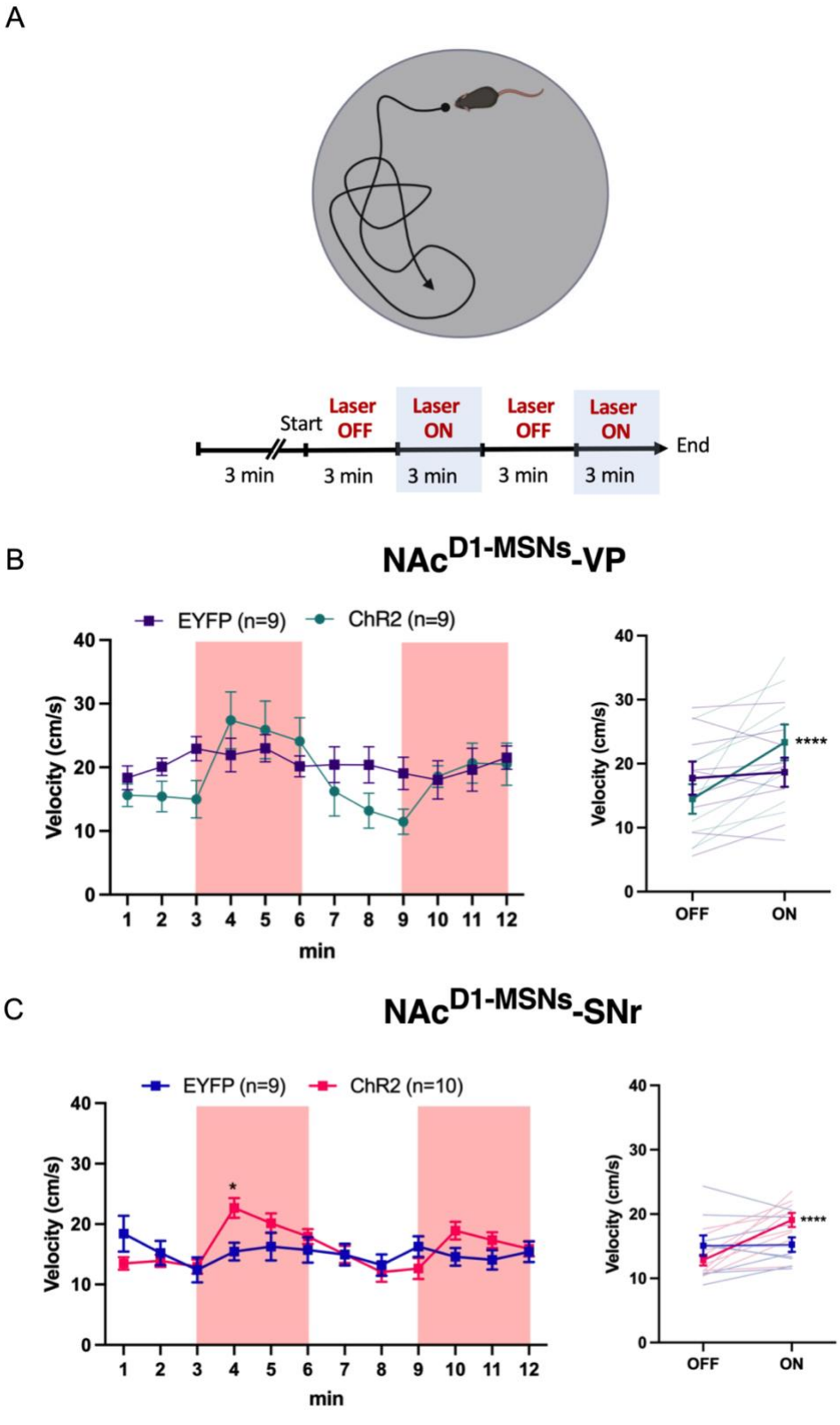
A
Start
Laser OFF
Laser ON
Laser OFF
Laser ON
End
3 min
3 min
3 min
3 min
3 min
B
NAc D1-MSNs -VP
EYFP (n=9)
ChR2 (n=9)
Velocity (cm/s)
min
OFF
ON
****
C
NAc D1-MSNs -SNr
EYFP (n=9)
ChR2 (n=10)
Velocity (cm/s)
min
OFF
ON
*
****

Fig 6. Bilateral stimulation of NAc D1-MSNs projecting to the VP and SNr promotes locomotor activity. (A) Schematic illustration and experimental timeline of the open field test (OFT) in which mice explore a circular chamber during alternating laser OFF and laser ON periods. (B) The velocity of D1-VP mice expressing EYFP (n=9) and ChR2 (n=9) during laser OFF and laser ON epochs throughout 12-minute sessions. The shaded areas represent the time intervals of laser delivery (Left), and the average velocity of D1-VP mice expressing EYFP (n=9), ChR2 (n=9) during both laser OFF and laser ON epochs (Right). (C) The velocity of D1-SNr mice expressing EYFP (n=9) and ChR2 (n=10) during laser OFF and laser ON epochs throughout 12-minute sessions (Two-way RM-ANOVA; EYFP vs ChR2; min 4, *p=0.0313). The shaded areas represent the time intervals of laser delivery (Left), and the average velocity of D1-SNr mice expressing EYFP (n=9), ChR2 (n=10) during both laser OFF and laser ON epochs (Right). Data represent the mean ± SEM, *post hoc* Bonferroni comparisons were performed with *p<0.05, ****p<0.0001 indicating statistical significance.

Figure 7.

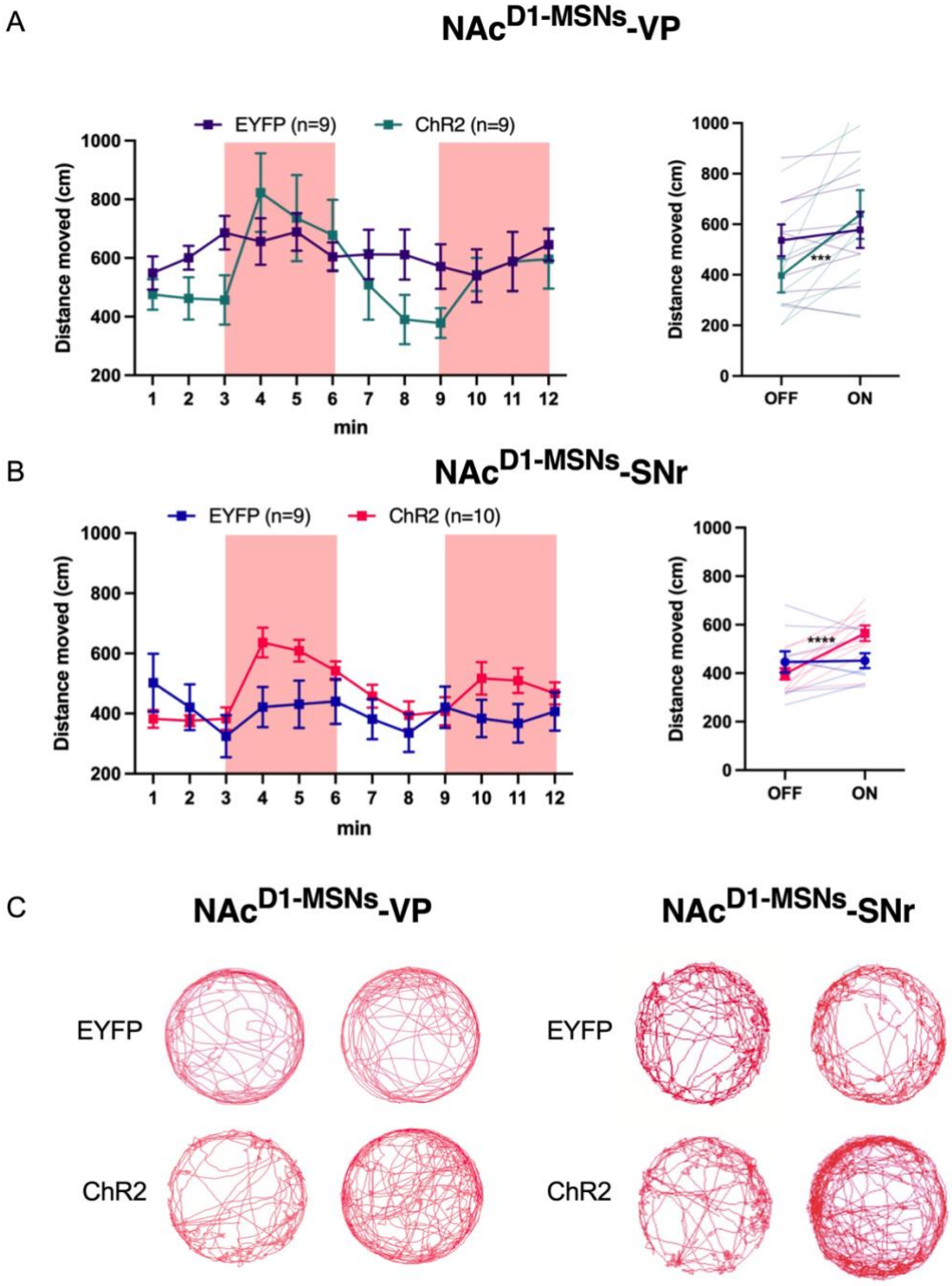

Fig 7. Bilateral stimulation of NAc D1-MSNs projecting to the VP and SNr enhances distance moved activity. (A) The distance moved of D1-VP mice expressing EYFP (n=9) and ChR2 (n=9) during laser OFF and laser ON epochs throughout 12-minute sessions. The shaded areas represent the time intervals of laser delivery (Left), and the average distance moved by D1-VP mice during

laser OFF and laser ON epochs (Right) (Two-way RM-ANOVA; ChR2; ON vs OFF, ***p=0.0005). (B) The distance moved of D1-SNr mice expressing EYFP (n=9) and ChR2 (n=10) during laser OFF and laser ON epochs throughout 12-minute sessions. The shaded areas represent the time intervals of laser delivery (Left), and the average velocity of D1-SNr mice expressing EYFP (n=9), ChR2 (n=10) during both laser OFF and laser ON epochs (Right). (C) Representative movement traces of an individual mouse in the circular chamber during laser OFF (combination between 0-3 min and 6-9 min) and laser ON (combination between 3-6 min and 9-12 min) epochs from D1-VP mice (Left) and D1-SNr mice (Right). Data represent the mean ± SEM, *post hoc* Bonferroni comparisons were performed with ***p<0.001, ****p<0.0001 indicating statistical significance.

Figure 8.

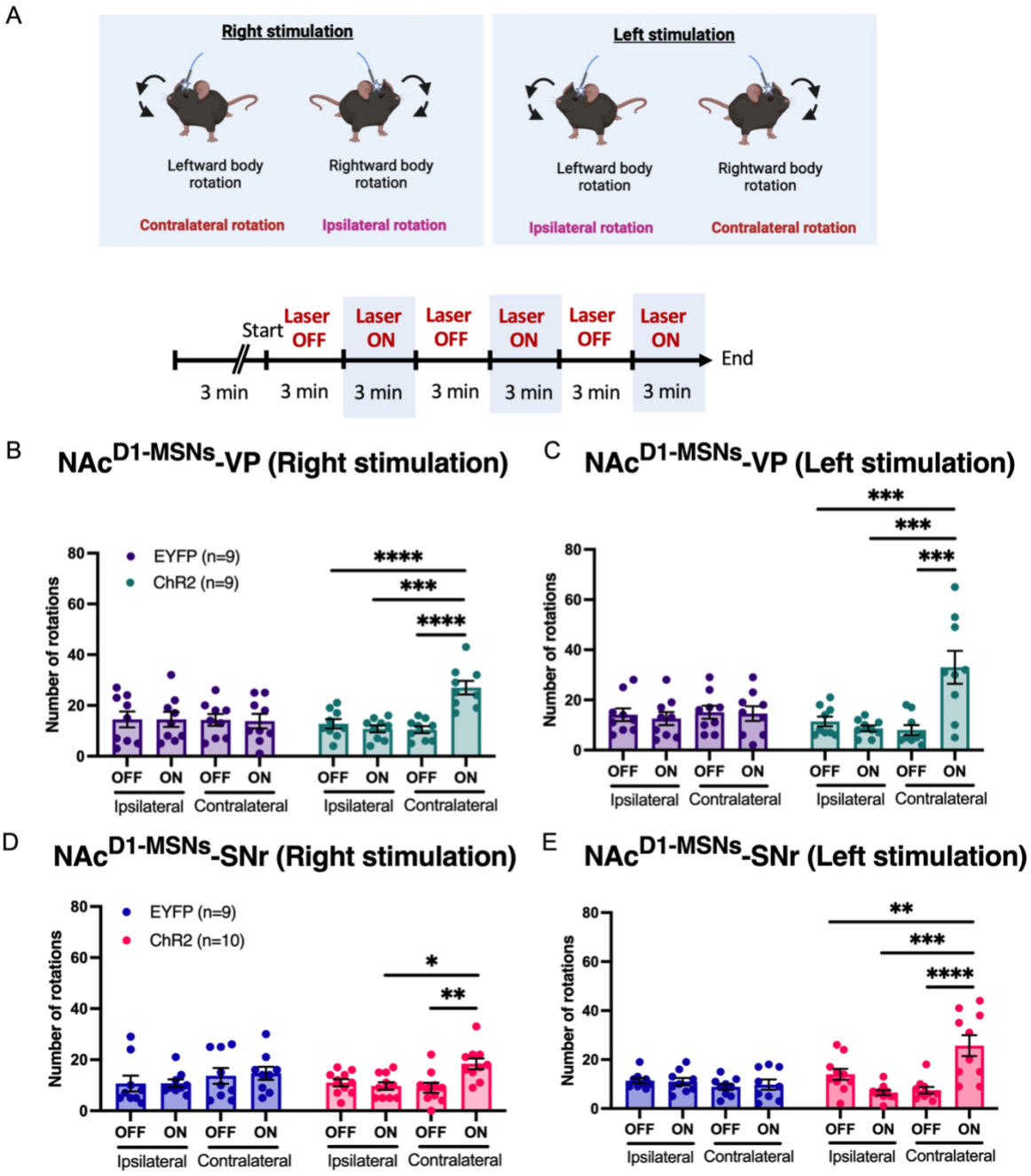

Fig 8. Unilateral stimulation of these pathways promotes contralateral rotations. (A) Illustrative representation of the body rotations observed from unilateral stimulation of either the right-hemisphere or left-hemisphere stimulation (Top) and experimental timeline in which mice received alternating laser OFF and laser ON periods in the open field arena (Bottom). (B) The total number of ipsilateral rotations (rotation on the same side as the stimulation side) and contralateral

rotations (rotation on the opposite side as the stimulation side) during right-hemisphere stimulation (Three-way RM-ANOVA; ChR2; Contralateral (OFF vs ON), ****p<0.0001; Ipsilateral vs Contralateral (ON), ***p=0.0002; Ipsilateral (OFF) vs Contralateral (ON), ****p<0.0001) and (C) left-hemisphere stimulation in D1-VP mice expressing EYFP (n=9) or ChR2 (n=9) (Three-way RM-ANOVA; ChR2; Contralateral (OFF vs ON), ***p=0.0003; Ipsilateral vs Contralateral (ON), ***p=0.0007; Ipsilateral (OFF) vs Contralateral (ON), ***p=0.0005). (D) The total number of ipsilateral rotations (rotation on the same side as the stimulation side) and contralateral rotations (rotation on the opposite side as the stimulation side) during right-hemisphere stimulation (Three-way RM-ANOVA; ChR2; Contralateral (OFF vs ON), **p=0.0039; Ipsilateral vs Contralateral (ON), *p=0.0340) and (E) left-hemisphere stimulation in D1-SNr mice expressing EYFP (n=9) or ChR2 (n=10) (Three-way RM-ANOVA; ChR2; Contralateral (OFF vs ON), ****p<0.0001; Ipsilateral vs Contralateral (ON), ***p=0.0002; Ipsilateral (OFF) vs Contralateral (ON), **p=0.0054). Data represent the mean ± SEM, *post hoc* Bonferroni comparisons were performed with *p<0.05, **p<0.01 ***p<0.001, ****p<0.0001 indicating statistical significance.

Figure 9.

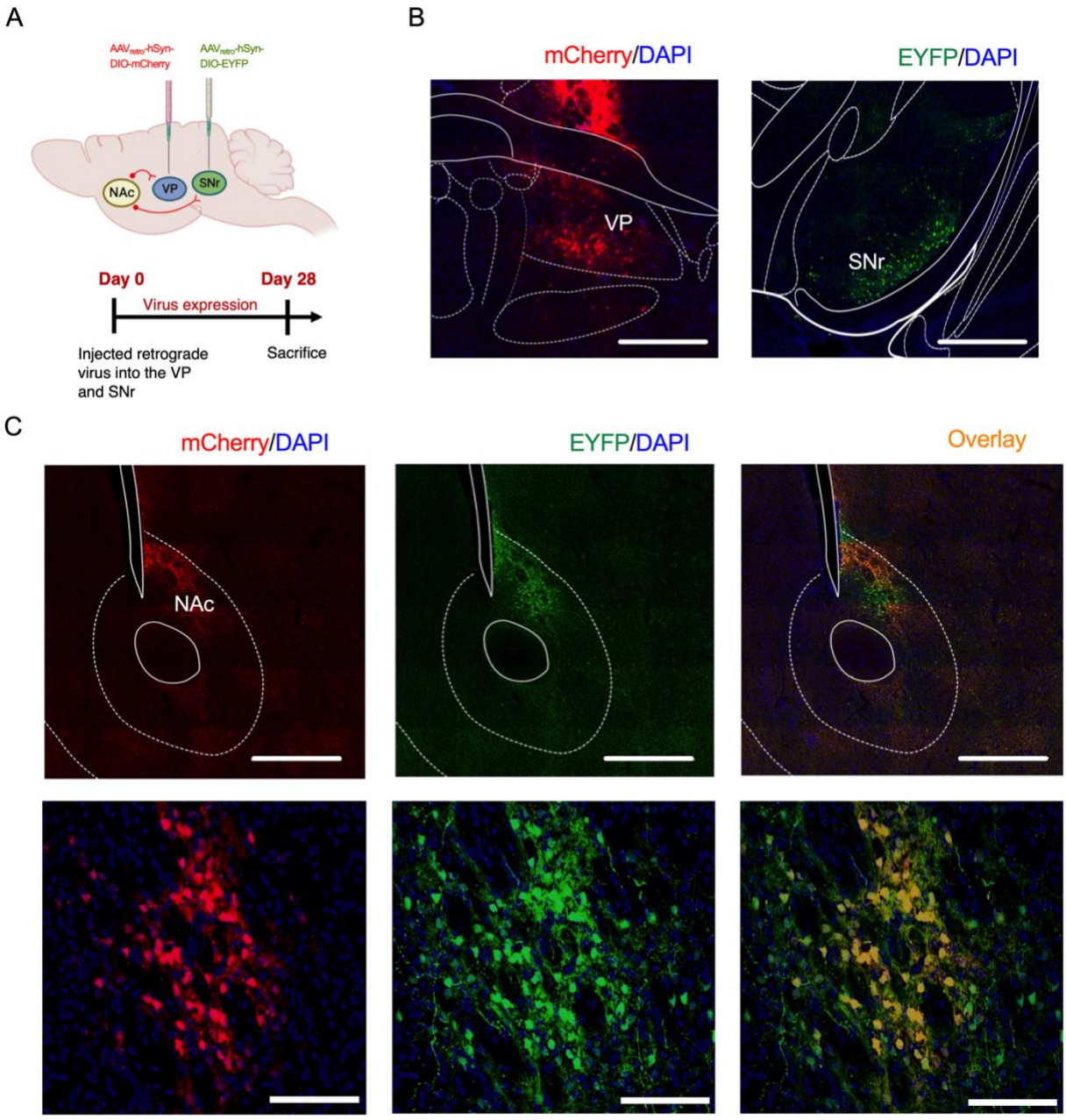

Fig 9. Retrograde tracing VP and SNr-projecting NAc core D1-MSNs. (A) Schematic represents retrograde-targeting of $NAc^{D1\text{-}MSNs}$-VP and $NAc^{D1\text{-}MSNs}$-SNr pathways and timeline for tracing study. (B) Representative coronal brain section of the injection site in VP (mCherry, Red) and SNr (EYFP, Green); nuclear marker (DAPI, Blue): scale bar, 500 μm. (C) Top, detection of monosynaptic connections between VP-projecting NAc D1-MSNs (mCherry, Red; DAPI, Blue)

(Left), SNr-projecting NAc D1-MSNs (EYFP, Green; DAPI, Blue) (Middle) and Overlap labeled neuron (mCherry, Red; EYFP, Green; co-labeled, yellow; DAPI, Blue) with a scale bar 100 μm (Right); Bottom, detection of monosynaptic connections in scale bar, 50 μm.

Figure 10.

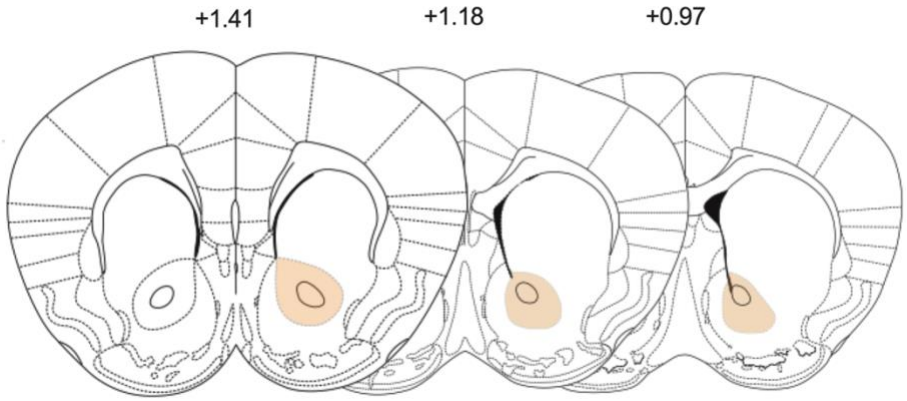

Fig 10. Representative coronal sections depicting the tracing of virus expression in the NAc core at three different anterior-posterior coordinates from the Bregma, located at +1.41 mm, +1.18 mm, and +0.97 mm. The colored indicates the area where I counted the number of activated neurons.

Figure 11.

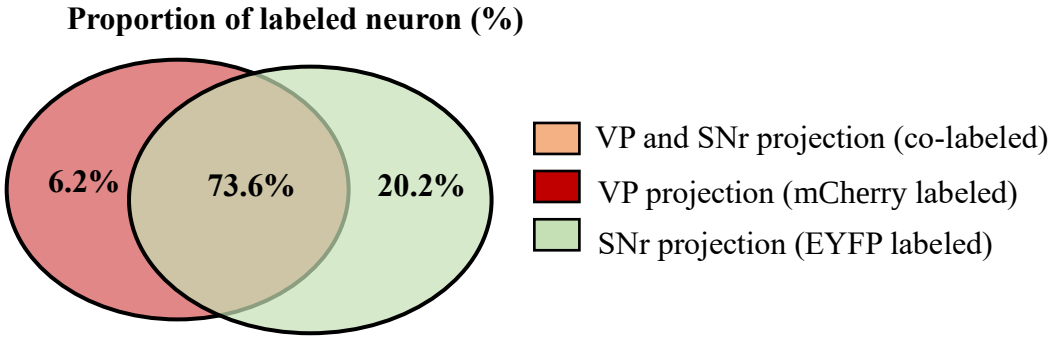

Fig 11. The retrograde tracing of monosynaptic pathway targeting the NAc core reveals a significant proportion of double-labeled neurons in the VP and SNr-projecting NAc D1-MSNs. The percentage of labeled neuron was measured from the total number of activated neurons in the NAc across three D1-Cre mice's brains.

3.4 Discussion

The major finding of these experiments is that both limbic and motor behaviors are modulated by the activity of NAc core D1-MSNs projecting to the VP and the SNr. Optogenetic activation of the $NAc^{D1\text{-}MSN}$-VP and $NAc^{D1\text{-}MSN}$-SNr pathways exhibited direct reinforcing effects and led to an augmentation of forward motion or rotations.

The results revealed that mice displayed a preference for a specific location paired with optogenetic activation of either the $NAc^{D1\text{-}MSN}$–VP or $NAc^{D1\text{-}MSN}$–SNr pathways. Moreover, mice actively responded in the operant chamber in order to receive the optogenetic stimulation alone or in combination with a liquid reward. These findings strongly support earlier studies that have reported that the stimulation of NAc D1-MSNs is rewarding and its ability to enhance the reinforcing effects of natural or drug rewards (Cole et al., 2018; Hikida et al., 2010; Lobo et al., 2010). These studies also suggest that the reinforcing effects observed from cell body stimulation might be mediated through projections from NAc D1-MSNs to both the VP and SNr. This finding contradicts a recent study that reported optogenetic activation of the $NAc^{D1\text{-}MSN}$–VP pathway in mice to be aversive rather than reinforcing (Liu et al., 2022). A possible explanation for this discrepancy may be due to the location of viral injection. Our experiments targeted the NAc core, whereas this previous paper (Liu et al., 2022) largely targeted the NAc shell. Given that opposing patterns of dopamine release have been reported in these two subregions in response to rewarding stimuli, it is plausible that these two subregions may oppositely control limbic functions.

In the self-stimulation operant tasks, a laser stimulation duration of 30 seconds was chosen based on the estimation that this specific duration would effectively enable the mice to rapidly learn the contingency between the laser and the instrumental response. Although directly comparing this stimulation protocol with other rewarding stimuli, such as food, drugs, or environmental stimuli conditioned to rewards, is challenging, previous evidence from *in vivo* calcium imaging has revealed that NAc D1-MSNs exhibited prolonged activation in response to the delivery of sucrose rewards (excitation lasting >5 seconds from the baseline for a single delivery of a 20 mg sucrose pellet or a 20 µl sucrose reward; (Liu et al., 2022) or entry into an environment associated with cocaine (excitation from baseline that slowly decreases over time during the time spent in the cocaine-paired chamber; Calipari et al., 2016). These findings indicate that the 30-second stimulation duration used in my study may elicit a neural response in D1-MSNs

similar to that observed during the prolonged consumption of a substantial reward. Interestingly, previous research has demonstrated that even brief (1 s) stimulation of D1-MSNs cell bodies in the NAc is enough to sustain optogenetic self-stimulation (Cole et al., 2018). However, it should be taken into consideration that this study largely targeted D1-MSNs in the medial shell region of the NAc, which primarily sends projections to dopaminergic neurons of the VTAs rather than to the SNr. As a result, this may lead to a stronger rewarding effect. Further investigation of the impact of various optogenetic stimulation protocols in specific subregions of the NAc could provide additional insights into the role of NAc D1-MSNs in modulating reward-related behaviors.

The observation that activating both the $NAc^{D1\text{-}MSN}$–VP and $NAc^{D1\text{-}MSN}$–SNr pathways leads to enhanced motor activity in an open field arena is consistent with previous research. It was shown that stimulating the axon terminals of NAc D1-MSNs in the VP increases locomotor activity (Napier et al., 1995) and another study has demonstrated that optogenetic activation of the axon terminals of NAc core D1-MSNs in the SNr lead to enhanced neural activity in the motor cortex (M1) (Aoki et al., 2019). In the current study, it is possible that the enhances in velocity observed after bilateral stimulation and contralateral turning observed after unilateral stimulation may be attributed to a facilitation of M1 activity. Furthermore, recent findings have shown that the limbic and motor basal ganglia circuits may converge within the thalamus, with overlapping patterns of innervation from both medial and lateral SNr regions, which in turn receive input from limbic-related nucleus accumbens and ventral pallidum areas, as well as motor-related dorsolateral striatum areas (Aoki et al., 2019; Foster et al., 2021; Hunnicutt et al., 2014; Macpherson et al., 2021). Importantly, even though motor activity was enhanced, our finding that instrumental responding in the self-stimulation experiments predominantly selective to the stimulation-paired panel rather than showing a general increase in responses at both panels, indicates that the findings of self-stimulation experiments are not simply the result of augmented motor activity.

A noteworthy limitation of the current study is that it only explored the behavioral effect of $NAc^{D1\text{-}MSN}$-SNr pathway stimulation, without investigating inhibition, was investigated. Previous research has shown that optogenetic stimulation and inhibition of NAc D1-MSN cell bodies can exert bilateral control reward and aversion, respectively. It is plausible to predict that optogenetic inhibition of the $NAc^{D1\text{-}MSN}$-VP and $NAc^{D1\text{-}MSN}$-SNr pathways could potentially induce aversion in rt-PP and self-stimulation studies. This is supported by evidence showing that the knockout of dopamine D1 receptors in mice lead to the elimination of prereward anticipatory

firing of NAc neurons during a place learning task and impairs intracranial self-stimulation responding (Tran et al., 2005). Interestingly, while chemicogenetic activation of NAc D1-MSNs has been demonstrated to enhance locomotor activity, inhibiting NAc D1-MSNs did not result in any changes in locomotion (Zhu et al., 2016). Consequently, future investigations that focus on exploring the behavioral effects of inhibiting NAc core D1-MSNs projecting to the VP or SNr, will help to verify whether these pathways can indeed bidirectionally regulate both limbic and motor functions.

Interestingly, various psychiatric conditions associated with alterations in NAc D1-MSNs signaling exhibit abnormal behaviors related to both limbic-related and motor-related behaviors. Indeed, locomotor sensitization, which involves an increase in motor activity, is a prevalent initial behavioral response observed in various addictive drugs, including methamphetamine, cocaine, ketamine, alcohol, nicotine, and opioids (Grahame et al., 2000; Ranaldi et al., 2009; Robinson & Berridge, 1993; Strong et al., 2017; Vezina, 2004), and has been reported to align with excessive dopamine release in the NAc core and enhanced activity in NAc D1-MSNs (Di Chiara, 2002; Van Zessen et al., 2021). On the contrary, motor retardation is a common observed symptom in both major depression and the depressed phase of bipolar disorder in humans (Buyukdura et al., 2011; Caligiuri & Ellwanger, 2000). Furthermore, this symptom has been observed in mouse model of depression, especially in chronic social defeat models (Huang et al., 2013; Ota et al., 2018). Consequently, chronic social defeat in mice is linked to decrease NAc dopamine release and diminished excitatory synaptic input onto NAc D1-MSNs (Francis & Lobo, 2017). This effect may potentially lead to a reduction in signaling through the $NAc^{D1\text{-}MSN}$–VP and $NAc^{D1\text{-}MSN}$–SNr pathways. Although the evidence supporting a shared underlying cause for the limbic and motor symptoms of psychiatric disorders, including substance abuse and depression, is not yet firmly established, these findings propose that the $NAc^{D1\text{-}MSN}$–VP and $NAc^{D1\text{-}MSN}$–SNr pathways may serve as attractive targets for future research.

Collectively, these findings provide evidence that the activity of NAc core D1-MSNs projecting to the VP and SNr can incluence both reinforcement and motor behavior, suggesting that these pathways play multifunctional roles. Moreover, these studies further support the idea of the limbic and motor basal ganglia circuits converging, potentially offering insights into the neural

circuit underlying the common cooccurrence of limbic and motor symptoms in psychiatric conditions such as depression and substance abuse.

Chapter 4

General Discussion

The research in this thesis has helped to clarify the functional roles of NAc D1- and D2-MSNs in cognitive, limbic, and motor control. Specifically, a new role for NAc D2-MSNs in error signaling was identified. This enabled mice to learn from their past mistakes and to use environmental cues to avoid inappropriate behaviors. Additionally, it was revealed that NAc D1-MSNs projecting to the SNr and VP both contribute to reinforcement and motor behavior. The possible physiological mechanisms underlying these findings, the limitation of these studies, and future directions for this research are discussed below.

4.1 The role of the NAc in cue-guided based decision-making

As described in section 2.3, it was identified that NAc D2-MSNs play an important role in learning to avoid making mistakes, thus guiding better decision-making in future. Using optogenetic suppression of NAc cell activity during specific periods of the test session (ITI, Cue, Outcome), it was revealed that NAc D2-MSNs activation after response errors is necessary for optimizing future decision-making behavior. This data is in agreement with previous evidence demonstrating local DA release onto D2-MSNs in NAc is necessary for inhibiting risk-taking behavior (Zalocusky et al., 2016), and avoiding non-rewarded strategies (Frank, 2006; Frank et al., 2004; Nakanishi et al., 2014) or negative outcomes (Mirenowicz & Schultz, 1996; Setlow et al., 2003).The recognition of these cells as “error signal generators” could guide the development of novel treatments for mental health disorders linked to compromised decision-making skills.

4.2 NAc D1-MSN pathways and limbic control

As shown in sections 3.3.1 and 3.3.2, it was revealed that NAc D1-MSNs projecting to either the SNr or VP contribute to limbic control. Indeed, optogenetic stimulation of $NAc^{D1\text{-}MSN}$-VP or $NAc^{D1\text{-}MSN}$-SNr pathways was able to drive reinforcement in real-time place preference and self-stimulation tests.

These findings support previous studies that have linked the VP to limbic control. It has previously been reported that GABAergic VP neurons encode the motivated approach behavior towards rewarding stimuli (Stephenson-Jones et al., 2020). Accordingly, inactivation of the VP by injection of muscimol (a $GABA_A$ agonist) impairs reward-related behaviors (Saga et al., 2022; Tachibana & Hikosaka, 2012). Based on the existing evidence that the VP can elicit both rewarding and aversion responses (Faget et al., 2018; Tooley et al., 2018), it is possible that the rewarding-related behaviors observed in our study could be influenced by the suppression of VP GLUT neurons activity. This suppression occurs when stimulating NAc D1-MSNs and may lead to impaired inhibition of reward effects.

Clinical evidence has similarly linked the VP to limbic control. Dysfunction of the VP has been observed in several psychiatric conditions associated with abnormal reward processing and motivated behaviors, including addiction and substance use disorders (Kupchik & Prasad, 2021; Scofield et al., 2016; Volkow et al., 2019), as well as depression (Francis & Lobo, 2017; Knowland et al., 2017; Soares-Cunha & Heinsbroek, 2023). It's important to note that the involvement of the VP in limbic disorder is complex, and more research is needed to fully understand its precise role and mechanism.

Previously, little was known about the role of the SNr in reinforcement and reward-related behavior. These studies provide evidence that connections between the NAc and the SNr are able to modulate limbic functions and suggest that this pathway, alongside the NAc D1-MSNs projection to the VP, might provide an efficacious target for the development of novel therapeutics targeted at limbic disorders.

4.3 NAc D1-MSN pathways and motor control

The motor experiments in section 3.3.3 indicate that stimulation of NAc D1-MSN projecting to either the SNr or VP is able to enhance locomotor activity. These findings suggest that both $NAc^{D1\text{-}MSN}$-VP and $NAc^{D1\text{-}MSN}$-SNr pathways may contribute to the motor cortico-basal ganglia-thalamo-cortical loop circuits.

These findings provide support for clinical evidence that has linked disruption of the VP and SNr to motor disorders. The VP has been implicated in various motor disorders, although its exact role in these conditions is still being investigated. Degeneration of the basal ganglia including VP can cause Huntington's disease that contributes to motor symptoms such as chorea (involuntary

movements) and dystonia (sustained muscle contraction) (Graybiel, 2000; Sanger et al., 2010). In addition, SNr is involved in hyperkinetic movement disorders characterized by excessive or abnormal involuntary movements (Lai et al., 2021), as well as in Parkinson's disease (Sitzia et al., 2020).

The findings of the current experiments indicate that the $NAc^{D1\text{-}MSN}$-VP and $NAc^{D1\text{-}MSN}$-SNr projection pathways might provide efficacious targets for the treatment of motor-related disorders.

4.4 Limitations and Future work

4.4.1 Further investigation of the functional role of D1- and D2-MSNs within specific NAc subregions

Previous evidence has indicated that different subregions of the NAc receive different innervation. Indeed, recent evidence has indicated that innervation of D1- and D2-MSNs differs between NAc core and NAc shell regions, with NAc core neurons receiving strong innervation from the anterior cortex and NAc shell regions receiving strong innervation from the lateral hypothalamus (Li et al., 2018). Similarly, it has been reported that the release of dopamine in response to rewarding or aversive stimuli also differs between NAc subregions, with increased and decreases in dopamine observed in response to rewarding and aversive stimuli, respectively, in the NAc core and lateral shell, but increased dopamine to both rewarding and aversive stimuli in the medial shell(de Jong et al., 2019). It is thought that these differences in innervation and neurotransmitter release likely confer different functional roles to neurons in these subregions. Indeed, it has recently been reported that activation of D2-MSNs in the dorsomedial shell induces reward, while activation of those in the dorsolateral shell induces aversion (Yao et al., 2021).

In the experiments presented in this thesis, manipulations were largely restricted to the NAc dorsal core region. Therefore, it is still unknown whether the identified role of NAc core D2-MSNs in error signaling also extends to D2-MSNs within the shell subregion. Similarly, the same is true for the roles of NAc core D1-MSNs projecting to the VP and SNr in limbic and motor control identified in chapter 3. Additionally, as recent evidence has indicated that innervation of the NAc core differs between dorsal and ventral core regions (Ma et al., 2020), it remains to be established whether the findings of experiments are true only of D1- and D2-MSNs in NAc dorsal

core region. Further investigation of the roles of D1- and D2-MSNs within various subregions of the NAc core and shell is needed to elucidate the complex control of cognitive, limbic, and motor functions by the NAc.

4.4.2 Further investigation of NAc D1- and D2-MSNs at the single cell level

Here, it was revealed that NAc core D2-MSNs play an important role in error signaling while NAc core D1-MSNs projecting to either the SNr or VP play important roles in reinforcement and motor control. However, a limitation of the methodological approach used in these studies is that optogenetic manipulation targeted NAc D1- and D2-MSN populations as a whole (or $NAc^{D1\text{-}MSN}$-VP and $NAc^{D1\text{-}MSN}$-SNr populations as a whole), potentially concealing heterogeneity within these cell populations. Indeed, single-cell RNA sequencing studies have recently revealed that there is a large degree of molecular and cellular heterogeneity within NAc D1- and D2-MSNs, with up to 15 different subtypes of D1-MSN and 9 different subtypes of D2-MSN being identified (Chen et al., 2021). In recent years, studies have begun to investigate how these subtypes of NAc D1- and D2-MSNs may demonstrate specific and sometimes unexpected functional roles. This includes the identification of subpopulations of D1-MSNs signaling aversive stimuli (Kim et al., 2020), in contrast to their canonical role in reward processing.

With the development of transactional viral expression techniques that enable the labeling of particular cell types that are activated at specific time periods (Kim et al., 2020; Yu et al., 2022), as well as the increased use of single-cell resolution in-vivo imaging (Nishioka et al., 2023), I am now beginning to understand how ensembles of D1- and D2-MSNs contribute to specific aspects of learning behavior. Further use of such technologies will help to better elucidate the role of subpopulations of NAc D1- and D2-MSNs in controlling cognitive, limbic, and motor functions.

Reference

Albin, R. L., Young, A. B., & Penney, J. B. (1989). The functional anatomy of basal ganglia disorders. *Trends in Neurosciences*, *12*(10). https://doi.org/10.1016/0166-2236(89)90074-X

Alcantara, A. A., Chen, V., Herring, B. E., Mendenhall, J. M., & Berlanga, M. L. (2003). Localization of dopamine D2 receptors on cholinergic interneurons of the dorsal striatum and nucleus accumbens of the rat. *Brain Research*, *986*(1–2). https://doi.org/10.1016/S0006-8993(03)03165-2

Alexander, G. E., & Crutcher, M. D. (1990). Functional architecture of basal ganglia circuits: neural substrates of parallel processing. In *Trends in Neurosciences* (Vol. 13, Issue 7). https://doi.org/10.1016/0166-2236(90)90107-L

Alexander, G. E., DeLong, M. R., & Strick, P. L. (1986). Parallel organization of functionally segregated circuits linking basal ganglia and cortex. *Annual Review of Neuroscience*, *VOL. 9*. https://doi.org/10.1146/annurev.ne.09.030186.002041

Ambroggi, F., Ghazizadeh, A., Nicola, S. M., & Fields, H. L. (2011). Roles of Nucleus Accumbens Core and Shell in Incentive-Cue Responding and Behavioral Inhibition. *Journal of Neuroscience*, *31*(18). https://doi.org/10.1523/JNEUROSCI.6491-10.2011

Antal, M., Beneduce, B. M., & Regehr, W. G. (2014). The substantia nigra conveys target-dependent excitatory and inhibitory outputs from the basal ganglia to the thalamus. *Journal of Neuroscience*, *34*(23). https://doi.org/10.1523/JNEUROSCI.0236-14.2014

Aoki, S., Smith, J. B., Li, H., Yan, X., Igarashi, M., Coulon, P., Wickens, J. R., Ruigrok, T. J., & Jin, X. (2019). An open cortico-basal ganglia loop allows limbic control over motor output via the nigrothalamic pathway. *ELife*. https://doi.org/10.7554/eLife.49995.001

Atasoy, D., Aponte, Y., Su, H. H., & Sternson, S. M. (2008). A FLEX switch targets channelrhodopsin-2 to multiple cell types for imaging and long-range circuit mapping. *Journal of Neuroscience*, *28*(28). https://doi.org/10.1523/JNEUROSCI.1954-08.2008

Balleine, B. W. (2019). The Meaning of Behavior: Discriminating Reflex and Volition in the Brain. In *Neuron* (Vol. 104, Issue 1). https://doi.org/10.1016/j.neuron.2019.09.024

Balleine, B. W., Delgado, M. R., & Hikosaka, O. (2007). The role of the dorsal striatum in reward and decision-making. In *Journal of Neuroscience* (Vol. 27, Issue 31). https://doi.org/10.1523/JNEUROSCI.1554-07.2007

Bornstein, A. M., & Daw, N. D. (2011). Multiplicity of control in the basal ganglia: Computational roles of striatal subregions. In *Current Opinion in Neurobiology* (Vol. 21, Issue 3). https://doi.org/10.1016/j.conb.2011.02.009

Boyden, E. S., Zhang, F., Bamberg, E., Nagel, G., & Deisseroth, K. (2005). Millisecond-timescale, genetically targeted optical control of neural activity. *Nature Neuroscience*, *8*(9). https://doi.org/10.1038/nn1525

Buyukdura, J. S., McClintock, S. M., & Croarkin, P. E. (2011). Psychomotor retardation in depression: Biological underpinnings, measurement, and treatment. In *Progress in Neuro-Psychopharmacology and Biological Psychiatry* (Vol. 35, Issue 2). https://doi.org/10.1016/j.pnpbp.2010.10.019

Caligiuri, M. P., & Ellwanger, J. (2000). Motor and cognitive aspects of motor retardation in depression. *Journal of Affective Disorders*, *57*(1–3). https://doi.org/10.1016/S0165-0327(99)00068-3

Calipari, E. S., Bagot, R. C., Purushothaman, I., Davidson, T. J., Yorgason, J. T., Peña, C. J., Walker, D. M., Pirpinias, S. T., Guise, K. G., Ramakrishnan, C., Deisseroth, K., & Nestler, E. J. (2016). In vivo imaging identifies temporal signature of D1 and D2 medium spiny neurons in cocaine reward. *Proceedings of the National Academy of Sciences of the United States of America*, *113*(10). https://doi.org/10.1073/pnas.1521238113

Castro, D. C., & Bruchas, M. R. (2019a). A Motivational and Neuropeptidergic Hub: Anatomical and Functional Diversity within the Nucleus Accumbens Shell. In *Neuron* (Vol. 102, Issue 3, pp. 529–552). Cell Press. https://doi.org/10.1016/j.neuron.2019.03.003

Castro, D. C., & Bruchas, M. R. (2019b). A Motivational and Neuropeptidergic Hub: Anatomical and Functional Diversity within the Nucleus Accumbens Shell. In *Neuron* (Vol. 102, Issue 3). https://doi.org/10.1016/j.neuron.2019.03.003

Chen, R., Blosser, T. R., Djekidel, M. N., Hao, J., Bhattacherjee, A., Chen, W., Tuesta, L. M., Zhuang, X., & Zhang, Y. (2021). Decoding molecular and cellular heterogeneity of mouse nucleus accumbens. *Nature Neuroscience*, *24*(12), 1757–1771. https://doi.org/10.1038/s41593-021-00938-x

Chow, B. Y., Han, X., Dobry, A. S., Qian, X., Chuong, A. S., Li, M., Henninger, M. A., Belfort, G. M., Lin, Y., Monahan, P. E., & Boyden, E. S. (2010). High-performance genetically targetable optical neural silencing by light-driven proton pumps. *Nature*, *463*(7277). https://doi.org/10.1038/nature08652

Chuhma, N., Mingote, S., Moore, H., & Rayport, S. (2014). Dopamine neurons control striatal cholinergic neurons via regionally heterogeneous dopamine and glutamate signaling. *Neuron*, *81*(4), 901–912. https://doi.org/10.1016/j.neuron.2013.12.027

Churchill, L., Klitenick, M. A., & Kalivas, P. W. (1998). Dopamine depletion reorganizes projections from the nucleus accumbens and ventral pallidum that mediate opioid-induced motor activity. *Journal of Neuroscience*, *18*(19). https://doi.org/10.1523/jneurosci.18-19-08074.1998

Claudia Pama, E. A., Colzato, L. S., & Hommel, B. (2013). Optogenetics as a neuromodulation tool in cognitive neuroscience. *Frontiers in Psychology*, *4*(SEP). https://doi.org/10.3389/fpsyg.2013.00610

Cole, S. L., Robinson, M. J. F., & Berridge, K. C. (2018). Optogenetic self-stimulation in the nucleus accumbens: D1 reward versus D2 ambivalence. *PLoS ONE*, *13*(11). https://doi.org/10.1371/journal.pone.0207694

Constantinople, C. M., Piet, A. T., & Brody, C. D. (2019). An Analysis of Decision under Risk in Rats. *Current Biology*, *29*(12). https://doi.org/10.1016/j.cub.2019.05.013

Creed, M., Ntamati, N. R., Chandra, R., Lobo, M. K., & Lüscher, C. (2016). Convergence of Reinforcing and Anhedonic Cocaine Effects in the Ventral Pallidum. *Neuron*, *92*(1), 214–226. https://doi.org/10.1016/j.neuron.2016.09.001

Crespo, J. A., Stöckl, P., Zorn, K., Saria, A., & Zernig, G. (2008). Nucleus accumbens core acetylcholine is preferentially activated during acquisition of drug- vs food-reinforced behavior. *Neuropsychopharmacology*, *33*(13). https://doi.org/10.1038/npp.2008.48

de Jong, J. W., Afjei, S. A., Pollak Dorocic, I., Peck, J. R., Liu, C., Kim, C. K., Tian, L., Deisseroth, K., & Lammel, S. (2019). A Neural Circuit Mechanism for Encoding Aversive Stimuli in the Mesolimbic Dopamine System. *Neuron*, *101*(1). https://doi.org/10.1016/j.neuron.2018.11.005

Deisseroth, K., Feng, G., Majewska, A. K., Miesenböck, G., Ting, A., & Schnitzer, M. J. (2006). Next-generation optical technologies for illuminating genetically targeted brain circuits.

Journal of Neuroscience, *26*(41), 10380–10386. https://doi.org/10.1523/JNEUROSCI.3863-06.2006

DeLong, M. R. (1990). Primate models of movement disorders of basal ganglia origin. In *Trends in Neurosciences* (Vol. 13, Issue 7). https://doi.org/10.1016/0166-2236(90)90110-V

DeLong, M. R., & Georgopoulos, A. P. (1981). Motor Functions of the Basal Ganglia. In *Comprehensive Physiology* (pp. 1017–1061). Wiley. https://doi.org/10.1002/cphy.cp010221

Di Chiara, G. (2002). Nucleus accumbens shell and core dopamine: Differential role in behavior and addiction. *Behavioural Brain Research*, *137*(1–2). https://doi.org/10.1016/S0166-4328(02)00286-3

Dreher, J. K., & Jackson, D. M. (1989). Role of D1 and D2 dopamine receptors in mediating locomotor activity elicited from the nucleus accumbens of rats. *Brain Research*, *487*(2). https://doi.org/10.1016/0006-8993(89)90831-7

Faget, L., Zell, V., Souter, E., McPherson, A., Ressler, R., Gutierrez-Reed, N., Yoo, J. H., Dulcis, D., & Hnasko, T. S. (2018). Opponent control of behavioral reinforcement by inhibitory and excitatory projections from the ventral pallidum. *Nature Communications*, *9*(1). https://doi.org/10.1038/s41467-018-03125-y

Floresco, S. B. (2015). The nucleus accumbens: An interface between cognition, emotion, and action. *Annual Review of Psychology*, *66*. https://doi.org/10.1146/annurev-psych-010213-115159

Foster, N. N., Barry, J., Korobkova, L., Garcia, L., Gao, L., Becerra, M., Sherafat, Y., Peng, B., Li, X., Choi, J. H., Gou, L., Zingg, B., Azam, S., Lo, D., Khanjani, N., Zhang, B., Stanis, J., Bowman, I., Cotter, K., … Dong, H. W. (2021). The mouse cortico–basal ganglia–thalamic network. *Nature*, *598*(7879). https://doi.org/10.1038/s41586-021-03993-3

Francis, T. C., & Lobo, M. K. (2017). Emerging Role for Nucleus Accumbens Medium Spiny Neuron Subtypes in Depression. In *Biological Psychiatry* (Vol. 81, Issue 8). https://doi.org/10.1016/j.biopsych.2016.09.007

Frank, M. J. (2006). Hold your horses: A dynamic computational role for the subthalamic nucleus in decision making. *Neural Networks*, *19*(8). https://doi.org/10.1016/j.neunet.2006.03.006

Frank, M. J., Seeberger, L. C., & O'Reilly, R. C. (2004). By carrot or by stick: Cognitive reinforcement learning in Parkinsonism. *Science*, *306*(5703). https://doi.org/10.1126/science.1102941

Gallo, E. F., Meszaros, J., Sherman, J. D., Chohan, M. O., Teboul, E., Choi, C. S., Moore, H., Javitch, J. A., & Kellendonk, C. (2018). Accumbens dopamine D2 receptors increase motivation by decreasing inhibitory transmission to the ventral pallidum. *Nature Communications*, *9*(1). https://doi.org/10.1038/s41467-018-03272-2

Gerashchenko, D., Blanco-Centurion, C. A., Miller, J. D., & Shiromani, P. J. (2006). Insomnia following hypocretin2-saporin lesions of the substantia nigra. *Neuroscience*, *137*(1). https://doi.org/10.1016/j.neuroscience.2005.08.088

Gerfen, C. R., Engber, T. M., Mahan, L. C., Susel, Z., Chase, T. N., Monsma, F. J., & Sibley, D. R. (1990a). D1 and D2 dopamine receptor-regulated gene expression of striatonigral and striatopallidal neurons. *Science*, *250*(4986). https://doi.org/10.1126/science.2147780

Gerfen, C. R., Engber, T. M., Mahan, L. C., Susel, Z., Chase, T. N., Monsma, F. J., & Sibley, D. R. (1990b). D1 and D2 dopamine receptor-regulated gene expression of striatonigral and striatopallidal neurons. *Science*, *250*(4986). https://doi.org/10.1126/science.2147780

Gerfen, C. R., & Surmeier, D. J. (2011). Modulation of striatal projection systems by dopamine. *Annual Review of Neuroscience*, *34*. https://doi.org/10.1146/annurev-neuro-061010-113641

gerfen1990. (n.d.).

Gibson, G. D., Prasad, A. A., Jean-Richard-dit-Bressel, P., Yau, J. O. Y., Millan, E. Z., Liu, Y., Campbell, E. J., Lim, J., Marchant, N. J., Power, J. M., Killcross, S., Lawrence, A. J., & McNally, G. P. (2018). Distinct Accumbens Shell Output Pathways Promote versus Prevent Relapse to Alcohol Seeking. *Neuron*, *98*(3). https://doi.org/10.1016/j.neuron.2018.03.033

Grace, A. A., Floresco, S. B., Goto, Y., & Lodge, D. J. (2007). Regulation of firing of dopaminergic neurons and control of goal-directed behaviors. In *Trends in Neurosciences* (Vol. 30, Issue 5, pp. 220–227). https://doi.org/10.1016/j.tins.2007.03.003

Grahame, N. J., Rodd-Henricks, K., Li, T. K., & Lumeng, L. (2000). Ethanol locomotor sensitization, but not tolerance correlates with selection for alcohol preference in high- and low-alcohol preferring mice. *Psychopharmacology*, *151*(2–3). https://doi.org/10.1007/s002130000388

Graybiel, A. M. (n.d.). *Primer The basal ganglia*.

Groenewegen, H. J., Wright, C. I., Beijer, A. V. J., & Voorn, P. (1999). Convergence and segregation of ventral striatal inputs and outputs. *Annals of the New York Academy of Sciences*, *877*. https://doi.org/10.1111/j.1749-6632.1999.tb09260.x

Guillaumin, A., Serra, G. Pietro, Georges, F., & Wallén-Mackenzie, Å. (2021). Experimental investigation into the role of the subthalamic nucleus (STN) in motor control using optogenetics in mice. *Brain Research*, *1755*. https://doi.org/10.1016/j.brainres.2020.147226

Haber, S. N. (2003). The primate basal ganglia: Parallel and integrative networks. *Journal of Chemical Neuroanatomy*, *26*(4). https://doi.org/10.1016/j.jchemneu.2003.10.003

Haber, S. N. (2016). Corticostriatal circuitry. *Dialogues in Clinical Neuroscience*, *18*(1). https://doi.org/10.1007/978-1-4614-6434-1_135-1

Han, X., Chow, B. Y., Zhou, H., Klapoetke, N. C., Chuong, A., Rajimehr, R., Yang, A., Baratta, M. V., Winkle, J., Desimone, R., & Boyden, E. S. (2011). A high-light sensitivity optical neural silencer: Development and application to optogenetic control of non-human primate cortex. *Frontiers in Systems Neuroscience*, *APRIL 2011*. https://doi.org/10.3389/fnsys.2011.00018

Heimer, L., Zahm, D. S., Churchill, L., Kalivas, P. W., & Wohltmann, C. (1991). Specificity in the projection patterns of accumbal core and shell in the rat. *Neuroscience*, *41*(1). https://doi.org/10.1016/0306-4522(91)90202-Y

Hikida, T., Kimura, K., Wada, N., Funabiki, K., & Nakanishi Shigetada, S. (2010). Distinct Roles of Synaptic Transmission in Direct and Indirect Striatal Pathways to Reward and Aversive Behavior. *Neuron*, *66*(6), 896–907. https://doi.org/10.1016/j.neuron.2010.05.011

Hikida, T., Yawata, S., Yamaguchi, T., Danjo, T., Sasaoka, T., Wang, Y., & Nakanishi, S. (2013). Pathway-specific modulation of nucleus accumbens in reward and aversive behavior via selective transmitter receptors. *Proceedings of the National Academy of Sciences of the United States of America*, *110*(1). https://doi.org/10.1073/pnas.1220358110

Horner, A. E., Heath, C. J., Hvoslef-Eide, M., Kent, B. A., Kim, C. H., Nilsson, S. R. O., Alsiö, J., Oomen, C. A., Holmes, A., Saksida, L. M., & Bussey, T. J. (2013). The touchscreen operant platform for testing learning and memory in rats and mice. *Nature Protocols*, *8*(10). https://doi.org/10.1038/nprot.2013.122

Huang, G. B., Zhao, T., Muna, S. S., Bagalkot, T. R., Jin, H. M., Chae, H. J., & Chung, Y. C. (2013). Effects of chronic social defeat stress on behaviour, endoplasmic reticulum proteins

and choline acetyltransferase in adolescent mice. *International Journal of Neuropsychopharmacology*, *16*(7). https://doi.org/10.1017/S1461145713000060

Hunnicutt, B. J., Long, B. R., Kusefoglu, D., Gertz, K. J., Zhong, H., & Mao, T. (2014). A comprehensive thalamocortical projection map at the mesoscopic level. *Nature Neuroscience*, *17*(9). https://doi.org/10.1038/nn.3780

Iino, Y., Sawada, T., Yamaguchi, K., Tajiri, M., Ishii, S., Kasai, H., & Yagishita, S. (2020). Dopamine D2 receptors in discrimination learning and spine enlargement. *Nature*, *579*(7800). https://doi.org/10.1038/s41586-020-2115-1

Ikeda, H., Kamei, J., Koshikawa, N., & Cools, A. R. (2012). Nucleus accumbens and dopamine-mediated turning behavior of the rat: Role of accumbal non-dopaminergic receptors. In *Journal of Pharmacological Sciences* (Vol. 120, Issue 3, pp. 152–164). Japanese Pharmacological Society. https://doi.org/10.1254/jphs.12R02CR

Ikemoto, S., & Panksepp, J. (1999). The role of nucleus accumbens dopamine in motivated behavior: A unifying interpretation with special reference to reward-seeking. In *Brain Research Reviews* (Vol. 31, Issue 1). https://doi.org/10.1016/S0165-0173(99)00023-5

Isaacson, J. S., & Scanziani, M. (2011). How inhibition shapes cortical activity. In *Neuron* (Vol. 72, Issue 2, pp. 231–243). https://doi.org/10.1016/j.neuron.2011.09.027

Kahneman, D., & Tversky, A. (1979). Prospect Theory: An Analysis of Decision under Risk Daniel Kahneman; Amos Tversky. *Econometrica*, *47*(2).

Kandel, E. R., Dudai, Y., & Mayford, M. R. (2014). The molecular and systems biology of memory. In *Cell* (Vol. 157, Issue 1). https://doi.org/10.1016/j.cell.2014.03.001

Kim, C. K., Sanchez, M. I., Hoerbelt, P., Fenno, L. E., Malenka, R. C., Deisseroth, K., & Ting, A. Y. (2020). A Molecular Calcium Integrator Reveals a Striatal Cell Type Driving Aversion. *Cell*, *183*(7). https://doi.org/10.1016/j.cell.2020.11.015

Kim, J., Park, B. H., Lee, J. H., Park, S. K., & Kim, J. H. (2011). Cell type-specific alterations in the nucleus accumbens by repeated exposures to cocaine. *Biological Psychiatry*, *69*(11). https://doi.org/10.1016/j.biopsych.2011.01.013

Klawonn, A. M., & Malenka, R. C. (2018). Nucleus accumbens modulation in reward and aversion. *Cold Spring Harbor Symposia on Quantitative Biology*, *83*. https://doi.org/10.1101/sqb.2018.83.037457

Knowland, D., Lilascharoen, V., Pacia, C. P., Shin, S., Wang, E. H. J., & Lim, B. K. (2017). Distinct Ventral Pallidal Neural Populations Mediate Separate Symptoms of Depression. *Cell*, *170*(2). https://doi.org/10.1016/j.cell.2017.06.015

Kravitz, A. V., Tye, L. D., & Kreitzer, A. C. (2012). Distinct roles for direct and indirect pathway striatal neurons in reinforcement. *Nature Neuroscience*, *15*(6). https://doi.org/10.1038/nn.3100

Kreitzer, A. C., & Malenka, R. C. (2007). Endocannabinoid-mediated rescue of striatal LTD and motor deficits in Parkinson's disease models. *Nature*, *445*(7128). https://doi.org/10.1038/nature05506

Kubanek, J., Snyder, L. H., & Abrams, R. A. (2015). Reward and punishment act as distinct factors in guiding behavior. *Cognition*, *139*, 154–167. https://doi.org/10.1016/j.cognition.2015.03.005

Kupchik, Y. M., Brown, R. M., Heinsbroek, J. A., Lobo, M. K., Schwartz, D. J., & Kalivas, P. W. (2015). Coding the direct/indirect pathways by D1 and D2 receptors is not valid for accumbens projections. *Nature Neuroscience*, *18*(9), 1230–1232. https://doi.org/10.1038/nn.4068

Kupchik, Y. M., & Kalivas, P. W. (2017). The Direct and Indirect Pathways of the Nucleus Accumbens are not What You Think. In *Neuropsychopharmacology* (Vol. 42, Issue 1). https://doi.org/10.1038/npp.2016.160

Kupchik, Y. M., & Prasad, A. A. (2021). Ventral pallidum cellular and pathway specificity in drug seeking. *Neuroscience and Biobehavioral Reviews*, *131*. https://doi.org/10.1016/j.neubiorev.2021.09.007

Kutlu, M. G., Zachry, J. E., Melugin, P. R., Cajigas, S. A., Chevee, M. F., Kelly, S. J., Kutlu, B., Tian, L., Siciliano, C. A., & Calipari, E. S. (2021). Dopamine release in the nucleus accumbens core signals perceived saliency. *Current Biology*, *31*(21). https://doi.org/10.1016/j.cub.2021.08.052

Lai, Y. Y., Kodama, T., Hsieh, K. C., Nguyen, D., & Siegel, J. M. (2021). Substantia nigra pars reticulata-mediated sleep and motor activity regulation. *Sleep*, *44*(1). https://doi.org/10.1093/sleep/zsaa151

Lee, J., Finkelstein, J., Choi, J. Y. Y., & Witten, I. B. B. (2016). Linking Cholinergic Interneurons, Synaptic Plasticity, and Behavior during the Extinction of a Cocaine-Context Association. *Neuron*, *90*(5), 1071–1085. https://doi.org/10.1016/j.neuron.2016.05.001

Li, Z., Chen, Z., Fan, G., Li, A., Yuan, J., & Xu, T. (2018). Cell-type-specific afferent innervation of the nucleus accumbens core and shell. *Frontiers in Neuroanatomy*, *12*. https://doi.org/10.3389/fnana.2018.00084

Liu, D., Li, W., Ma, C., Zheng, W., Yao, Y., Tso, C. F., Zhong, P., Chen, X., Song, J. H., Choi, W., Paik, S.-B., Han, H., & Dan, Y. (2020). *A common hub for sleep and motor control in the substantia nigra*. https://www.science.org

Liu, Z., Le, Q., Lv, Y., Chen, X., Cui, J., Zhou, Y., Cheng, D., Ma, C., Su, X., Xiao, L., Yang, R., Zhang, J., Ma, L., & Liu, X. (2022). A distinct D1-MSN subpopulation down-regulates dopamine to promote negative emotional state. *Cell Research*, *32*(2), 139–156. https://doi.org/10.1038/s41422-021-00588-5

Lobo, M. K., Covington, H. E., Chaudhury, D., Friedman, A. K., Sun, H. S., Damez-Werno, D., Dietz, D. M., Zaman, S., Koo, J. W., Kennedy, P. J., Mouzon, E., Mogri, M., Neve, R. L., Deisseroth, K., Han, M. H., & Nestler, E. J. (2010). Cell type - Specific loss of BDNF signaling mimics optogenetic control of cocaine reward. *Science*, *330*(6002). https://doi.org/10.1126/science.1188472

Lu, X. Y., Ghasemzadeh, M. B., & Kalivas, P. W. (1997). Expression of D1 receptor, D2 receptor, substance P and enkephalin messenger RNAs in the neurons projecting from the nucleus accumbens. *Neuroscience*, *82*(3). https://doi.org/10.1016/S0306-4522(97)00327-8

Ma, L., Chen, W., Yu, D., & Han, Y. (2020). Brain-Wide Mapping of Afferent Inputs to Accumbens Nucleus Core Subdomains and Accumbens Nucleus Subnuclei. *Frontiers in Systems Neuroscience*, *14*. https://doi.org/10.3389/fnsys.2020.00015

Macpherson, T., & Hikida, T. (2018). Nucleus accumbens dopamine D1-receptor-expressing neurons control the acquisition of sign-tracking to conditioned cues in mice. *Frontiers in Neuroscience*, *12*(JUN). https://doi.org/10.3389/fnins.2018.00418

Macpherson, T., & Hikida, T. (2019). Role of basal ganglia neurocircuitry in the pathology of psychiatric disorders. In *Psychiatry and Clinical Neurosciences* (Vol. 73, Issue 6). https://doi.org/10.1111/pcn.12830

Macpherson, T., Matsumoto, M., Gomi, H., Morimoto, J., Uchibe, E., & Hikida, T. (2021). Parallel and hierarchical neural mechanisms for adaptive and predictive behavioral control. *Neural Networks*, *144*, 507–521. https://doi.org/10.1016/j.neunet.2021.09.009

Macpherson, T., Morita, M., & Hikida, T. (2014). Striatal direct and indirect pathways control decision-making behavior. In *Frontiers in Psychology* (Vol. 5, Issue NOV). https://doi.org/10.3389/fpsyg.2014.01301

Mannella, F., Gurney, K., & Baldassarre, G. (2013). The nucleus accumbens as a nexus between values and goals in goal-directed behavior: A review and a new hypothesis. *Frontiers in Behavioral Neuroscience*, *OCT*. https://doi.org/10.3389/fnbeh.2013.00135

Mannella, F., Mirolli, M., & Baldassarre, G. (2016). Goal-directed behavior and instrumental devaluation: A neural system-level computational model. *Frontiers in Behavioral Neuroscience*, *10*(OCT). https://doi.org/10.3389/fnbeh.2016.00181

Matsui, A., & Alvarez, V. A. (2018). Cocaine Inhibition of Synaptic Transmission in the Ventral Pallidum Is Pathway-Specific and Mediated by Serotonin. *Cell Reports*, *23*(13). https://doi.org/10.1016/j.celrep.2018.05.076

McHaffie, J. G., Stanford, T. R., Stein, B. E., Coizet, V., & Redgrave, P. (2005). Subcortical loops through the basal ganglia. *Trends in Neurosciences*, *28*(8). https://doi.org/10.1016/j.tins.2005.06.006

Milardi, D., Quartarone, A., Bramanti, A., Anastasi, G., Bertino, S., Basile, G. A., Buonasera, P., Pilone, G., Celeste, G., Rizzo, G., Bruschetta, D., & Cacciola, A. (2019). The Cortico-Basal Ganglia-Cerebellar Network: Past, Present and Future Perspectives. In *Frontiers in Systems Neuroscience* (Vol. 13). https://doi.org/10.3389/fnsys.2019.00061

Mirenowicz, J., & Schultz, W. (1996). Preferential activation of midbrain dopamine neurons by appetitive rather than aversive stimuli. *Nature*, *379*(6564). https://doi.org/10.1038/379449a0

Mogenson, G. J., Jones, D. L., & Yim, C. Y. (1980). From motivation to action: Functional interface between the limbic system and the motor system. In *Progress in Neurobiology* (Vol. 14, Issues 2–3). https://doi.org/10.1016/0301-0082(80)90018-0

Nagel, G., Szellas, T., Huhn, W., Kateriya, S., Adeishvili, N., Berthold, P., Ollig, D., Hegemann, P., & Bamberg, E. (2003). Channelrhodopsin-2, a directly light-gated cation-selective membrane channel. *Proceedings of the National Academy of Sciences of the United States of America*, *100*(SUPPL. 2). https://doi.org/10.1073/pnas.1936192100

Nakanishi, S., Hikida, T., & Yawata, S. (2014). Distinct dopaminergic control of the direct and indirect pathways in reward-based and avoidance learning behaviors. In *Neuroscience* (Vol. 282). https://doi.org/10.1016/j.neuroscience.2014.04.026

Nambu, A. (2004). A new dynamic model of the cortico-basal ganglia loop. *Progress in Brain Research*, *143*. https://doi.org/10.1016/S0079-6123(03)43043-4

Napier, T. C., Mitrovic, I., Churchill, L., Klitenick, M. A., Lu, X. Y., & Kalivas, P. W. (1995). Substance P in the ventral pallidum: Projection from the ventral striatum, and electrophysiological and behavioral cinsequences of pallidal substance P. *Neuroscience*, *69*(1). https://doi.org/10.1016/0306-4522(95)00218-8

Nicola, S. M. (2007). The nucleus accumbens as part of a basal ganglia action selection circuit. In *Psychopharmacology* (Vol. 191, Issue 3). https://doi.org/10.1007/s00213-006-0510-4

Nicola, S. M. (2010). The flexible approach hypothesis: Unification of effort and cue-responding hypotheses for the role of nucleus accumbens dopamine in the activation of reward-seeking behavior. *Journal of Neuroscience*, *30*(49). https://doi.org/10.1523/JNEUROSCI.3958-10.2010

Nishioka, T., Attachaipanich, S., Hamaguchi, K., Lazarus, M., de Kerchove d'Exaerde, A., Macpherson, T., & Hikida, T. (2023). Error-related signaling in nucleus accumbens D2

receptor-expressing neurons guides inhibition-based choice behavior in mice. *Nature Communications*, *14*(1), 2284. https://doi.org/10.1038/s41467-023-38025-3

Nonomura, S., Nishizawa, K., Sakai, Y., Kawaguchi, Y., Kato, S., Uchigashima, M., Watanabe, M., Yamanaka, K., Enomoto, K., Chiken, S., Sano, H., Soma, S., Yoshida, J., Samejima, K., Ogawa, M., Kobayashi, K., Nambu, A., Isomura, Y., & Kimura, M. (2018). Monitoring and Updating of Action Selection for Goal-Directed Behavior through the Striatal Direct and Indirect Pathways. *Neuron*, *99*(6). https://doi.org/10.1016/j.neuron.2018.08.002

O'Connor, E. C., Kremer, Y., Lefort, S., Harada, M., Pascoli, V., Rohner, C., & Lüscher, C. (2015). Accumbal D1R Neurons Projecting to Lateral Hypothalamus Authorize Feeding. *Neuron*, *88*(3). https://doi.org/10.1016/j.neuron.2015.09.038

Ota, S. M., Suchecki, D., & Meerlo, P. (2018). Chronic social defeat stress suppresses locomotor activity but does not affect the free-running circadian period of the activity rhythm in mice. *Neurobiology of Sleep and Circadian Rhythms*, *5*. https://doi.org/10.1016/j.nbscr.2018.03.002

Pardo-Garcia, T. R., Garcia-Keller, C., Penaloza, T., Richie, C. T., Pickel, J., Hope, B. T., Harvey, B. K., Kalivas, P. W., & Heinsbroek, J. A. (2019). Ventral pallidum is the primary target for accumbens D1 projections driving cocaine seeking. *Journal of Neuroscience*, *39*(11), 2041–2051. https://doi.org/10.1523/JNEUROSCI.2822-18.2018

Parent, A., & Hazrati, L. N. (1995). Functional anatomy of the basal ganglia. I. The cortico-basal ganglia-thalamo-cortical loop. In *Brain Research Reviews* (Vol. 20, Issue 1). https://doi.org/10.1016/0165-0173(94)00007-C

Patel, S., & Slater, P. (1988). Effects of GABA compounds injected into the subpallidal regions of rat brain on nucleus accumbens evoked hyperactivity. *Behavioral Neuroscience*, *102*(4). https://doi.org/10.1037/0735-7044.102.4.596

Peak, J., Hart, G., & Balleine, B. W. (2019). From learning to action: the integration of dorsal striatal input and output pathways in instrumental conditioning. In *European Journal of Neuroscience* (Vol. 49, Issue 5). https://doi.org/10.1111/ejn.13964

Penner, M. R., & Mizumori, S. J. Y. (2012). Neural systems analysis of decision making during goal-directed navigation. In *Progress in Neurobiology* (Vol. 96, Issue 1). https://doi.org/10.1016/j.pneurobio.2011.08.010

Plaznik, A., Stefanski, R., & Kostowski, W. (1989). Interaction between accumbens D1 and D2 receptors regulating rat locomotor activity. *Psychopharmacology*, *99*(4). https://doi.org/10.1007/BF00589908

Ranaldi, R., Egan, J. R., Kest, K., Fein, M., & Delamater, A. R. (2009). Repeated heroin in rats produces locomotor sensitization and enhances appetitive Pavlovian and instrumental learning involving food reward. *Pharmacology Biochemistry and Behavior*, *91*(3). https://doi.org/10.1016/j.pbb.2008.08.006

Rasmussen, E. B., & Newland, M. C. (2008). ASYMMETRY OF REINFORCEMENT AND PUNISHMENT IN HUMAN CHOICE. *Journal of the Experimental Analysis of Behavior*, *89*(2). https://doi.org/10.1901/jeab.2008.89-157

Rein, M. L., & Deussing, J. M. (2012). The optogenetic (r)evolution. In *Molecular Genetics and Genomics* (Vol. 287, Issue 2). https://doi.org/10.1007/s00438-011-0663-7

Reynolds, S. M., & Berridge, K. C. (2002). Positive and negative motivation in nucleus accumbens shell: Bivalent rostrocaudal gradients for GABA-elicited eating, taste "liking"/"disliking" reactions, place preference/avoidance, and fear. *Journal of Neuroscience*, *22*(16). https://doi.org/10.1523/jneurosci.22-16-07308.2002

Robbins, T. W., Gillan, C. M., Smith, D. G., de Wit, S., & Ersche, K. D. (2012). Neurocognitive endophenotypes of impulsivity and compulsivity: Towards dimensional psychiatry. In *Trends in Cognitive Sciences* (Vol. 16, Issue 1). https://doi.org/10.1016/j.tics.2011.11.009

Robertson, G. S., & Jian, M. (1995). D1 and D2 dopamine receptors differentially increase fos-like immunoreactivity in accumbal projections to the ventral pallidum and midbrain. *Neuroscience*, *64*(4). https://doi.org/10.1016/0306-4522(94)00426-6

Robinson, M. J. F., Warlow, S. M., & Berridge, K. C. (2014). Optogenetic excitation of central amygdala amplifies and narrows incentive motivation to pursue one reward above another. *Journal of Neuroscience*, *34*(50). https://doi.org/10.1523/JNEUROSCI.2013-14.2014

Robinson, T. E., & Berridge, K. C. (1993). The neural basis of drug craving: An incentive-sensitization theory of addiction. In *Brain Research Reviews* (Vol. 18, Issue 3). https://doi.org/10.1016/0165-0173(93)90013-P

Robinson, T. E., Yager, L. M., Cogan, E. S., & Saunders, B. T. (2014). On the motivational properties of reward cues: Individual differences. In *Neuropharmacology* (Vol. 76, Issue PART B, pp. 450–459). https://doi.org/10.1016/j.neuropharm.2013.05.040

Root, D. H., Melendez, R. I., Zaborszky, L., & Napier, T. C. (2015). The ventral pallidum: Subregion-specific functional anatomy and roles in motivated behaviors. In *Progress in Neurobiology* (Vol. 130, pp. 29–70). Elsevier Ltd. https://doi.org/10.1016/j.pneurobio.2015.03.005

Saga, Y., Galineau, L., & Tremblay, L. (2022). Impulsive and compulsive behaviors can be induced by opposite GABAergic dysfunctions inside the primate ventral pallidum. *Frontiers in Systems Neuroscience*, *16*. https://doi.org/10.3389/fnsys.2022.1009626

Salgado, S., & Kaplitt, M. G. (2015). The nucleus accumbens: A comprehensive review. In *Stereotactic and Functional Neurosurgery* (Vol. 93, Issue 2). https://doi.org/10.1159/000368279

Sanger, T. D., Chen, D., Fehlings, D. L., Hallett, M., Lang, A. E., Mink, J. W., Singer, H. S., Alter, K., Ben-Pazi, H., Butler, E. E., Chen, R., Collins, A., Dayanidhi, S., Forssberg, H., Fowler, E., Gilbert, D. L., Gorman, S. L., Gormley, M. E., Jinnah, H. A., … Valero-Cuevas, F. (2010). Definition and classification of hyperkinetic movements in childhood. In *Movement Disorders* (Vol. 25, Issue 11). https://doi.org/10.1002/mds.23088

Schlosburg, J. E., Whitfield, T. W., Park, P. E., Crawford, E. F., George, O., Vendruscolo, L. F., & Koob, G. F. (2013). Long-term antagonism of κ opioid receptors prevents escalation of and increased motivation for heroin intake. *Journal of Neuroscience*, *33*(49). https://doi.org/10.1523/JNEUROSCI.1979-13.2013

Schultz, W., Dayan, P., & Montague, P. R. (1997). A neural substrate of prediction and reward. *Science*, *275*(5306). https://doi.org/10.1126/science.275.5306.1593

Scofield, M. D., Heinsbroek, J. A., Gipson, C. D., Kupchik, Y. M., Spencer, S., Smith, A. C. W., Roberts-Wolfe, D., & Kalivas, P. W. (2016). The nucleus accumbens: Mechanisms of addiction across drug classes reflect the importance of glutamate homeostasis. *Pharmacological Reviews*, *68*(3). https://doi.org/10.1124/pr.116.012484

Scudder, S. L., Baimel, C., Macdonald, E. E., & Carter, A. G. (2018). Hippocampal-evoked feedforward inhibition in the nucleus accumbens. *Journal of Neuroscience*, *38*(42), 9091–9104. https://doi.org/10.1523/JNEUROSCI.1971-18.2018

Setlow, B., Schoenbaum, G., & Gallagher, M. (2003). Neural encoding in ventral striatum during olfactory discrimination learning. *Neuron*, *38*(4). https://doi.org/10.1016/S0896-6273(03)00264-2

Shen, W., Flajolet, M., Greengard, P., & Surmeier, D. J. (2008). Dichotomous dopaminergic control of striatal synaptic plasticity. *Science*, *321*(5890). https://doi.org/10.1126/science.1160575

Sicre, M., Meffre, J., Louber, D., & Ambroggi, F. (2020). The nucleus accumbens core is necessary for responding to incentive but not instructive stimuli. *Journal of Neuroscience*, *40*(6), 1332–1343. https://doi.org/10.1523/JNEUROSCI.0194-19.2019

Sitzia, G., Mantas, I., Zhang, X., Svenningsson, P., & Chergui, K. (2020). NMDA receptors are altered in the substantia nigra pars reticulata and their blockade ameliorates motor deficits in experimental parkinsonism. *Neuropharmacology*, *174*. https://doi.org/10.1016/j.neuropharm.2020.108136

Smith, K. S., Tindell, A. J., Aldridge, J. W., & Berridge, K. C. (2009). Ventral pallidum roles in reward and motivation. In *Behavioural Brain Research* (Vol. 196, Issue 2). https://doi.org/10.1016/j.bbr.2008.09.038

Soares-Cunha, C., Coimbra, B., David-Pereira, A., Borges, S., Pinto, L., Costa, P., Sousa, N., & Rodrigues, A. J. (2016). Activation of D2 dopamine receptor-expressing neurons in the nucleus accumbens increases motivation. *Nature Communications*, *7*. https://doi.org/10.1038/ncomms11829

Soares-Cunha, C., de Vasconcelos, N. A. P., Coimbra, B., Domingues, A. V., Silva, J. M., Loureiro-Campos, E., Gaspar, R., Sotiropoulos, I., Sousa, N., & Rodrigues, A. J. (2020). Nucleus accumbens medium spiny neurons subtypes signal both reward and aversion. *Molecular Psychiatry*, *25*(12). https://doi.org/10.1038/s41380-019-0484-3

Soares-Cunha, C., Domingues, A. V., Correia, R., Coimbra, B., Vieitas-Gaspar, N., de Vasconcelos, N. A. P., Pinto, L., Sousa, N., & Rodrigues, A. J. (2022). Distinct role of nucleus accumbens D2-MSN projections to ventral pallidum in different phases of motivated behavior. *Cell Reports*, *38*(7). https://doi.org/10.1016/j.celrep.2022.110380

Soares-Cunha, C., & Heinsbroek, J. A. (2023). Ventral pallidal regulation of motivated behaviors and reinforcement. In *Frontiers in Neural Circuits* (Vol. 17). https://doi.org/10.3389/fncir.2023.1086053

Stefanik, M. T., Kupchik, Y. M., Brown, R. M., & Kalivas, P. W. (2013). Optogenetic evidence that pallidal projections, not nigral projections, from the nucleus accumbens core are necessary for reinstating cocaine seeking. *Journal of Neuroscience*, *33*(34), 13654–13662. https://doi.org/10.1523/JNEUROSCI.1570-13.2013

Stephenson-Jones, M., Bravo-Rivera, C., Ahrens, S., Furlan, A., Xiao, X., Fernandes-Henriques, C., & Li, B. (2020). Opposing Contributions of GABAergic and Glutamatergic Ventral Pallidal Neurons to Motivational Behaviors. *Neuron*, *105*(5). https://doi.org/10.1016/j.neuron.2019.12.006

Strickland, J. C., Bolin, B. L., Lile, J. A., Rush, C. R., & Stoops, W. W. (2016). Differential sensitivity to learning from positive and negative outcomes in cocaine users. *Drug and Alcohol Dependence*, *166*, 61–68. https://doi.org/10.1016/j.drugalcdep.2016.06.022

Strong, C. E., Schoepfer, K. J., Dossat, A. M., Saland, S. K., Wright, K. N., & Kabbaj, M. (2017). Locomotor sensitization to intermittent ketamine administration is associated with nucleus accumbens plasticity in male and female rats. *Neuropharmacology*, *121*. https://doi.org/10.1016/j.neuropharm.2017.05.003

Surmeier, D. J., Ding, J., Day, M., Wang, Z., & Shen, W. (2007). D1 and D2 dopamine-receptor modulation of striatal glutamatergic signaling in striatal medium spiny neurons. In *Trends in Neurosciences* (Vol. 30, Issue 5). https://doi.org/10.1016/j.tins.2007.03.008

Surmeier, D. J., Song, W.-J., & Yan, Z. (1996). *Coordinated Expression of Dopamine Receptors in Neostriatal Medium Spiny Neurons*.

Svenningsson, P., Le Moine, C., Kull, B., Sunahara, R., Bloch, B., & Fredholm, B. B. (1997). Cellular expression of adenosine A(2a) receptor messenger RNA in the rat central nervous system with special reference to dopamine innervated areas. *Neuroscience*, *80*(4). https://doi.org/10.1016/S0306-4522(97)00180-2

Swadlow, H. A. (2003). Fast-spike interneurons and feedforward inhibition in awake sensory neocortex. *Cerebral Cortex*, *13*(1). https://doi.org/10.1093/cercor/13.1.25

Swerdlow, N. R., & Koob, G. F. (1987). Lesions of the dorsomedial nucleus of the thalamus, medial prefrontal cortex and pedunculopontine nucleus: effects on locomotor activity mediated by nucleus accumbens-ventral pallidal circuitry. *Brain Research*, *412*(2). https://doi.org/10.1016/0006-8993(87)91129-2

Tachibana, Y., & Hikosaka, O. (2012). The Primate Ventral Pallidum Encodes Expected Reward Value and Regulates Motor Action. *Neuron*, *76*(4). https://doi.org/10.1016/j.neuron.2012.09.030

Tai, L. H., Lee, A. M., Benavidez, N., Bonci, A., & Wilbrecht, L. (2012). Transient stimulation of distinct subpopulations of striatal neurons mimics changes in action value. *Nature Neuroscience*, *15*(9). https://doi.org/10.1038/nn.3188

Tepper, J. M., & Bolam, J. P. (2004). Functional diversity and specificity of neostriatal interneurons. In *Current Opinion in Neurobiology* (Vol. 14, Issue 6, pp. 685–692). https://doi.org/10.1016/j.conb.2004.10.003

Tooley, J., Marconi, L., Alipio, J. B., Matikainen-Ankney, B., Georgiou, P., Kravitz, A. V., & Creed, M. C. (2018). Glutamatergic Ventral Pallidal Neurons Modulate Activity of the Habenula–Tegmental Circuitry and Constrain Reward Seeking. *Biological Psychiatry*, *83*(12). https://doi.org/10.1016/j.biopsych.2018.01.003

Tran, A. H., Tamura, R., Uwano, T., Kobayashi, T., Katsuki, M., & Ono, T. (2005). Dopamine D1 receptors involved in locomotor activity and accumbens neural responses to prediction of reward associated with place. *Proceedings of the National Academy of Sciences of the United States of America*, *102*(6). https://doi.org/10.1073/pnas.0409726102

Tsutsui-Kimura, I., Natsubori, A., Mori, M., Kobayashi, K., Drew, M. R., de Kerchove d'Exaerde, A., Mimura, M., & Tanaka, K. F. (2017). Distinct Roles of Ventromedial versus Ventrolateral Striatal Medium Spiny Neurons in Reward-Oriented Behavior. *Current Biology*, *27*(19). https://doi.org/10.1016/j.cub.2017.08.061

Tye, K. M., & Deisseroth, K. (2012). Optogenetic investigation of neural circuits underlying brain disease in animal models. In *Nature Reviews Neuroscience* (Vol. 13, Issue 4, pp. 251–266). https://doi.org/10.1038/nrn3171

Tye, K. M., Mirzabekov, J. J., Warden, M. R., Ferenczi, E. A., Tsai, H. C., Finkelstein, J., Kim, S. Y., Adhikari, A., Thompson, K. R., Andalman, A. S., Gunaydin, L. A., Witten, I. B., & Deisseroth, K. (2013). Dopamine neurons modulate neural encoding and expression of depression-related behaviour. *Nature*, *493*(7433). https://doi.org/10.1038/nature11740

Van Zessen, R., Li, Y., Marion-Poll, L., Hulo, N., Flakowski, J., & Lüscher, C. (2021). Dynamic dichotomy of Accumbal population activity underlies cocaine sensitization. *ELife*, *10*. https://doi.org/10.7554/eLife.66048

Vezina, P. (2004). Sensitization of midbrain dopamine neuron reactivity and the self-administration of psychomotor stimulant drugs. *Neuroscience and Biobehavioral Reviews*, *27*(8). https://doi.org/10.1016/j.neubiorev.2003.11.001

Volkow, N. D., Michaelides, M., & Baler, R. (2019). The neuroscience of drug reward and addiction. *Physiological Reviews*, *99*(4). https://doi.org/10.1152/physrev.00014.2018

Voorn, P., Vanderschuren, L. J. M. J., Groenewegen, H. J., Robbins, T. W., & Pennartz, C. M. A. (2004). Putting a spin on the dorsal-ventral divide of the striatum. In *Trends in Neurosciences* (Vol. 27, Issue 8). https://doi.org/10.1016/j.tins.2004.06.006

Wallace, L. J., & Uretsky, N. J. (1991). Effect of GABAergic and glutamatergic drugs injected into the ventral pallidum on locomotor activity. In *Advances in Experimental Medicine and Biology* (Vol. 295). https://doi.org/10.1007/978-1-4757-0145-6_16

Wang, L., Shen, M., Yu, Y., Tao, Y., Zheng, P., Wang, F., & Ma, L. (2014). Optogenetic activation of GABAergic neurons in the nucleus accumbens decreases the activity of the ventral pallidum and the expression of cocaine-context-associated memory. *International Journal of Neuropsychopharmacology*, *17*(5). https://doi.org/10.1017/S1461145713001570

Whitfield, T. W., Schlosburg, J. E., Wee, S., Gould, A., George, O., Grant, Y., Zamora-Martinez, E. R., Edwards, S., Crawford, E., Vendruscolo, L. F., & Koob, G. F. (2015). K opioid receptors in the nucleus accumbens shell mediate escalation of methamphetamine intake. *Journal of Neuroscience*, *35*(10). https://doi.org/10.1523/JNEUROSCI.1978-13.2015

Wise, R. A. (2004). Dopamine, learning and motivation. In *Nature Reviews Neuroscience* (Vol. 5, Issue 6). https://doi.org/10.1038/nrn1406

Xiong, Q., Znamenskiy, P., & Zador, A. M. (2015). Selective corticostriatal plasticity during acquisition of an auditory discrimination task. *Nature*, *521*(7552). https://doi.org/10.1038/nature14225

Yao, Y., Gao, G., Liu, K., Shi, X., Cheng, M., Xiong, Y., & Song, S. (2021). Projections from D2 Neurons in Different Subregions of Nucleus Accumbens Shell to Ventral Pallidum Play Distinct Roles in Reward and Aversion. *Neuroscience Bulletin*, *37*(5). https://doi.org/10.1007/s12264-021-00632-9

Yawata, S., Yamaguchi, T., Danjo, T., Hikida, T., & Nakanishi, S. (2012). Pathway-specific control of reward learning and its flexibility via selective dopamine receptors in the nucleus accumbens. *Proceedings of the National Academy of Sciences of the United States of America*, *109*(31). https://doi.org/10.1073/pnas.1210797109

Yee, J., Famous, K. R., Hopkins, T. J., McMullen, M. C., Pierce, R. C., & Schmidt, H. D. (2011). Muscarinic acetylcholine receptors in the nucleus accumbens core and shell contribute to cocaine priming-induced reinstatement of drug seeking. *European Journal of Pharmacology*, *650*(2–3). https://doi.org/10.1016/j.ejphar.2010.10.045

Yin, H. H., Ostlund, S. B., & Balleine, B. W. (2008). Reward-guided learning beyond dopamine in the nucleus accumbens: The integrative functions of cortico-basal ganglia networks. In *European Journal of Neuroscience* (Vol. 28, Issue 8). https://doi.org/10.1111/j.1460-9568.2008.06422.x

Yizhar, O., Fenno, L. E., Davidson, T. J., Mogri, M., & Deisseroth, K. (2011). Optogenetics in Neural Systems. In *Neuron* (Vol. 71, Issue 1). https://doi.org/10.1016/j.neuron.2011.06.004

Yorgason, J. T., Zeppenfeld, D. M., & Williams, J. T. (2017). Cholinergic interneurons underlie spontaneous dopamine release in nucleus accumbens. *Journal of Neuroscience*, *37*(8), 2086–2096. https://doi.org/10.1523/JNEUROSCI.3064-16.2017

Young, C. B., & Sonne, J. (2019). Neuroanatomy, Basal Ganglia. In *StatPearls*.

Yu, X., Zhao, G., Wang, D., Wang, S., Li, R., Li, A., Wang, H., Nollet, M., Chun, Y. Y., Zhao, T., Yustos, R., Li, H., Zhao, J., Li, J., Cai, M., Vyssotski, A. L., Li, Y., Dong, H., Franks, N.

P., & Wisden, W. (2022). A specific circuit in the midbrain detects stress and induces restorative sleep. *Science*, *377*(6601). https://doi.org/10.1126/science.abn0853

Zalocusky, K. A., Ramakrishnan, C., Lerner, T. N., Davidson, T. J., Knutson, B., & Deisseroth, K. (2016). Nucleus accumbens D2R cells signal prior outcomes and control risky decision-making. *Nature*, *531*(7596). https://doi.org/10.1038/nature17400

Zhu, X., Ottenheimer, D., & DiLeone, R. J. (2016). Activity of D1/2 receptor expressing neurons in the nucleus accumbens regulates running, locomotion, and food intake. *Frontiers in Behavioral Neuroscience*, *10*(APRIL). https://doi.org/10.3389/fnbeh.2016.00066